Alma Mater Studiorum – University of Bologna

School of Engineering and Architecture

Department of Electrical, Electronic and Information Engineering (DEI)

Master Course in

Electrical Energy Engineering

Thesis in:

High Voltage Engineering

LIFE ESTIMATION OF HVDC CABLES SUBJECTED TO QUALIFICATION TEST CONDITIONS

Student:

BASSEL DIBAN

Supervisor:

Prof. Dr. Ing. GIOVANNI MAZZANTI

Co-supervisors:

Dr. Ing. Paolo Seri

Dr. Ing. Marco Landini

Dr. Ing. Ivan Troia

Academic year: 2018/2019

October 2019

Acknowledgement:

To my beloved family which has always supported me…

To my bleeding home Syria which will be in my heart forever…

To Italy which gave me this golden opportunity through the scholarship program of the Italian Ministry of Foreign Affairs…

I would like to express my special thanks of gratitude to my supervisor Prof. Giovanni Mazzanti who helped me to do this thesis and to obtain new knowledge from his experience as well.

Index:

Abstract:

The goal of the Master Thesis is estimating the life of HVDC XLPE-insulated cables subjected to the Electrical Type Test conditions according to CIGRÉ Technical Brochure 496, during which a series of load cycles (LC) with DC voltage *UT=1.85 U0* (rated voltage) are applied in three stages, i.e.:

- 12 cycles lasting 24 hours each with a negative polarity of the applied voltage (12 days).
- 12 cycles lasting 24 hours each with a positive polarity of the applied voltage (12 days).
- 3 cycles lasting 48 hours each with a positive polarity of the applied voltage (3×48 h=6 days).

It is worth noting that according to CIGRÉ brochure 496 Load Cycles are of two types:

1. A 24-hour Load Cycle consists of 8 hours heating (with steady conductor temperature equal to the rated one during at least the last 2 hours), followed by 16 hours of natural cooling.
2. A 48-hour Load Cycle consists of 24 hours heating (with steady conductor temperature equal to the rated one during at least the last 18 hours), followed by 24 hours of natural cooling.

The simulation of the above-mentioned test has been realized by implementing a Matlab code consisting in 3 stages:

1) Transient thermal gradient calculations over the insulation thickness for 24-hour Load Cycle and 48-hour Load Cycle defined according to the Brochure of CIGRÉ 496 (Fig. 1).
2) Electric field calculations over the insulation thickness using the exact (Fig. 2) and the approximated method. This process considers the exponential dependence of electrical conductivity on electric field *E* and temperature *T* by means of the coefficients *a* & *b* as shown in the following equation:

$$\sigma = \sigma_0 \, exp(aT + bE)$$

where:

σ_0 = electrical conductivity of the insulation at an electric field *E=0 [kV/mm]* and a temperature *T=0 [°C]*.

a, b = coefficients whose values depends on the compound of the material of the insulation.

3) Calculations of cable life in many noteworthy points within the insulation thickness (Fig. 3).

Results: The results completely change according to the values of *a*, *b* as shown in Figs. (2),(3):

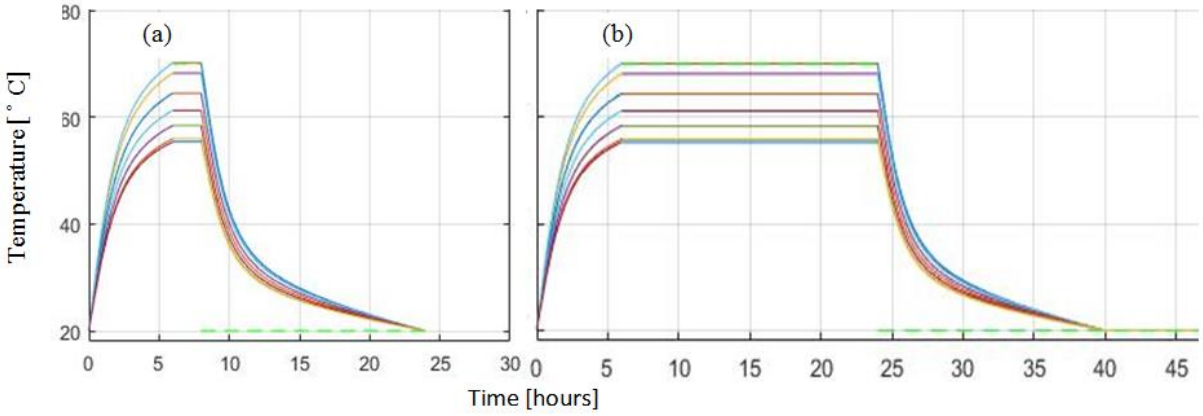

Figure 1 -Transient Temperature profile in case of (a) 24-hour Load Cycle (b) 48-hour Load Cycle for 7 points inside the XLPE insulation of an extruded HVDC cable

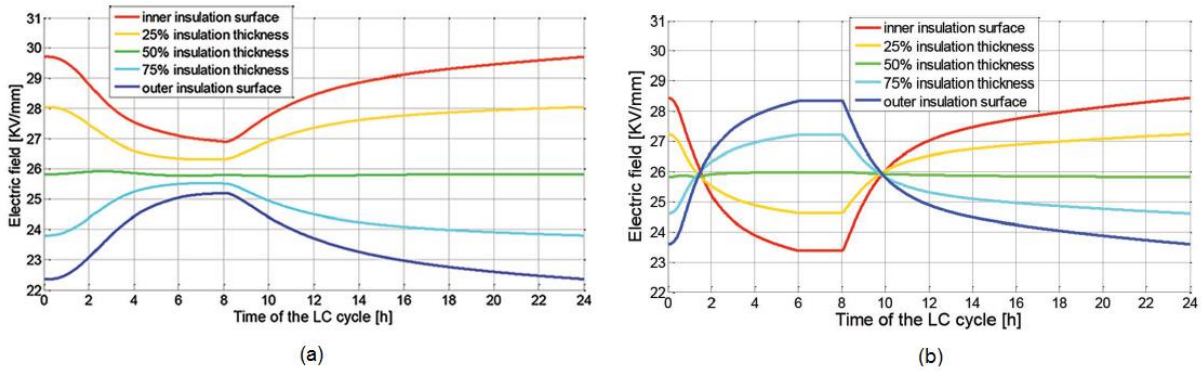

Figure 2 – Electric field at five points of cable insulation thickness calculated with the exact method for: (a) Low values of the coefficients *a*, *b* (a_L=*0.042 K-1;* b_L=*0.032 mm/kV*); (b) High values of *a*, *b* (a_H=*0.101* K^{-1}*;* b_H=*0.0775 mm/kV).*

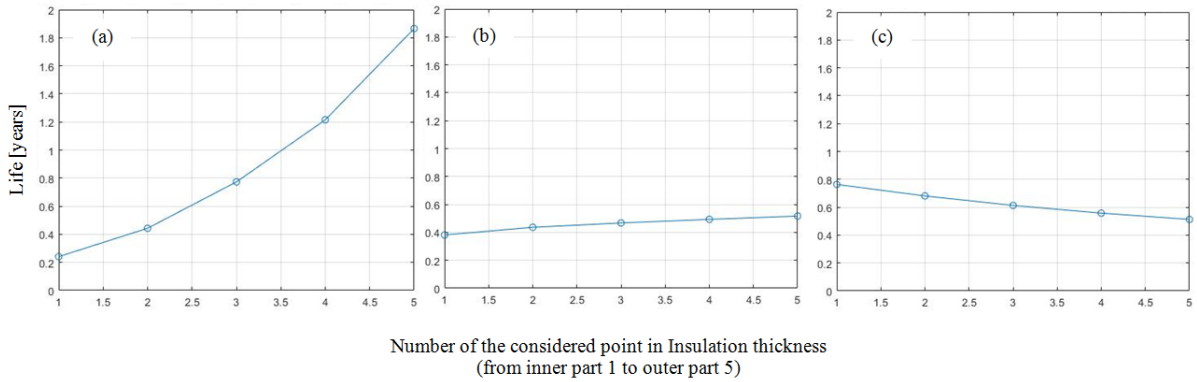

Figure 3 – Life of cable in years at five point of the insulation thickness for: (a) Low values of the coefficients *a*, *b* (a_L=*0.042 K-1;* b_L=*0.032 mm/kV*); (b) for Medium values of *a*, *b* (a_M=*0.084* K^{-1}*;* b_M=*0.0645 mm/kV*); (c) for High values of *a*, *b* (a_H=*0.101 K-1;* b_H=*0.0775 mm/kV*)

Discussion: The phenomenon called "Field Inversion" takes place only in the case of high values of "*a*" and "*b*" coefficients (Fig. 2.b) where the outer part of the insulation is stressed more than the inner part; accordingly, the outer part has a shorter life (Fig. 3.c). On this basis, the longer life corresponds to the cable with high values of "*a*" and "*b*" coefficients.

It is clear from Figure (3) in case of low "*a*" and "*b*" that the lower those values are, the more the inner part of the insulation is stressed. Consequently, the overall life becomes shorter because the life of the cable is determined by the shortest one over the cable thickness.

It can be clearly noticed that the life of the cable under the Type Test condition (around 90 days) is three times longer than the Type Test duration (30 days), considering the worst case which corresponds to low values of "*a*" and "*b*" (in the inner part of the insulation). However, this does not necessarily mean that the high values of "*a*" and "*b*" are overall better, since there are a lot of considerations to be considered in the selection of "*a*" and "*b*" in the manufacturing process.

Introduction:

Due the continuous expansion of the transmission systems as well as the need for long subsea power links, the importance of HVDC (High Voltage DC) adoption has been revealed as a solution to overhead lines concerns. On the other hand, HVDC has many notable advantages over the HVAC (High Voltage AC) which are summarised in the following:

- HVDC allows to control the quantity as well as the direction of the electrical power flow that in turn improve the characteristic and the efficiency of the electrical network itself.
- HVDC power lines have a lower risk due to the magnetic field (the magnetic field limits in HVDC are much lower than that in HVAC according to ICNIRP - International Commission on Non-Ionizing Radiation Protection), in addition to the lesser visual pollution.
- HVDC has lower capital and O&M (Operation and Maintenance) costs in case of distances longer than a certain value called “Break-even Distance” which ranges between 400 and 500 km in the case of overhead power lines (it depends on the operating voltage and the transmitted power). In this case, despite the additional cost of the converter station in HVDC, it is compensated by the lower electrical losses along the power lines resulting in a lower cost in case of HVDC.

For the above-mentioned reasons, during the last twenty years, HVDC cables have attained a considerable market share, especially, those that are insulated with DC-XLPE (cross-Linked PolyEthylene specifically designed for DC applications) which hereinafter called DC-XLPE extruded cables.

This thesis will provide a contribution to the previous studies of extruded HVDC cables, to be exact, this will cover the life of cables subjected to Type Test.

The first chapter “Thermal Calculations of HVDC Power Cables”

The second chapter “Electric Field Calculations”

The third chapter “Life Model of HVDC cables”.

CHAPTER 1

THERMAL CALCULATIONS of HVDC POWER CABLES

1.1 Typical structure of HVDC extruded cables:

a unipolar HVDC extruded cable has a similar structure as a unipolar HVAC extruded cable which is shown in the Figure 1.1.

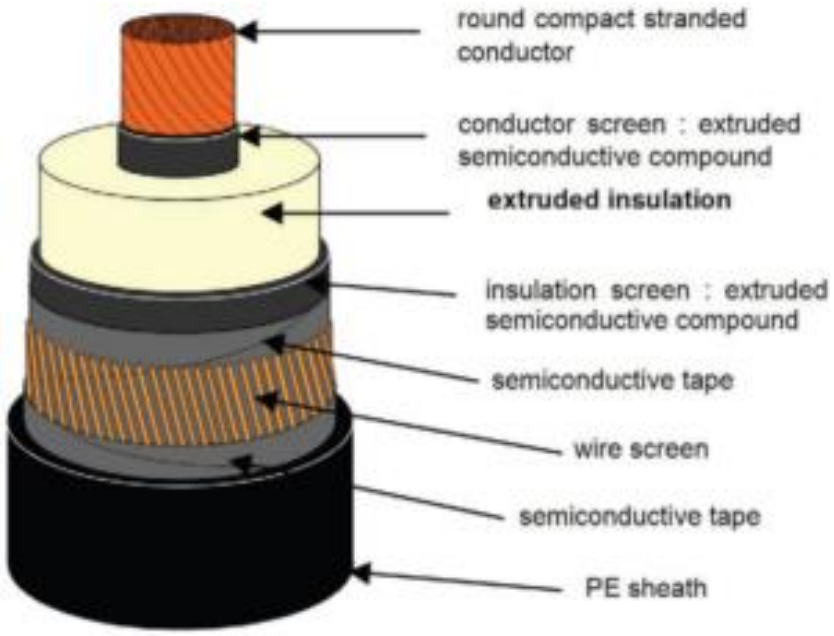

Figure 1.1 - Structure of a unipolar HVDC cable with extruded insulation.

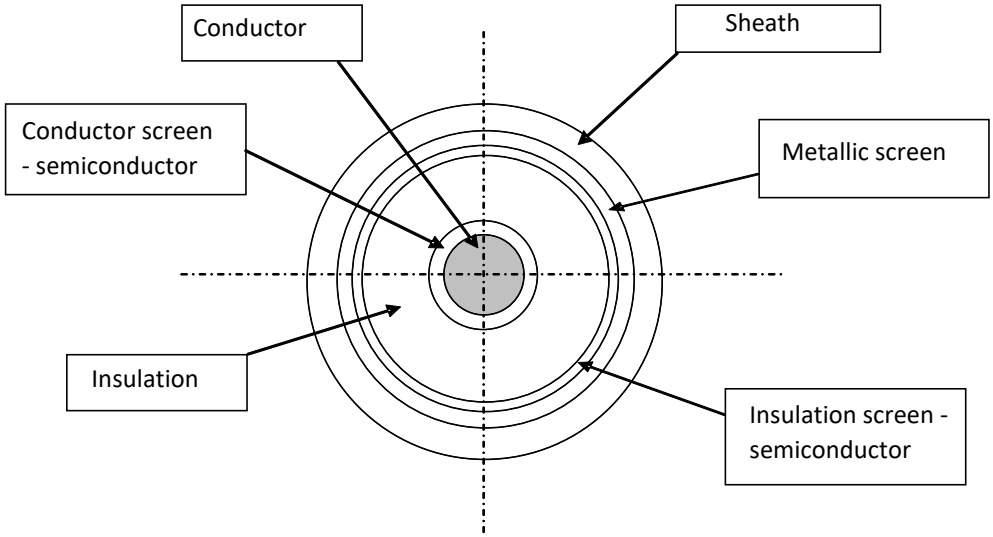

Figure 1.2 - Cross-section of a unipolar HVDC cable with extruded insulation.

The cable consists of the following layers (from the inner to the outer layer):

1) Conductor: it can be made from either copper or aluminium, which is formed in a compact arrangement of thin round wires.
2) Inner Semiconductive Layer: which is extruded directly on the conductor surface to make the electric field on the surface of the conductor as radial as possible, additionally, the semiconductive layer ensures a good adherence to the conductor, this in turn prevents microgaps formation. This layer is typically made of the same insulation material with adding carbon particles to increase its conductivity.
3) Insulation Layer: is extruded directly on the inner semiconductive layer. This layer is designed to withstand the rated voltage of the cable to isolate the active part of the cable.
4) Outer Semiconductive Layer is placed on the insulation layer and plays the same role as the Inner Semiconductive Layer does.
5) Metallic Screen: provides a mechanical strength to the cable.
6) Thermoplastic sheath: is usually made of Polyethylene (PE) (and sometimes Polyvinylcloride - PVC). This layer protects the cable from corrosion and other environmental factors.

In the case of undersea cables, another layer of steel wire (called Armoring) is added on the outer layer to enhance the mechanical strength of the cable (against external actions such as anchoring, shark bites…etc). Finally, this layer is covered with an External Sheath.

1.2 Thermal design of HVDC extruded cable:

One of the main functions of the insulation in HVDC cable is to withstand the nominal current flow (I_n) at which the temperature does not exceed the maximum permissible temperature of the insulation θ_{max}. The temperature profile inside the insulation depends on the characteristics of the insulation. As a result, the current flowing through the conductor strongly depends on the type of insulation used in the cable which is considered the most sensitive part of the cable to the electrical and thermal stresses, it is also worth noting that the insulation is the most expensive component of the HVDC cable.

The thermal calculations shown here are based on the International Electrotechnical Commission standards (IEC 60287) [1].

With regards to an XLPE extruded cable, the maximum permissible temperature in the case of continuous current flow:

$$\vartheta_{max} = 70\ ℃ \tag{1.1}$$

The ambient temperature should also be taken into account during this process, this temperature equals to the temperature of the soil which corresponds to 20 $℃$ [1], it is worth noting that the HV cables have a relatively high weight, therefore, they are usually installed either directly into the ground or in special channels unlike MV (Medium Voltage) or LV (Low voltage cables) which can be aerial :

$$\vartheta_a = 20\ ℃ \tag{1.2}$$

The temperature drop is defined as the difference between the maximum and the ambient temperatures:

$$\Delta\vartheta_{tot} = f(I) = \vartheta_{max} - \vartheta_a \tag{1.3}$$

In the case of an XLPE cable, the total temperature drop is:

$$\Delta\vartheta_{tot} = \vartheta_{max} - \vartheta_a = 50\ ℃ \tag{1.4}$$

The total temperature drop is a limit which must not be exceeded, otherwise the life of insulation decreases due to the insulation deterioration overtime.

The purpose of this thermal design is to determine the maximum current. During this process, it is necessary to define the power dissipated from the surface of the conductor into the insulation (W), in order to calculate the temperature drop $\Delta\vartheta$ in the layer R_T of the insulation using "Thermal Ohm's Law":

$$\Delta\vartheta = R_T W \tag{1.5}$$

Where:

- $\Delta\vartheta$[° C] is the temperature drop in considered layer.
- $R_T \left[\frac{℃\ m}{W}\right]$ is the thermal resistance of the considered layer.
- $W \left[\frac{W}{m}\right]$ is the thermal power per unit length that crosses the considered layer.

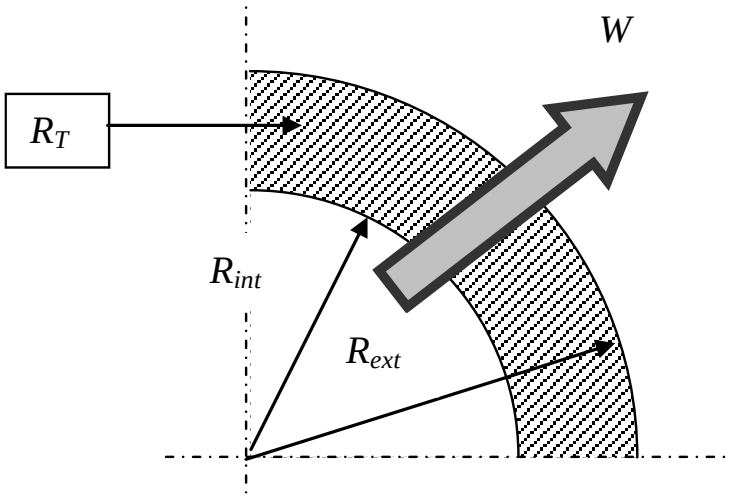

Figure 1.3 - Cross-section of one of the layers that constitutes the cable.

To derive R_T , the insulation thickness is divided into infinitesimal elements. For each infinitesimal element dx, the thermal resistance for the layer delimited between x and $x + dx$ is given by:

$$dR_T = \rho_t \frac{dx}{2\pi x} \tag{1.6}$$

Where: ρ_t is the thermal resistivity of the material of the layer.

Hereinafter, the quantities per unit length of the cable will be considered, for example, the area of a cylindrical surface of the insulation with a radius of x is $2\pi x1 = 2\pi x$.

By integrating the equation (1.6) in the range [R_{int}, R_{ext}] yields:

$$R_T = \int_{R_{int}}^{R_{ext}} \rho_T \frac{dx}{2\pi x} = \frac{\rho_T}{2\pi} ln\left(\frac{R_{ext}}{R_{int}}\right) \tag{1.7}$$

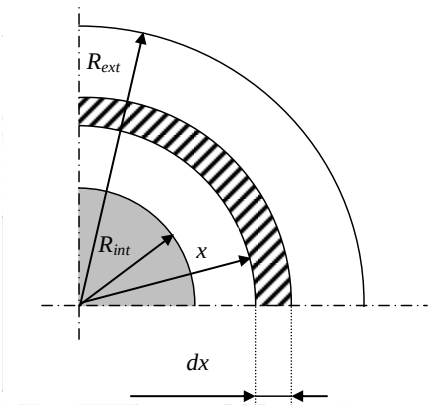

Figure 1.4 - Infinitesimal element dx of the layer that composes the cable.

in this chapter, the temperature profile will be considered not only in the cable but also until a point in the soil which has an ambient temperature ϑ_{amb} , since it is not necessary that the outer surface of the cable has the ambient temperature as it can be shown in the Figure (1.5):

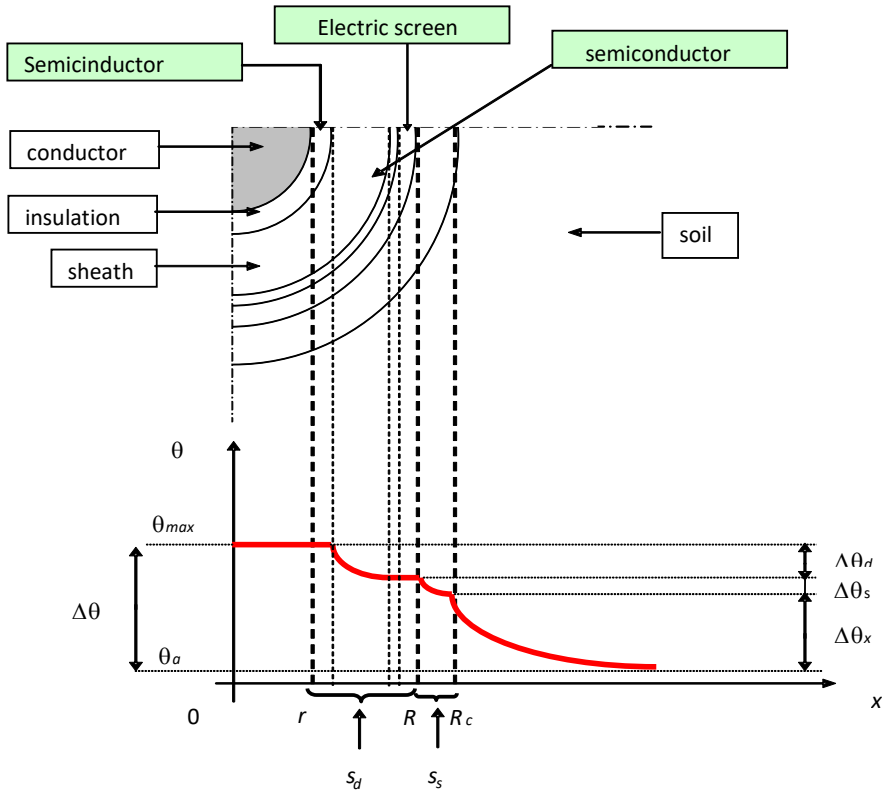

Figure 1.5 – Temperature drop in the insulation and the soil.

It is worth noting that the semiconductive layers as well as the screen are neglected in the thermal design due to their small thicknesses. As a consequence, the outer surface of the inner semiconductive layer and the inner surface of the outer semiconductive layer will only be considered rather than the conductor surface and the outer semiconductor – screen surface, respectively. Consequently, three temperature drops are introduced:

- $\Delta\theta_d \equiv$ temperature drop in the insulation layer;
- $\Delta\theta_s \equiv$ temperature drop in the thermoplastic sheath;
- $\Delta\theta_x \equiv$ temperature drop in the soil.

$$\Delta\vartheta_{tot} = \Delta\vartheta_d + \Delta\vartheta_s + \Delta\vartheta_x \tag{1.8}$$

Because the temperature drop in the soil $\Delta\vartheta_x$ is 3-5 times higher than those in the insulation $\Delta\vartheta_d$ and the sheath $\Delta\vartheta_s$, each temperature drop have to be defined individually.

It is noteworthy that in the case of alternating current (AC) there are three types of loss in the cable:

- Losses due to Joule effect in the conductor P_J .
- Dielectric losses in the insulation P_d .
- Additional Joule effect losses in the screen P_{add} due to the presence of currents generated by magnetic induction.

In DC systems, the additional losses do not take place at all, the dielectric losses in the insulation are considered negligible. As a result, In DC systems only Joule effect losses in the conductor take place.

$$P_d = P_{add} = 0 \tag{1.9}$$

1.2.1 Temperature drop in the insulation:

By applying Ohm's thermal law, the temperature drop in the insulation can be determined:

$$\Delta\vartheta_d = R_{Td}(P_J + \beta P_d) = R_{Td}\, P_J \tag{1.10}$$

Where:

- $\beta = 0.5 \div 1$ because not the whole P_d power is dissipated through the insulation thickness.
- $R_{Td} = \frac{\rho_{Td}}{2\pi} ln\left(\frac{R}{r}\right)$ is the thermal resistance of the dielectric, calculated according to (1.7).
- The power dissipated in the conductor due to Joule effect is given by:

$$P_J = R_{cc}\, I^2 \tag{1.11}$$

Where: R_{cc} is the electrical resistance of the conductor in the case of DC current operating under the maximum temperature θ_{max}.

I is the rms value of the electrical current flowing in the conductor.

By substituting (1.11) in (1.10) yields:

$$\Delta\vartheta_d = R_{Td} R_{cc} {I_n}^2 \tag{1.12}$$

1.2.2 temperature drop in the sheath:

By applying Ohm's thermal law yields:

$$\Delta\vartheta_s = R_{Ts}\left(P_J + P_d + P_{add}\right) \tag{1.13}$$

In the same way as in the dielectric, the temperature drop in the sheath can be found:

$$\Delta\vartheta_s = R_{Ts}R_{cc}{I_n}^2 \tag{1.14}$$

It is noteworthy to mention that unlike AC systems, in DC systems no induction losses in the sheath take place.

1.2.3 temperature drop in the soil:

In order to derive the temperature drop in the soil, three unipolar cables placed at a certain depth from the ground (b) separated from each other by a horizontal distance (a) as it is shown in the Figure 1.6:

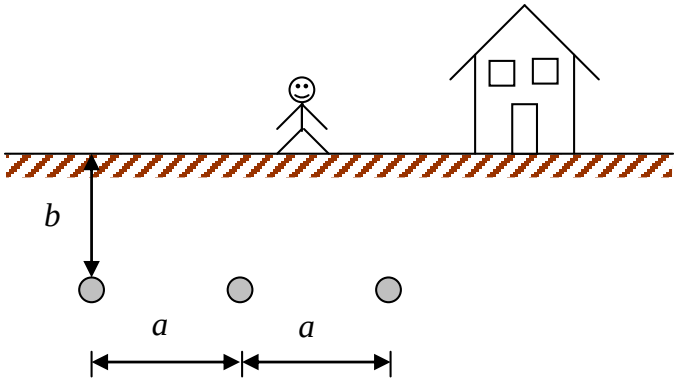

Figure 1.6 - Three unipolar cables placed at a depth (b) in the ground, and separated by a horizontal distance (a)

By applying Ohm's thermal law (1.5), the temperature drop in the soil $\Delta\vartheta_x$ can be derived:

$$\Delta\vartheta_x = R_{Tx}(P_J + P_d + P_{add}) \tag{1.15}$$

For the hottest cable of a set of three unipolar cables (as shown in Figure 1.6) center, the thermal resistance of the soil has one of the following expressions depending on the type of standarad in use:

- IEC 60287 (old version):

$$R_{Tt} = \frac{\rho_{Tx}}{2\pi}\left\{ln\left(\frac{2b - R_c}{R_c}\right) + ln\left[1 + \left(\frac{2b}{a}\right)^2\right]\right\} \quad (1.16)$$

- IEC 60287 (new version):

$$R_{Tt} = \frac{\rho_{Tx}}{2\pi}\left\{ln\left(uu + \sqrt{uu^2 - 1}\right)\right\} \quad (1.17)$$

In (1.16) and (1.17):

- *Rc* represents the outer radius of the cable expressed in meters;
- *to* represents the distance between cables (in case of more than one);
- *b* represents the burial depth;
- $uu = \frac{b}{R_c}$;
- ρ_{Tt} represents the soil thermal resistivity.

It is worth noting that the expression 1.15 is different from that of the insulation and the sheath because the soil does not have a cylindrical shape, not to mention that the fatigue rate is not the same for the the three cables (it has a higher value in the central cable than the side ones).

Based on the above-mentioned expressions, the temperature drop in the soil is expressed as the following:

$$\Delta\vartheta_x = R_{Tx}R_{cc}{I_n}^2 \quad (1.18)$$

1.2.4 total temperature drop:

The total temperature drop can be written by substituting (1.12), (1.16) in (1.8) yields:

$$\Delta\vartheta_{tot} = R_{cc}{I_n}^2[R_{Td} + R_{Ts} + R_{Tx}] \quad (1.19)$$

By rewriting the expression (1.19) one can obtain the maximum allowable current of the cable:

$$I_n = \sqrt{\frac{\Delta\vartheta_{tot}}{R_{cc}[R_{Td} + R_{Ts} + R_{Tx}]}} \quad (1.20)$$

The expressions (1.17) and (1.18) are valid only for unipolar cables, however, they can be modified to take into consideration (n) number of phases in the cable. Then, they become as the following:

$$\Delta\vartheta_{tot} = R_{cc}{I_n}^2[R_{Td} + n(R_{Ts} + R_{Tx})] \tag{1.21}$$

$$I_n = \sqrt{\frac{\Delta\vartheta_{tot}}{R_{cc}[R_{Td} + R_{Ts} + R_{Tx}]}} \tag{1.22}$$

It should be noticed that if the cable is not single-sheath, then each phase must have its own sheath, meaning the presence of (n) sheath, therefore, in this case only the soil passes the heat of all the phases (which is usually used in MV three-phase cables).

$$\Delta\vartheta_{tot} = R_{cc}{I_n}^2[R_{Td} + R_{Ts} + nR_{Tx}] \tag{1.23}$$

$$I_n = \sqrt{\frac{\Delta\vartheta_{tot}}{R_{ca}[R_{Td} + R_{Ts} + nR_x]}} \tag{1.24}$$

1.2.5 Transient temperature profile in the cable thickness:

The previous equations show a dependence of the temperature ϑ on the electrical resistance R_{cc} , However, there is a dependence of the electrical resistance R_{cc} on the temperature ϑ in all points of the cable thickness, as follows:

$$R_{cc} = \frac{\rho_{el,20℃}}{S_{eff}}[1 + \alpha_{20}(\vartheta_c - 20)] = R_{cc,20}[1 + \alpha_{20}(\vartheta_c - 20)] \tag{1.25}$$

Where: α_{20} is the temperature coefficient of the electrical resistivity at 20 ℃.

By substituting the equation (1.25) in (1.12), (1.14) and (1.18) yields:

Temperature drop in the dielectric:

$$\Delta\vartheta_d = \vartheta_c - \vartheta_s = P_J R_{Td} = R_{cc}I^2R_{Td} = R_{Td}R_{cc,20}I^2 + R_{Td}R_{cc,20}\alpha_{20}(\vartheta_c - 20)I^2 \tag{1.26}$$

Temperature drop in the sheath:

$$\Delta\vartheta_s = \vartheta_s - \vartheta_x = R_{Ts}R_{cc}I^2 = R_{Ts}R_{cc,20}I^2 + R_{Ts}R_{cc,20}\alpha_{20}(\vartheta_c - 20)I^2 \tag{1.27}$$

Temperature drop in the soil:

$$\Delta\vartheta_x = \vartheta_x - \vartheta_a = R_{Tx}R_{cc}I^2 = R_{Tx}R_{cc,20}I^2 + R_{Tx}R_{cc,20}\alpha_{20}(\vartheta_c - 20)I^2 \tag{1.28}$$

The total temperature drop in the cable and the soil can be obtained by substituting (1.26), (1.27) and (1.28) in (1.8) and manipulating the resulting expression:

$$\vartheta_c = \frac{[R_{Td} + (R_{Ts} + R_{Tx})]\xi I^2 + \vartheta_a}{1 - [R_{Td} + (R_{Ts} + R_{Tx})]\eta I^2} \tag{1.29}$$

Where: $\xi = R_{cc,20}(1 - \alpha_{20}20)$

$\eta = R_{cc,20}\alpha_{20}$

1.3 The thermal response of a cable to a current step:

The thermal response to a current step is used to calculate the transient temperature in a power cable. It depends on the thermal capacitance and resistance of the insulation layers as well as the soil. The thermal Ohm's Law is the basis of the transient temperature calculations considering the following analogies:

Electrical Ohm's Law	**Thermal Ohm's Law**
Voltage	Temperature
Current	Thermal flow
Electrical Resistance	Thermal Resistance
Electrical Capacitance	Thermal Capacitance

The method recommended for calculating the temperature response of a cable to a suddenly applied constant value of conductor current is to consider that the whole thermal circuit is divisible into two independent parts. One part is made up of the cable components out of the outer surface of the cable, the second part is the environment of the cable. The individual responses of these two parts are partial transients, with which the total transient for the. complete system can be built up.

The derivation of these two parts of the thermal circuit and the temperature transients across them are given separately in the sub-sections which follow, but the method for combining the transients will be described first.

The method of combination, due to Morello (1958), makes an allowance for the heat which accumulates in the first part of the thermal circuit and which results in a corresponding reduction in the heat entering the second part during the transient. This is done by assuming that the following ratio (the so-called *Attainment factor* $a(t)$):

$$a(t) = \frac{Heat\ emitted\ from\ the\ first\ part\ at\ time\ t\ during\ a\ transient}{Heat\ emitted\ from\ the\ first\ part\ in\ the\ steady\ state}$$

$$= \frac{Temperature\ rise\ across\ the\ first\ part\ at\ time\ t\ during\ a\ transient}{Temperature\ rise\ across\ the\ first\ part\ in\ the\ steady\ state}$$

Then, the temperature transient of the second part of the thermal circuit is composed of its response to a step function of heat input multiplied by a reduction coefficient (variable in time) equal to the attainment factor of the first part.

If the period is long enough to complete the transient in the first part of the thermal circuit, then the *attainment factor* may be assumed equal to 1. [23]

1.4 The thermal Circuit:

1.4.1 The thermal circuit of the insulation:

It can be expressed by the representation of Van Wormer's technique Figure (1.7):

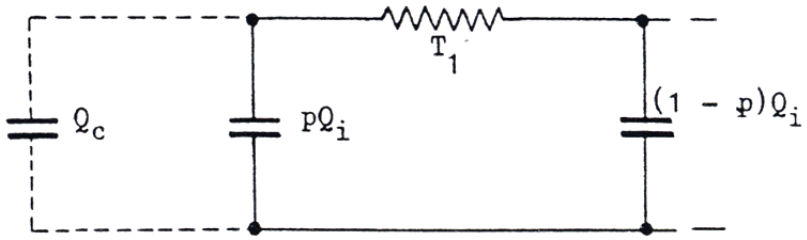

Figure 1.7 - the representation of the insulation Van Wormer's technique.

$$p = \frac{1}{2\ln\left(\frac{D_i}{d_c}\right)} - \frac{1}{\left(\frac{D_i}{d_c}\right)^2 - 1} \qquad (1.30)$$

Where:

- T_1 is the total thermal resistance of dielectric per conductor (or equivalent conductor in multi-core cable).
- Q_i total thermal capacitance of dielectric per conductor (or equivalent conductor in multi-core cable).
- D_i is the outer diameter of dielectric.
- Q_0 is the thermal capacitance of conductor.
- d_0 is the outer diameter of dielectric.

1.4.2 The thermal circuit considering the outer covering:

The cable can be represented by the following thermal circuit which considers both the insulation and the covering:

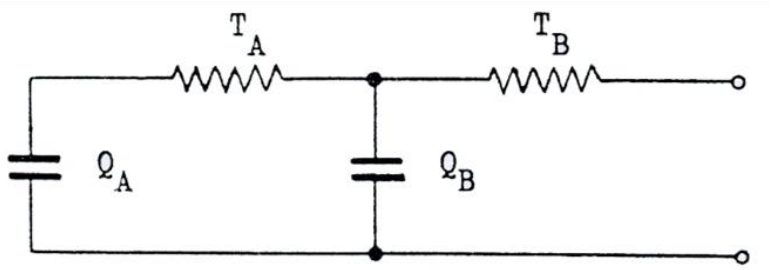

Figure 1.8 - the representation of the thermal circuit of the cable.

$$T_A = T_1 \tag{1.30}$$

$$T_B = q_s T_3 \tag{1.31}$$

$$Q_A = Q_c + pQ_i \tag{1.32}$$

$$Q_B = (1-p)Q_i + \frac{Q_s + p'Q_j}{q_s} \tag{1.33}$$

Where:

- T_3 is the thermal resistance of the outer thermoplastic sheath.
- Q_c is the thermal capacity of the equivalent conductor.
- Q_s is the thermal capacity of the electric screen.
- Q_j is the thermal capacity of the outer sheath.
- $q_s = \frac{losses\ in\ the\ conductor\ and\ the\ sheath}{losses\ in\ the\ conductor}$
- $p' = \frac{1}{2\log\left(\frac{D_e}{D_s}\right)} - \frac{1}{\left(\frac{D_e}{D_s}\right)^2 - 1}$ (1.34)
- $D_e\ and\ D_s$ are the outer and the inner diameters of the sheath.

Calculation of the response of the cable circuit:

The transient response of these cable circuits to a step function of load current is found as follows:

$$M_0 = \frac{1}{2}\left(Q_A(T_A + T_B) + Q_B T_B\right) \tag{1.35}$$

$$N_0 = Q_A T_A Q_B T_B \tag{1.36}$$

$$a = \frac{M_0 + \sqrt{{M_0}^2 + N_0}}{N_0} \tag{1.37}$$

$$b = \frac{M_0 - \sqrt{{M_0}^2 - N_0}}{N_0} \tag{1.38}$$

$$T_a = \frac{1}{a-b}\left[\frac{1}{Q_A} - b(T_A + T_B)\right] \tag{1.39}$$

$$T_b = T_A + T_B - T_a \tag{1.40}$$

the transient temperature rise of the outer surface of the cable is given by the equation:

$$\vartheta_c(t) = W_c\left[T_a(1 - e^{-at}) + T_b\left(1 - e^{-bt}\right)\right] \tag{1.41}$$

Where: W_c is the power loss per unit length in the conductor based on the maximum conductor temperature attained. W_c is assumed to be constant during the transient.

1.4.3 The thermal circuit of the laying environment:

The transient response of the cable environment is calculated by an exponential integral formula. Therefore, the transient temperature rise, $\vartheta_e(t)$, of the outer surface of the hottest cable of a group of cables, and similarly loaded, is:

$$\vartheta_e(t) = \alpha(t)\frac{\rho_{T,S}\Delta W_1}{4\pi}\left\{\left[-E_i\left(-\frac{D_e^2}{16t\delta}\right) + E_i\left(-\frac{L^2}{t\delta}\right)\right] + \sum_{k=1}^{k=N-1}\left[-E_i\left(-\frac{d_{p,k}^2}{4t\delta}\right) + E_i\left(-\frac{{d'}_{p,k}^2}{4t\delta}\right)\right]\right\} \tag{1.42}$$

Where:

- ΔW_1 is the total power loss per unit length of each cable in the group.
- $-E_i(-x)$ is the exponential integral function.
- $\alpha(t)$ is the conductor to cable surface attainment factor.
- $\rho_{T,S}$ is the soil thermal resistivity.
- D_e is the external surface diameter of the cable.
- δ is the soil thermal diffusivity.
- t is the time from the moment of application of heating.
- L is the axial depth of the burial of the hottest cable.
- $d_{p,k}$ is the distance from centre of cable k to centre of hottest cable p

- $d'_{p,k}$ is the distance from the image of the centre of the cable k to centre of hottest cable p'.
- *N* is the number of cables.

1.4.4 calculation of the total thermal transient of both the cable and the laying environment:

the complete temperature transient is given by the following equation:

$$\vartheta(t) = \vartheta_c(t) + \vartheta_e(t) \tag{1.43}$$

However, the temperature of the conductor cannot be considered constant, since it varies due to the variation of the resistance of the conductor material.

$$\vartheta_\alpha(t) = \frac{\vartheta(t)}{1 + \alpha_R(\vartheta(\infty) - \vartheta(t))} \tag{1.44}$$

Where:

- $\vartheta(t)$ is the conductor transient temperature rise above ambient without correction for variation in conductor loss, and is based on the conductor resistance at the end of the transient.
- $\vartheta(\infty)$ is the conductor steady state temperature rise above ambient.
- α_R is the temperature coefficient of electrical resistivity of the conductor material at the commencement of the transient.

CHAPTER 2

Electric Field Calculations

2.1 The Difference between HVAC and HVDC:

The electric field calculation in HVAC is much simpler than HVDC cables because in AC cables the electric field depends only on the dielectric permittivity, the geometry of the cable and the applied voltage unlike the DC systems in which the electric field depends on the electrical conductivity of the dielectric in addition to the permittivity, the geometry and the applied voltage. The difficulty in calculations lies on the fact that the electric conductivity in the dielectric depends on both the electric field and the temperature:

$$\sigma = \sigma_0 \, exp(aT + bE) \tag{2.1}$$

Where:

σ_0 = the electrical conductivity of the dielectric at 0 ° C and for an electric field equal to 0 KV/mm.

a = temperature coefficient of electrical conductivity (1/K or 1/ ° C).

b = stress coefficient of electrical conductivity (mm/kV, or m/MV).

According to (2.1) the electrical conductivity increases when the temperature increases resulting in a possible inversion in the electric field distribution (field inversion) in the cable thickness. This phenomenon depends on the values of the coefficients a and b which may take low, medium or high values. It can be noticed from (2.1) that high values of of the coefficients a and b increase the electrical conductivity resulting in field inversion inside the cable.

In other words, the electric field in HVDC cables has the same distribution as in HVAC cables under no load (which is called capacitive or Laplacian distribution) and begin to change towards the inversion after the cable is loaded and temperature increases and in turn the electrical conductivity as well in the inner part of the insulation.

Due to this aforementioned dependence, the electric field calculation in HVDC have to consider the electrical conductivity which varies with the temperature over time according to the load cycles to which the cable is subjected. On this basis, the electric field calculation is an iterative process as it can be seen later in this chapter.

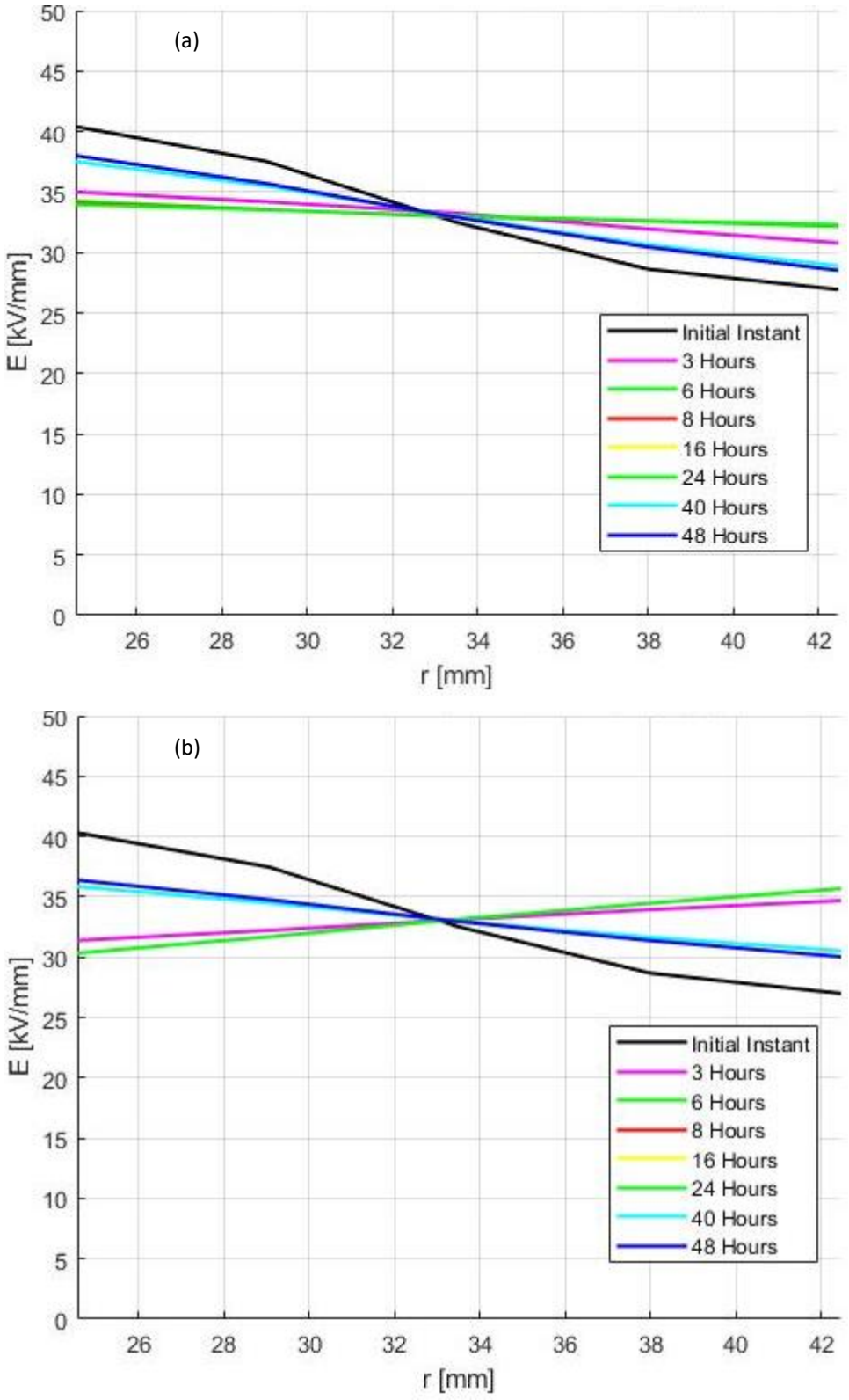

Figure 2.1 – Transient exact electric field profile during the 1'st cycle of the 48-hour Load Cycles period (LC) under the Type Test conditions at 5 points of the insulation of the sample cable for (a) a_L, b_L and (b) a_H, b_H.

2.2 Steady electric field distribution in HVDC cables:

2.2.1 Exact electric field:

To calculate the electric field distribution in HVDC cables, it is necessary to know:

- Temperature distribution ΔT_d.
- Insulation geometry (r_o, r_i).
- Field and temperature dependence of resistivity (a, b).

The temperature distribution can be calculated using "the thermal Ohm's law"

$$\Delta T(r) = T(r) - T(r_o) = \frac{W_c}{2\pi\lambda_{T,d}}\, ln\frac{r_o}{r} \tag{2.2}$$

Where: $T(r)$ and $T(r_o)$ are the temperature at the points r and r_o , respectively.

$\Delta T(r)$ is the temperature drop between the point r and the outer insulation r_o.

W_c is Joule losses in the conductor per unit length [W/m].

$\lambda_{T,d}$ is the thermal conductivity of the dielectric [W/K m].

The current density as function of the radius (r) can be expressed as follows:

$$J = \frac{I_d}{2\pi r} \tag{2.3}$$

By substituting (2.3) and (2.1) in the Ohm's law for current density yields:

$$J = \sigma E(r) = \frac{E(r)}{\rho} = \frac{I_d}{2\pi r}\rho_0\, exp[-(aT(r) + bE(r))] \tag{2.4}$$

By substituting (2.2) in (2.4) one obtains:

$$\ln\left(E(r)\frac{2\pi r}{I_d\rho_0}\right) = -aT(r_o) - \frac{aW_c}{2\pi\lambda_{T,d}}\ln\frac{r_o}{r} + bE(r) \tag{2.5}$$

By replacing:

$$A = \frac{aW_c}{2\pi\lambda_{T,d}} = \frac{a\Delta T_d}{\ln\frac{r_o}{r_i}} \tag{2.6}$$

The expression (2.5) can be rewritten in the form:

$$\ln\left(E(r)\frac{2\pi r}{I_d\rho_0}\right) = -aT(r_o) - \ln\left(\frac{r_o}{r}\right)^A + bE(r) \tag{2.7}$$

$$E(r) = U_0 \frac{r^{z-1}\, exp[-b \cdot E(r)]}{\int_{r_i}^{r_o} r^{z-1}\, exp[-b \cdot E(r)]\ dr} \tag{2.8}$$

Where:

$$z = \frac{a \cdot \Delta T_d}{ln\left(\frac{r_o}{r_i}\right)} \tag{2.9}$$

However, such an equation cannot be rewritten in a closed form, hence, the electric field can only be estimated numerically using this method. On the other hand, a closed form of the equation (2.7) can be obtained using one of two approximations:

2.2.2 The approximated expression of the electric field according to Jeroense-Morshuis [3]

In this approximation the stress coefficient of the electrical conductivity *b=0*, therefore the expression of the electric field becomes:

$$E(r) = U_0 \frac{r^{z-1}}{\int_{r_i}^{r_o} r^{z-1} dr} \tag{2.10}$$

The error in this approximation becomes significant in the presence of high electric fields because the dependence of the electric conductivity on the electric field can no longer be neglected.

2.2.3 The approximated expression of the electric field according to Eoll [2]

According to Eoll, a closed form of the electric field equation cab be derived by using the following approximation:

$$exp[bE(r)] \approx \left[\frac{eE(r)}{E_m}\right]^{-bE_m} \tag{2.11}$$

Where: *e* is the Neper number.

E_m is the mean value of the electric field in the insulation:

$$E_m = \frac{U_0}{r_o - r_i} \tag{2.12}$$

Considering (2.11) the expression (2.7) can be rewritten as follows:

$$E(r) = \left\{\frac{I_d \rho_0}{2\pi r_0}\, E_m^B \left(\frac{r}{r_o}\right)^{A-1} \quad exp[-(aT(r_o) + B)]\right\}^{\frac{1}{1+B}} \tag{2.13}$$

Where:

$$B = bE_m = \frac{bU_0}{r_o - r_i} \tag{2.14}$$

From the definition of the voltage U_0:

$$U_0 = \int_{r_i}^{r_o} E(r)dr \tag{2.15}$$

By substituting (2.15) in (2.13) one obtains:

$$U_0 = \frac{\kappa}{\delta}\left(\frac{I_d\rho_0}{2\pi r_0}\right)^{\frac{1}{1+B}}\left({r_o}^{\delta} - {r_i}^{\delta}\right) \tag{2.16}$$

Where:

$$\kappa = \left\{ E_m^B \left(\frac{1}{r_o}\right)^{A-1} exp[-(aT(r_o) + B)]\right\}^{\frac{1}{1+I}} \tag{2.17}$$

$$\delta = \frac{A+B}{1+B} = \frac{\frac{aW_c}{2\pi\lambda_{T,d}} + bE_m}{1+bE_m} = \frac{\frac{aW_c}{2\pi\lambda_{T,d}} + \frac{bU_0}{r_o - r_i}}{1 + \frac{bU_0}{r_o - r_i}} = \frac{\frac{a\Delta T_d}{\ln\frac{r_o}{r_i}} + \frac{bU_0}{r_o - r_i}}{1 + \frac{bU_0}{r_o - r_i}} \tag{2.18}$$

By substituting (2.16) in (2.13) yields:

$$E(r) = U_0 \frac{\delta}{r_o \cdot [1 - (r_i/r_o)^{\delta}]} (r/r_o)^{\delta - 1} \tag{2.19}$$

It can be noticed from the expressions (2.18) and (2.19) that the electric field is a function only of the temperature drop through the insulation but not the absolute temperature.

It is noteworthy to mention that Eoll approximation is used in the life model in this thesis.

2.3 Transient Electric Field Distribution:

The expressions (2.18) and (2.19) are valid only for steady-state DC electric field calculations, which means that neglecting the divergence caused by the difference in temperature inside the insulation thickness. However, in reality, each variation in the temperature will cause a transient which require a certain time to reach a steady state, this time is expressed as a unitless quantity called “time to stability” which is equal to 10τ where $\tau = \varepsilon\,\rho_E = \frac{\varepsilon}{\sigma_E}$ (2.20) where ε is the permittivity, ρ_E and σ_E are the electrical resistivity and the electrical conductivity, respectively.[4]

It is noteworthy to mention that both the Prequalification Test and the Type Test in the CIGRE Technical Brochure 496 considers the time to stability in load cycles, high load and zero load periods as it will be discussed later. [5]

2.3.1 Definition of Operational Stages of HVDC Cables:

According to [3], there are seven stages can be defined in HVDC cables as shown in the Figure (2.2):

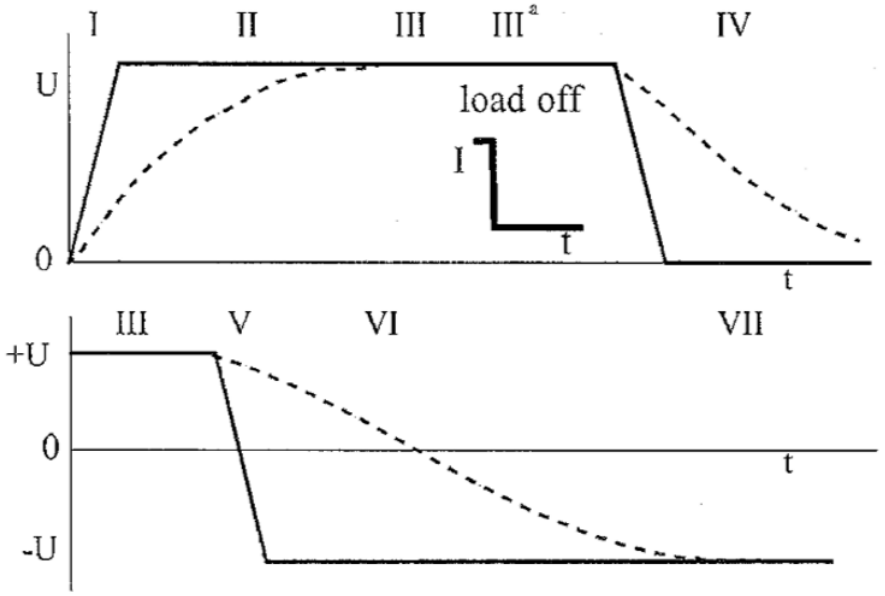

Figure 2.2 - The different stages when switching on and off a dc voltage (top) and after a polarity reversal (bottom). The dotted lines represent the growth and decay of space charges in the insulation

Stage I: Raising the voltage:

In this stage the voltage U is raised to its desired value within $\sim 1\ s$ which is much shorter than the time constant of the insulation τ. For this reason, the field in this stage is a capacitive field which can be calculated using the equation:

$$E(r) = \frac{U_0}{r\ ln\frac{r_o}{r_i}} \tag{2.21}$$

Where: U_0 is the nominal voltage.

r is a generic radius.

r_o is the outer radius of the insulation.

r_i is the inner radius of the insulation.

Stage II: The voltage has reached its final value:

The electric field in this stage changes from purely capacitive to purely resistive. The field in this stage is called "intermediate field". This field cannot be calculated analytically, instead, it has to be calculated numerically using:

Gauss law $$\nabla.(\varepsilon_o \varepsilon_r E) = \rho \quad (2.22)$$

Continuity equation $$\nabla.J = -\frac{\partial \rho}{\partial t} \quad (2.23)$$

Ohm's law $$J = \sigma E \quad (2.24)$$

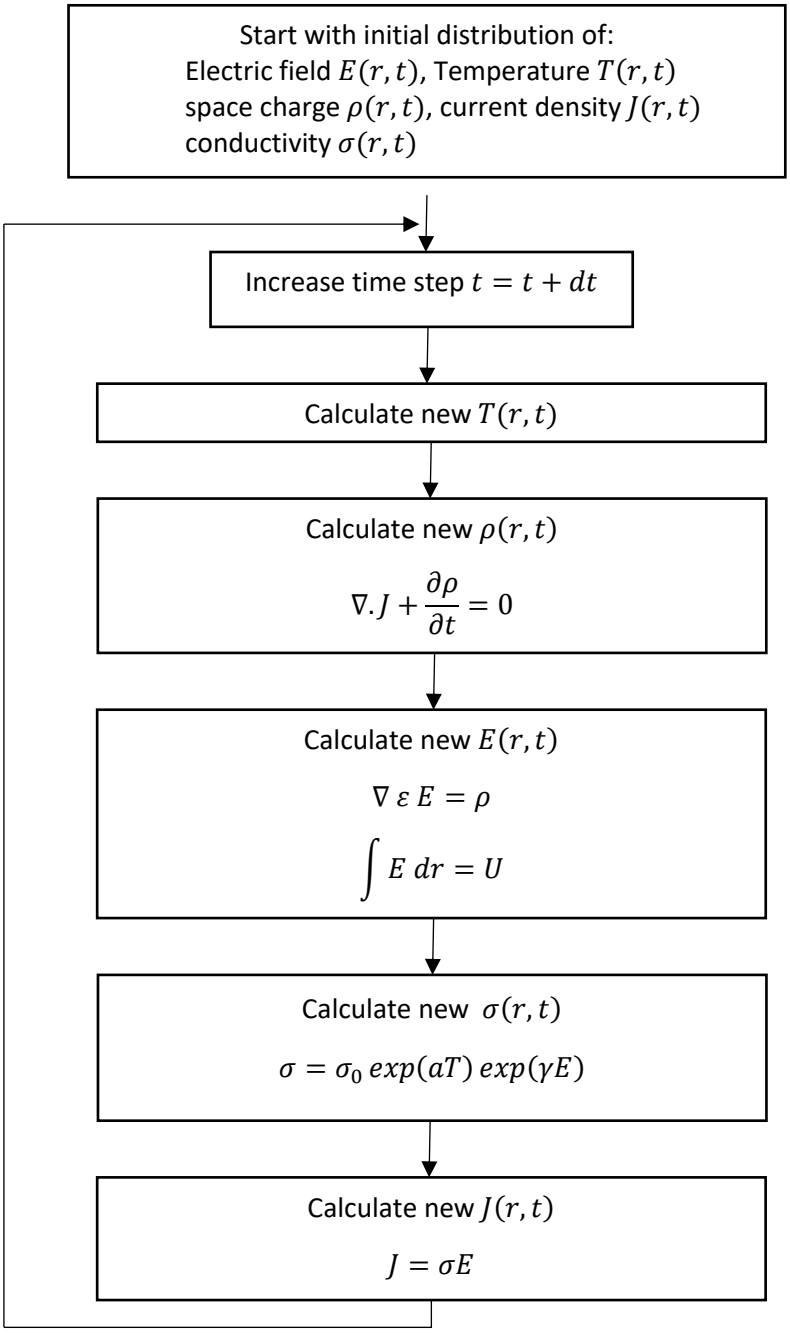

Figure 2.3 - Flow chart of the numerical method of the electric field calculation according to [3].

Stage III: Stable resistive field:

In this stage, the electric field becomes purely resistive which means that it no longer varies with time. Therefore, the analytical closed form of the electric field calculation (2.8) and (2.9) can be used provided that field inversion phenomenon may take place due to the variation in the electrical conductivity σ according to the values of the stress and temperature coefficients of the electrical conductivity a and b.

$$E(r) = U_0 \frac{r^{z-1}\, exp[-b \cdot E(r)]}{\int_{r_i}^{r_o} r^{z-1}\, exp[-b \cdot E(r)]\; dr} : \quad z = \frac{a \cdot \Delta T_d}{ln\left(\frac{r_o}{r_i}\right)} \qquad (2.8)(2.9)$$

In this thesis in addition to the exact electric field calculations, the simplified expression of the analytical closed form according to Eoll approximation (2.19) is also used to calculate the electric field for the sake of comparison.

Furthermore, the space charge can be derived as follows:

$$\nabla \cdot J = -\frac{\partial \rho}{\partial t} \rightarrow \frac{\partial}{\partial t} = 0\ (steady) \rightarrow \nabla \cdot J = 0 \qquad (2.25)$$

$$\nabla \cdot D = \rho \rightarrow D = \varepsilon_0 \varepsilon_r E \rightarrow \nabla \cdot (\varepsilon_0 \varepsilon_r E) = \rho \rightarrow \nabla \cdot \left(\frac{\varepsilon_0 \varepsilon_r}{\sigma} J\right) : \qquad (2.26)$$

$$J \cdot \nabla\left(\frac{\varepsilon_0 \varepsilon_r}{\sigma}\right) + \left(\frac{\varepsilon_0 \varepsilon_r}{\sigma}\right) \nabla \cdot J = \rho \qquad (2.27)$$

$$\sigma E \cdot \nabla\left(\frac{\varepsilon}{\sigma}\right) = \rho \qquad (2.28)$$

As a result, in this stage the considered space charge is only that due to discontinuities of permittivity and conductivity.

Stage III[a]: Stable resistive field: special case when the load current is switched off.

Stage IV: The applied voltage is reduced to zero.

Stage V: Voltage reversal has been initiated to achieve power reversal in case of CSC (Current-Source Converters) but voltage is still positive (from +U_o.)

Stage VI: Voltage has been reversed but the electric field is not stable yet.

Stage VII: Voltage has been reversed and the electric field becomes stable.

The explanation of the other operational stages is omitted for the sake of brevity since they are not considered in the model in this thesis.

2.3.2 Implementation of the transient electric field calculation in MATLAB:

The voltage is considered constant throughout the whole period. In this study, the simulation is separately carried out under two voltages for the sake of comparison:

1. The rated voltage U_o. (Normal operation)
2. Voltage equal to $1.85U_o$. (Electrical Type Test according to [5]).

The space charge accumulation phenomenon is neglected in this study. However, this space charges cause aging in the extruded cables especially for high voltage levels.

The current varies over time to impose a certain temperature profile in the 24-h and 48-hour Load Cycles of the Electrical Type Test according to CIGRÉ Technical Brochure 496 [5].

The Electrical Type Test according to CIGRÉ Technical Brochure 496 consists of a series of Load Cycles (LC) with DC voltage U_T=1.85 U_0 (rated voltage) are applied in three stages, i.e.:

- 12 cycles lasting 24 hours each with a negative polarity of the applied voltage (12 days).
- 12 cycles lasting 24 hours each with a positive polarity of the applied voltage (12 days).
- 3 cycles lasting 48 hours each with a positive polarity of the applied voltage (3×48 h=6 days).

It is worth noting that in this study the polarity of the applied voltage is always considered positive for all Load Cycles because the effect of space charges is neglected. Furthermore, positive polarity was selected for the “48 hours” load cycles as this is believed to be the most stringent condition for accessories.

According to CIGRÉ Technical Brochure 496, Load Cycles are of two types [5]:

1) A 24-hour Load Cycle consists of 8 hours heating (with steady conductor temperature equal to the rated one during at least the last 2 hours), followed by 16 hours of natural cooling.
2) A 48-hour Load Cycle consists of 24 hours heating (with steady conductor temperature equal to the rated one during at least the last 18 hours), followed by 24 hours of natural cooling.

2.3.2.1 The algorithm of transient electric field calculation:

The electric field is calculated numerically depending on the Maxwell's equations as discussed in the stage II of the operational stages of HVDC cables according to [3]. The algorithm used in this study to calculate the transient electric field is mentioned in [6].

The first step: initialization of the following quantities:

1. Temperature *T(r,0)* is defined using the temperature profile in a generic point *r* in the insulation at the initial instant *t=0*, this temperature is equal to the ambient temperature:

$$T(r,0) = T_{amb} = 20°C \tag{2.25}$$

2. Initial distribution of the electric field in the insulation thickness *E(r,0)* is considered a capacitive field (Laplacian field) which can be calculated from (2.21).
3. Initial distribution of the space charge density is considered zero inside the insulation:

$$\rho(r,0) = 0 \tag{2.26}$$

4. Initial distribution of the electrical conductivity in the insulation thickness is a function of both the initial distributions of the temperature and the electric field:

$$\sigma(r,0) = \sigma_0\, exp[aT(r,0) + bE(r,0)] \tag{2.27}$$

5. Initial distribution of the current density can be calculated from the initial distributions of both the electric field and the electrical conductivity.

$$J(r,0) = \sigma(r,0)\, E(r,0) \tag{2.28}$$

The second step is to increase the time by a certain time step *dt*:

$$t(i) = t(i-1) + dt \tag{2.29}$$

and to update the temperature value to that of the next time step:

$$T(r,t_{i-1}) \rightarrow T(r,t_i) \tag{2.30}$$

This iteration which includes the iteration mentioned in the third step continues until the last instant of the period.

The third step (for the instant *i* and the temperature *T(i)*) is calculating the transient electric field iteratively until the difference between the electric field in the current and the last step becomes equal to or lower than 0.1%. This process includes:

1. Recalculate the space charge density $\rho(r, t(i), k)$ using the equation (2.23).
2. Recalculate the electric field $E(r, t(i), k)$ using the equation (2.22).
3. Recalculate the electrical conductivity $\sigma(r, t(i), k)$ using the equation (2.1).
4. Recalculate the current density $J(r, t(i), k)$ using the equation (2.24).

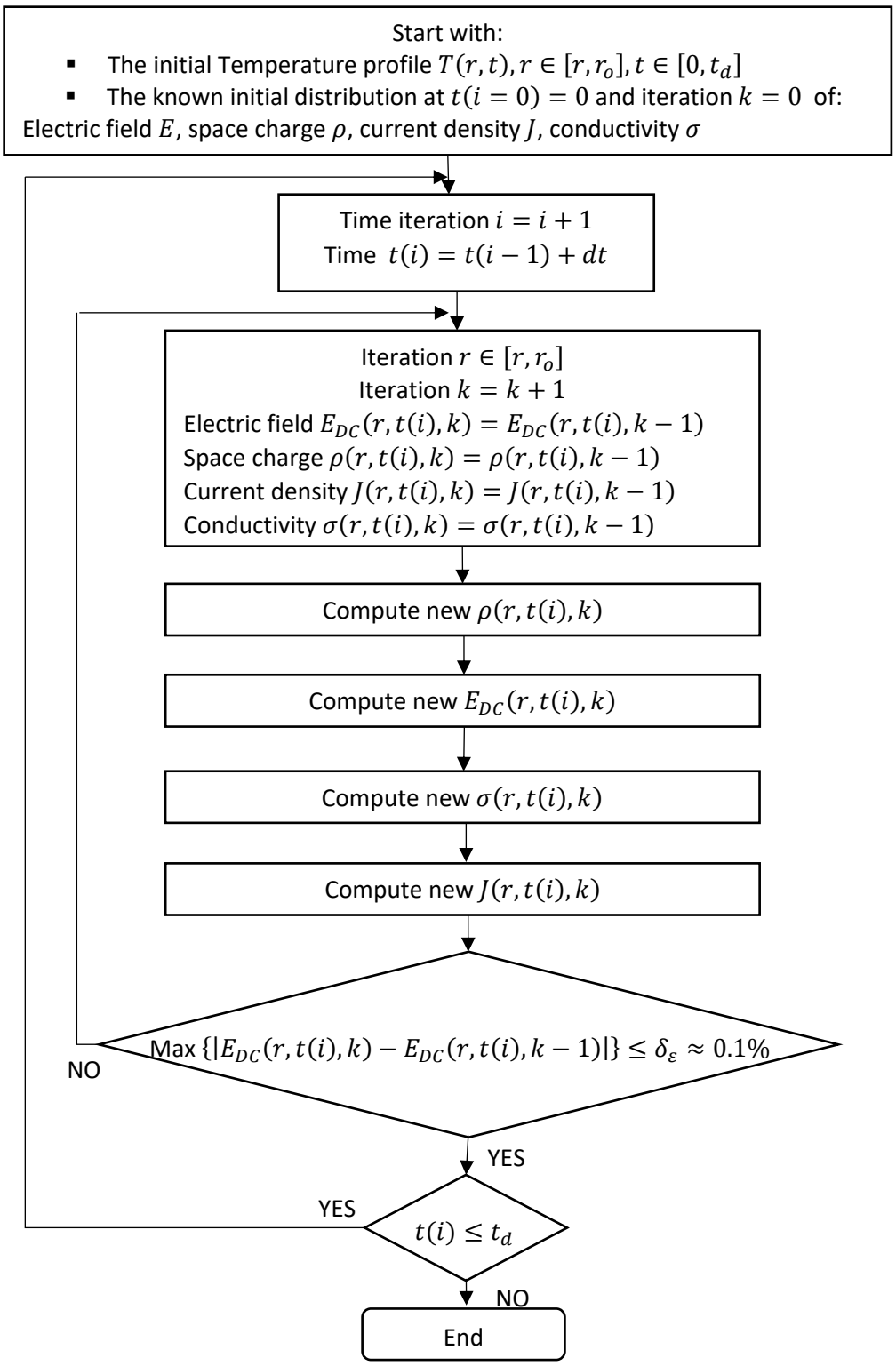

Figure 2.4 - Flow chart of the numerical method of the transient electric field calculation.

2.3.2.2 Electric field convergence test:

It can be noticed from the Figure (2.1) that the beginning points of the five cycles are not the same especially in the first cycle because the Eoll approximation is applied to calculate the electric field at the first instant. For this reason, five consecutive cycles of the Load Cycles are calculated to observe the convergence of the algorithm which occurs only if the difference between the electric field calculated using Eoll and the electric field calculated iteratively become lower than 0.1%.

CHAPTER 3

Life Model of HVDC cables

3.1. Introduction:

insulations in power systems are subjected to a progressive aging process which is an irreversible change of the material properties and this may lead to the breakdown in which the insulation is no longer able to withstand the applied stress. The time required to reach the breakdown is called “time-to-failure”, alternatively called “insulation life”. [7]

Life modelling means the modelling of the expected life of the insulation, this includes finding out the relationship between insulation life and stresses.

$$L\,(S_1, S_2, \ldots, S_N) = f\,(S_1, S_2, \ldots, S_N;\ p_1, p_2, \ldots .P_M) \quad (3.1)$$

Where L is the insulation life, $(S_1, S_2, \ldots, S_N)$ are the stresses to which the insulation is subjected, $(p_1, p_2, \ldots .P_M)$ are the parameters of the model.
Generally speaking, those stresses can be classified as:

- Electrical stress: due to the applied electric field.
- Thermal stress.
- Mechanical stress: static (bending, compression) or dynamic (vibration).
- Environmental stress (pollution, humidity, solar and cosmic radiation, corrosion)

However, the stresses of interest in the extruded insulation are only the electrical and the thermal stresses since both voltage and temperature are progressively applied on the insulation in HVDC extruded cables. Furthermore, the aging effect of the electrical stress is more important than that of the thermal stress especially in MV and HV cables where the electric field is relatively high.

The parameters of the life model can be derived by applying the best-fitting techniques on the so-called Accelerated Life Tests which aims at reducing the test duration from the real duration (40 years) to an acceptable test duration (1 month). This acceleration can be achieved by increasing the stress value to be higher than that under the normal conditions. For the sake of generality of the model, the extrapolation is used to keep the relationship between life and stresses constant even for stress values lower than values under the test conditions. [8]

Two approaches have been proposed for the life model of HVDC cables:

1) The macroscopic (phenomenological) approach: This approach depends only on the description of aging. It has been used to fit parameters in the accelerated life tests.

2) The microscopic (physical) approach: it is an advance in the phenomenological approach. This approach considers the loss of life due to the localized degradation because of the space charge accumulation in microdefects (voids, protrusions …etc) inside the insulation bulk which in turn leads to either a failure or a different aging mechanism. [8]

It is worth noting that the general complete model (which accurately describes all relationships between the life and all possible stresses in the insulation bulk) does not exist in the literature since impurities formation is probabilistic and charge density dynamics are dependent on multiple probabilistic factors, such as the amplitude and duration of the applied electric field, temperature, moisture content, electrode material, interface condition between conductor and polymer, geometry of the polymer and material properties, chemical composition, morphology, impurities and additives, and aging status.[9] However, many advances in the life model of HVDC cables have been achieved in the literature [10-17].

Due to the randomness of the breakdown process, it can be argued that the *life* (*time to failure)* of the insulation is a random variable which is always dependent on the *failure probability*. In other words, the failure process is stochastic even for all specimen manufactured using the same techniques and are subjected to the same operating conditions. The results of the past experiments have shown that the Weibull distribution is the best distribution to represent the relationship between the time to failure and the failure probability [8].

3.2. Life Models of the HVDC Cables:

3.2.1 Life Model considering only the thermal stress (Arrhenius model):

The Arrhenius life model is the most common model to represent the temperature effect on the degradation of the insulating materials (according to Dakin's theory) [18]:

$$L(T) = L_0 \, exp\left[-B\left(\frac{1}{T_0} - \frac{1}{T}\right)\right] \tag{3.1}$$

Where:

- $L(T)$ is the thermal life of the insulation at the absolute reference temperature T_0.
- $B = \Delta W / K_B$, ΔW is the activation energy of the main thermal degradation reaction, $K_B = 1.38 \times 10^{-23}\, J/K$ is the Boltzmann constant.
- L_0 is the life at the reference temperature T_0.

The Arrhenius life equation has 2 parameters L_0 and B (L_0 is considered a parameter because T_0 must be known in advance). The life according to Arrhenius is represented in the so-called Arrhenius graph which has the coordinates *log(life)* versus *-1/T*.

It can be noticed in the figure (3.1) that the higher the coefficient *B*, the better the insulation. Therefore, the insulation having an activation energy *B1* is better than the one which has an activation energy *B2*.

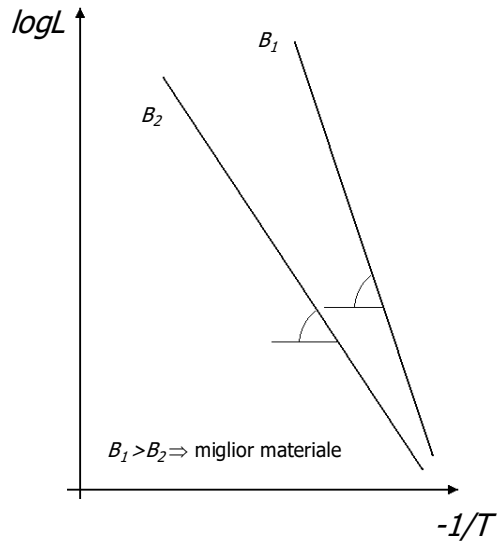

Figure 3.1 – Arrhenius graph in the coordinates *log(life)* vs *-1 / T*.

Arrhenius expression (3.1) can be expressed in a compact way as follows:

$$L(T) = L_0 \, exp[-BT'] \tag{3.2}$$

Where:

$$T' = \frac{1}{T_0} - \frac{1}{T} \tag{3.3}$$

Arrhenius life model is valid only in the absence of the electrical stress (which means that there is no voltage applied on the cable). Thus, the Arrhenius model parameters can only be determined through a test carried out in an oven.

3.2.2 Life Model considering only the electrical stress (Inverse Power Model - IPM model):

IPM is a phenomenological model used to express a relationship between the life of the insulation *L* and the electric field *E* (or the voltage *U*). This model can be expressed in two forms according to the reference parameter:

a) The maximum electric field applied during the test E_H

$$L(E) = L_H \left(\frac{E}{E_H}\right)^{-n} \tag{3.4}$$

Where:

- $L(E)$ is the life corresponding to the electric field E.
- L_H is the life corresponding to the electric field E_H.
- *n* is the voltage endurance coefficient (VEC).

b) The reference electric field of the cable E_0 (the design electric field or the electric field bellow which the aging process caused by the electric field is negligible):

$$L(E) = L_0 \left(\frac{E}{E_0}\right)^{-n} \tag{3.5}$$

Where:

- $L(E)$ is the life corresponding to the electric field E.
- L_0 is the life corresponding to the electric field E_0.
- *n* is the voltage endurance coefficient (VEC).

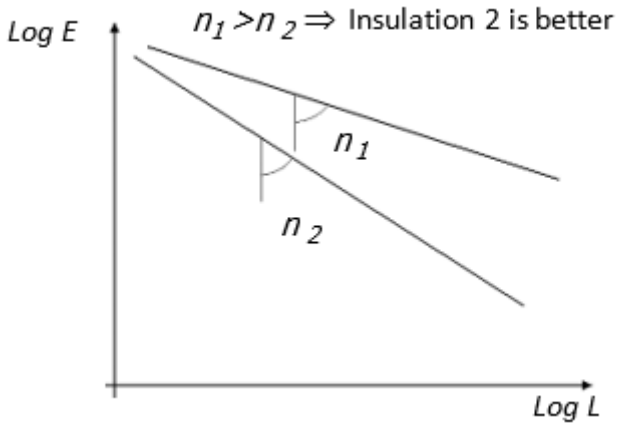

Figure 3.2 – Inverse Power Model (IPM) in (*log E*) versus (*log L*) coordinates.

It is noteworthy to mention that the equations (3.4) and (3.5) are valid only in the absence of the thermal stress. Therefore, the above-mentioned equations are valid only for a constant temperature which may be either the ambient temperature or the nominal operating temperature, in this case the parameters L_0 and n must be recalculated at the considered temperature.

3.2.3 Life Model considering both electrical and thermal stresses – the Electrothermal model (Arrhenius-IPM):

Arrhenius-IPM model is a combination between both Arrhenius and IPM models to consider both the electrical and the thermal stresses (the electrothermal stress).

The proposed expression in the literature is based on the IPM expression (since the electrical stress has a major effect on the degradation process especially in the MV and HV) considering the non-negligible effect of the thermal stress on the insulation. This model can be expressed as follows [19]:

$$L(E,T) = L_0 \left(\frac{E}{E_0}\right)^{-(n_0 - b_{ET}T')} exp[-BT'] \tag{3.6}$$

Where:

- $L(E,T)$ is the life corresponding to the electric field E at the temperature T.
- L_0 is the life corresponding to the reference electric field E_0 and the reference temperature T_0.
- n_0 is the value of VEC at the reference temperature T_0.
- b_{ET} represents the synergism between the electrical and thermal stress.
- $B = \Delta W / K_B$, ΔW is the activation energy of the main thermal degradation reaction, $K_B = 1.38 \times 10^{-23}\ J/K$ is the Boltzmann constant.
- $T' = \frac{1}{T_0} - \frac{1}{T}$

It can be noticed from the equation (3.6) that the value $b_{ET} = 0$ corresponds to the highest synergism and the increase in $b_{ET} > 0$ will reduce the synergism because the exponent $(n_0 - b_{ET}T')$ goes down.

Since the life of insulations has a stochastic nature, it can be expressed as a probabilistic function using a probability distribution function, Weibull probability distribution function is the best one to be used in the case of polymeric insulations [20].

$$P(t_F, E, T) = 1 - exp\left\{-\left[\frac{t_F}{\alpha_t(E,T)}\right]^{\beta_t}\right\} \tag{3.7}$$

Where:

- t_F is the P-th percentile of the electrothermal life (time-to-failure).

- α_t is the scale parameter of Weibull probability distribution of the life. It corresponds to the 63.2-th percentile of the life.
- β_t is the shape parameter of Weibull probability distribution of the life

By definition, the reliability is the probability of no failure before the time t_F and is expressed as the complement to 1 of the failure probability at the time t_F. Therefore, it can be expressed as follows:

$$R(t_F, E, T) = 1 - P(t_F, E, T) = exp\left\{-\left[\frac{t_F}{\alpha_t(E,T)}\right]^{\beta_t}\right\} \tag{3.8}$$

The failure rate can be calculated using the hazard function:

$$h(t_F, E, T) = -\frac{R'(t_F, E, T)}{R(t_F, E, T)} = \frac{\beta_t}{\alpha_t(E,T)}\left[\frac{t_F}{\alpha_t(E,T)}\right]^{\beta_t - 1} \tag{3.9}$$

The life model of the insulation can be derived from (3.7):

$$t_F = [-\ln(1-P)]^{1/\beta_t}\alpha_t(E,T) \tag{3.10}$$

By substituting $\alpha_t(E,T)$ in (3.10) with $L(E,T)$ in (3.6) yields:

$$t_F = [-\ln(1-P)]^{1/\beta_t}\alpha_0\left(\frac{E}{E_0}\right)^{-(n_0 - b_{ET}T')} exp[-BT'] \tag{3.11}$$

Where: α_0 corresponds to a 63.2-th percentile of failure probability.

The parameters of the model (3.11) can be determined by tests performed in the laboratory on specimens of the considered power cable. Then, those parameters are extrapolated to consider the full-scale power cable by considering the Dimensional Factor D [21].

$$\begin{gathered} L_D = L_T\left[\frac{1}{D}\cdot\frac{ln(1-P_D)}{ln(1-P_T)}\right]^{\frac{1}{\beta_t}} \\ D \approx \frac{l_D}{l_T}\left(\frac{r_D}{r_T}\right)^2 \end{gathered} \tag{3.12}$$

Where:

- P_D is the failure probability for the full-scale cable.
- P_T is the failure probability for the specimens in the test.
- l_D, r_D is the length of the power cable and the radius of the conductor, respectively.
- l_T, r_T is the length of the specimen and the radius of the conductor, respectively.

Calculating the life from the equation (3.6) would be difficult because the parameter L_0 is not easy to be determined. Thus, it would be practical to express the life L as a function of the design life L_D which is easy to be determined.

$$L(E_D, T_D) = L_0 \left(\frac{E_D}{E_0}\right)^{-(n_0 - b_{ET} T_D')} exp[-BT_D'] \tag{3.13}$$

Where $T_D' = \frac{1}{T_0} - \frac{1}{T_D}$

$$\frac{L(E,T)}{L(E_D,T_D)} = \left(\frac{E}{E_0}\right)^{-n_0} \left(\frac{E}{E_0}\right)^{b_{ET}T'} \left(\frac{E_D}{E_0}\right)^{n_0} \left(\frac{E_D}{E_0}\right)^{-b_{ET}T_D'} exp[-B(T' - T_D')] \tag{3.14}$$

$$L(E,T) = L_D \left(\frac{E}{E_0}\right)^{-n_0} \left(\frac{E}{E_0}\right)^{b_{ET}T'} \left(\frac{E_D}{E_0}\right)^{n_0} \left(\frac{E_D}{E_0}\right)^{-b_{ET}T_D'} exp[-B(T' - T_D')] =$$

$$= L_D \left(\frac{E}{E_D}\right)^{-n_0} \left(\frac{E}{E_0}\right)^{b_{ET}T'} \left(\frac{E_D}{E_0}\right)^{-b_{ET}T_D'} exp[-B(T' - T_D')] =$$

$$= L_D \left(\frac{E}{E_D}\right)^{-n_0} \left(\frac{E}{E_0}\right)^{b_{ET}\left(\frac{1}{T_0} - \frac{1}{T}\right)} \left(\frac{E_D}{E_0}\right)^{-b_{ET}\left(\frac{1}{T_0} - \frac{1}{T_D}\right)} exp\left[-B\left(\frac{1}{T_0} - \frac{1}{T} - \frac{1}{T_0} + \frac{1}{T_D}\right)\right] =$$

$$= L_D \left(\frac{E}{E_D}\right)^{-n_0} \left(\frac{E}{E_0}\right)^{b_{ET}\left(\frac{1}{T_0} - \frac{1}{T}\right)} \left(\frac{E_D}{E_0}\right)^{-b_{ET}\left(\frac{1}{T_0} - \frac{1}{T_D}\right)} exp\left[-B\left(\frac{1}{T_D} - \frac{1}{T}\right)\right] \tag{3.15}$$

$$L(E,T) = L_D \left(\frac{E}{E_D}\right)^{-n_0} \left(\frac{E}{E_D}\frac{E_D}{E_0}\right)^{b_{ET}\left(\frac{1}{T_0} - \frac{1}{T}\right)} \left(\frac{E_D}{E_0}\right)^{-b_{ET}\left(\frac{1}{T_0} - \frac{1}{T_D}\right)} exp\left[-B\left(\frac{1}{T_D} - \frac{1}{T}\right)\right] =$$

$$= L_D \left(\frac{E}{E_D}\right)^{-n_0} \left(\frac{E}{E_D}\right)^{b_{ET}\left(\frac{1}{T_0} - \frac{1}{T}\right)} \left(\frac{E_D}{E_0}\right)^{\frac{b_{ET}}{T_0}} \left(\frac{E_D}{E_0}\right)^{-\frac{b_{ET}}{T}} \left(\frac{E_D}{E_0}\right)^{-\frac{b_{ET}}{T_0}} \left(\frac{E_D}{E_0}\right)^{\frac{b_{ET}}{T_D}} exp\left[-B\left(\frac{1}{T_D} - \frac{1}{T}\right)\right]$$

$$= L_D \left(\frac{E}{E_D}\right)^{-n_0} \left(\frac{E}{E_D}\right)^{b_{ET}\left(\frac{1}{T_0} - \frac{1}{T}\right)} \left(\frac{E_D}{E_0}\right)^{b_{ET}\left(\frac{1}{T_D} - \frac{1}{T}\right)} exp\left[-B\left(\frac{1}{T_D} - \frac{1}{T}\right)\right] \tag{3.16}$$

By defining VEC at the design temperature $n_D = n_0 - b\left(\frac{1}{T_0} - \frac{1}{T_D}\right)$, one gets:

$$L(E,T) = L_D \left(\frac{E}{E_D}\right)^{-n_0} \left(\frac{E}{E_D}\right)^{b_{ET}\left(\frac{1}{T_0} - \frac{1}{T}\right)} \left(\frac{E_D}{E_0}\right)^{b_{ET}\left(\frac{1}{T_D} - \frac{1}{T}\right)} exp\left[-B\left(\frac{1}{T_D} - \frac{1}{T}\right)\right] =$$

$$= L_D \left(\frac{E}{E_D}\right)^{-\left[n_0 - b_{ET}\left(\frac{1}{T_0} - \frac{1}{T}\right)\right]} \left(\frac{E_D}{E_0}\right)^{b_{ET}\left(\frac{1}{T_D} - \frac{1}{T}\right)} exp\left[-B\left(\frac{1}{T_D} - \frac{1}{T}\right)\right] =$$

$$= L_D \left(\frac{E}{E_D}\right)^{-\left[n_0 - b_{ET}\left(\frac{1}{T_0}-\frac{1}{T_D}+\frac{1}{T_D}-\frac{1}{T}\right)\right]} \left(\frac{E_D}{E_0}\right)^{b_{ET}\left(\frac{1}{T_D}-\frac{1}{T}\right)} exp\left[-B\left(\frac{1}{T_D}-\frac{1}{T}\right)\right] =$$

$$= L_D \left(\frac{E}{E_D}\right)^{-\left[n_0 - b_{ET}\left(\frac{1}{T_0}-\frac{1}{T_D}\right)-b\left(\frac{1}{T_D}-\frac{1}{T}\right)\right]} \left(\frac{E_D}{E_0}\right)^{b_{ET}\left(\frac{1}{T_D}-\frac{1}{T}\right)} exp\left[-B\left(\frac{1}{T_D}-\frac{1}{T}\right)\right] =$$

$$= L_D \left(\frac{E}{E_D}\right)^{-\left[n_D - b_{ET}\left(\frac{1}{T_D}-\frac{1}{T}\right)\right]} \left(\frac{E_D}{E_0}\right)^{b_{ET}\left(\frac{1}{T_D}-\frac{1}{T}\right)} exp\left[-B\left(\frac{1}{T_D}-\frac{1}{T}\right)\right] \quad (3.17)$$

$$L(E,T) = L_D \left(\frac{E}{E_D}\right)^{-[n_D - b_{ET}T'']} \left(\frac{E_D}{E_0}\right)^{b_{ET}T''} exp[-BT''] \quad (3.18)$$

it is also possible to express the life with reference to the failure probability P_D using Weibull probability distribution as follows:

$$t_{D,F}\,(E,T) = \left[\frac{-ln\,(1-F)}{-ln\,(1-\,P_D)}\right]^{1/\beta_t} L_D \left(\frac{E}{E_D}\right)^{-[n_D - b_{ET}T'']} \left(\frac{E_D}{E_0}\right)^{b_{ET}T''} exp[-BT''] \quad (3.19)$$

Where:

- $t_{D,F}\,(E,T)$ is the time-to-failure (or the life) of the cable with reference to the design parameters.
- F the desired failure probability.
- P_D the design failure probability.

The equation (3.19) can be simplified if $F = PD$ to be:

$$t_{D,F}\,(E,T) = L_D \left(\frac{E}{E_D}\right)^{-[n_D - b_{ET}T'']} \left(\frac{E_D}{E_0}\right)^{b_{ET}T''} exp[-BT''] \quad (3.20)$$

The Miner's Law:

Due to the regular repetition of the load cycles during the Type Test, it can be acceptable to consider the stresses constant according to Miner's Law in cumulative damage. This can be achieved by dividing the insulation life into M equal intervals corresponding to the load cycles. Miner's law is expressed as follows:

$$L = M \cdot t_D \quad (3.21)$$

Where: M is the number of the load cycles to failure, t_D is the duration of the load cycle, L is the life (or time-to-failure).

By dividing each t_D into *N* intervals representing the current step in the load cycle (i.e. Loading period, High Load, Zero Load), Δt_i can be expressed in this form $\Delta t_i = t_D/N$.

Each Δt_i is divided into infinitesimal intervals during which both the electric field and the temperature is considered constant, then the loss of life of the insulation can be written in the form:

$$dLF = dLF(E_i(t), T_i(t)) = \frac{dt}{L[E_i(t), T_i(t)]} \tag{3.22}$$

The loss of life during the step *i* (or LF_i) is calculated by applying (3.13) on each infinitesimal interval dt of each step of the cycle replacing $\Delta t_i = 1$ (since the sum of loss of life fractions during Δt_i is equal to 1):

$$LF_i = \int_0^{\Delta t_i} \frac{dt}{L[E_i(t), T_i(t)]} \tag{3.23}$$

$$\int_0^{L} dLF = M \sum_{i=1}^{N} \left\{ \int_0^{\Delta ti} dLF(E_i(t), T_i(t)) \right\} = M \sum_{i=0}^{N} LF_i = 1 \tag{3.24}$$

Where *M* can be written in the form:

$$M = \left(\sum_{i=0}^{N} LF_i \right)^{-1} \tag{3.25}$$

The life of cable corresponds to the life of the points in the cable which has the shortest life (the so-called hot spots)

It can be easily noticed that the equation (3.16) can only be calculated numerically because of the integral in the expression. Thus, a simplified approach can be proposed to make the calculations faster and less time-consuming. This can be achieved by neglecting the transient of both the temperature and the electric field (which means that it is assumed that the temperature and the electric field are known and constant during the *i-th* step of the load cycle). Then, the equation (3.14) can be simplified to be written in the form:

$$LF_{i,\infty} = \int_0^{\Delta ti} \frac{dt}{L[E_{i,\infty}, T_{i,\infty}]} = \frac{\Delta t_i}{L[E_{i,\infty}, T_{i,\infty}]} = \frac{t_D}{L[E_{i,\infty}, T_{i,\infty}]N} \tag{3.26}$$

By neglecting the transient electric field and temperature, the life equation becomes:

$$L_\infty = M_\infty \cdot t_D = \left(\sum_{i=1}^{N} LF_{i,\infty} \right)^{-1} \cdot t_D \tag{3.27}$$

As a result, the use of the simplified method to calculate the loss of life will make an error in the results since the thermal inertia of the cable material as well as the soil will not reach immediately (or maybe will never reach) the steady-state temperature which corresponds to the current value in the considered step.

3.3 The basic parameters of the cable:

The cable properties have been chosen to correspond with that mentioned in the literature [6]:

Parameter		**value**
Conductor	Material	Copper
	Cross-section area	1600 mm^2
	$R_{DC,cu}$	1.13×10^{-5}
	$a_{20,cu}$	3.93×10^{-3}
	$\rho_{T,cu}$ the electrical resistivity	$1.7241\times 10^{-2}\left[\frac{mm^2}{m}\right]$
	$C_{T,cu}$ the thermal capacity	$3.45\times 10^{6}\left[\frac{J}{m^3.°C}\right]$
Insulation	Material	DC-XLPE (Cross-Linked PolyEthylene for Direct Current applications)
	Thickness	17.9 [mm]
	ε_r	2.5
	$tan\ \delta$	0.001
	$\rho_{T,d}$ the thermal resistivity	$3.5\left[\frac{°C.m}{W}\right]$
	$C_{T,d}$ the thermal capacity	$2.4\times 10^{6}\left[\frac{J}{m^3.°C}\right]$
Sheath	$\rho_{T,d}$ the thermal resistivity	$3.5\left[\frac{°C.m}{W}\right]$
	$C_{T,d}$ the thermal capacity	$2.4\times 10^{6}\left[\frac{J}{m^3.°C}\right]$
Rated voltage U_0		320 KV
Rated power		1000 MW
Rated conductor temperature		70 $[°C]$
Loading factor		1.3694
Cooling factor (K_{cool})		2.236
Inner semiconductor thickness		2 [mm]

outer semiconductor thickness	1 [mm]
PVC sheath thickness	4.5 [mm]
Electric screen thickness	1 [mm]

It is noteworthy to mention that the loading factor is the factor by which the current is multiplied for heating the dielectric up to reach the required temperature within 6 hours.

3.4 The basic parameters of the soil:

Parameter		**value**
Soil	$\rho_{T,d}$ the thermal resistivity	1.3 $\left[\frac{^\circ C.m}{W}\right]$
	δ the thermal diffusivity	0.5 $\times 10^{-6}$ $\left[\frac{m^2}{s}\right]$
	L_B depth of burial	1.3 [m]

3.5 The parameters of the life model:

Parameter	**value**
B	12430 $[K]$
Synergism parameter b	0 $[K]$
β_t	1
Voltage Endurance Coefficient (at T_0) n_0	10
The reference electric field E_0	6 $[Kv/mm]$
Design Life L_D	40 $[y]$
Design Failure Probability P_D	1%

3.6 The considered values of the stress and temperature coefficients of the electrical conductivity *a* and *b:*

This study considers three different values of the stress and temperature coefficients of the electrical conductivity *a* and *b,* [6]

	$\boldsymbol{a}$ $[K^{-1}]$	$\boldsymbol{b}$ $[mm/KV]$
Low	0.042	0.032
Medium	0.084	0.0645
High	0.101	0.0775
Very High	0.168	0.129

3.7 The Electrical Type Test according to the CIGRE technical Brochure 496 [5]:

A Test made before supplying on a general commercial basis a type of cable system covered by this recommendation, in order to demonstrate satisfactory performance characteristics to meet the intended application.

3.7.1 Range of approval

The type approval shall be accepted as valid for cable systems supplied within the scope of this recommendation if the following conditions are fulfilled:

a) The actual designs, materials, manufacturing processes and service conditions for the cable system are in all essential aspects equal.
b) All service voltages are less than or equal to those of the tested cable system.
c) The mechanical stresses to be applied during preconditioning are less than or equal to those of the tested cable system.
d) The service maximum conductor temperature $T_{cond,max}$ is less than or equal to that of the tested cable system.
e) The maximum temperature drop across the insulation layer ΔT_{max} (excluding the semiconducting screens) is less than or equal to that of the tested cable system.
f) The actual conductor cross-section is not larger than that of the tested cable system.
g) The calculated average electrical stress in the insulation (given by U_0 which is the rated DC voltage divided by the nominal insulation thickness) is less than or equal to that of the tested system.
h) The calculated Laplace electrical stress (using nominal dimensions) at the cable conductor and insulation screen is less than or equal to that of the tested system.

i) A cable system qualified according to this recommendation for LCC is also qualified for VSC. A cable system qualified according to this recommendation for VSC is not qualified for LCC.

where:

- LCC: A HVDC system using Line Commutated Converters. LCC is a converter that has the feature of changing voltage polarity on the cable system when the direction of power flow is reversed IEC 60633.
- VSC: A HVDC system using Voltage Source Converters. VSC is a converter that does not change the voltage polarity of the cable system when the direction of power flow is reversed Cigré TB 289.

3.7.2 Test objects:

All components of the cable system (cable and accessories) shall be subjected to type testing. It is acceptable to test different parts of a system in different test loops. However, these test loops must cover all relevant cable system components.

By definition, an accessory includes 0.5 m of cable on each side, measured from the point on the cable where no disassembling or dismantling for the purpose of installation of the accessory has taken place. The non-interrupted cable length between accessories in a test loop shall be a minimum of 5 m. A minimum of 10 m of continuous non-interrupted cable shall be included in a test loop.

Any non-continuous design feature (such as a metallic connection between metallic layers) shall be included in the cable test object.

Test objects for land or submarine application shall be subjected to the appropriate mechanical preconditioning.

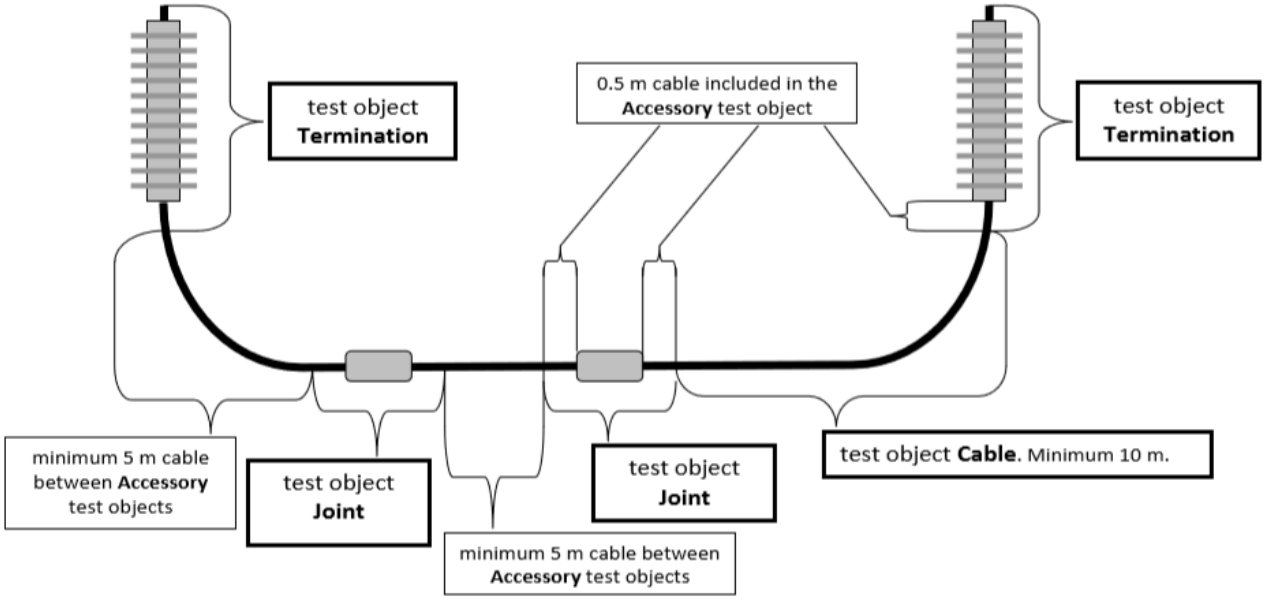

Figure 3.3 – Possible configuration of test objects within a test loop

3.7.3 Load cycle test for cable system to be qualified for VSC (Voltage Source Converters):

The test objects shall be subjected to the following conditions:

- Twelve “24 hours” load cycles at negative polarity at U_T.

- Twelve “24 hours” load cycles at positive polarity at U_T.

- Three “48 hours” load cycles at positive polarity at U_T.

Positive polarity was selected for the “48 hours” load cycles as this is believed to be the most stringent condition for accessories. However, in this study the polarity effect is not considered.

3.7.4 Definition of the Load Cycles:

Load cycles consist of both a heating period and a cooling period.

- “24 hours” load cycles (for prequalification and type tests) consist of at least 8 hours of heating followed by at least 16 hours of natural cooling. During at least the last 2 hours of the heating period, a conductor temperature $\geq T_{cond,max}$ and a temperature drop across the insulation $\geq \Delta T_{max}$ shall be maintained.

- "48 hours" load cycles (for type test only) consist of at least 24 hours of heating followed by at least 24 hours of natural cooling. During at least the last 18 hours of the heating period, a conductor temperature $\geq T_{cond,max}$ and a temperature drop across the insulation $\geq \Delta T_{max}$ shall be maintained. 48-hour load cycles are only required as part of the type test procedure to ensure that electrical stress inversion is well advanced within the cycle.

Where:

$T_{cond,max}$ is the maximum temperature at which the cable conductor is designed to operate. This value is to be stated by the supplier.

ΔT_{max} is the maximum temperature difference over the cable insulation in steady state (not including semiconducting screens) at which the cable is designed to operate. This value is to be calculated and stated by the supplier, who shall also provide evidence of the correlation between this design value and data measured during testing.

OUTCOMES OF MATLAB SIMULATION

Load Cycles:

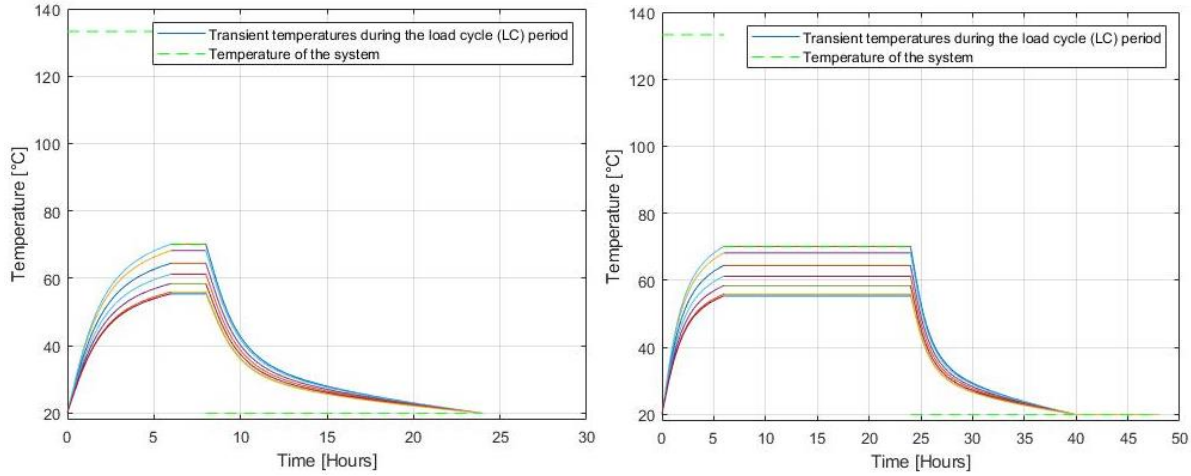

Figure 4.1 - Thermal profiles of 24-hour and 48-hour Load Cycles

1) Test under the rated voltage U_o:

- **24-hour Load Cycles**

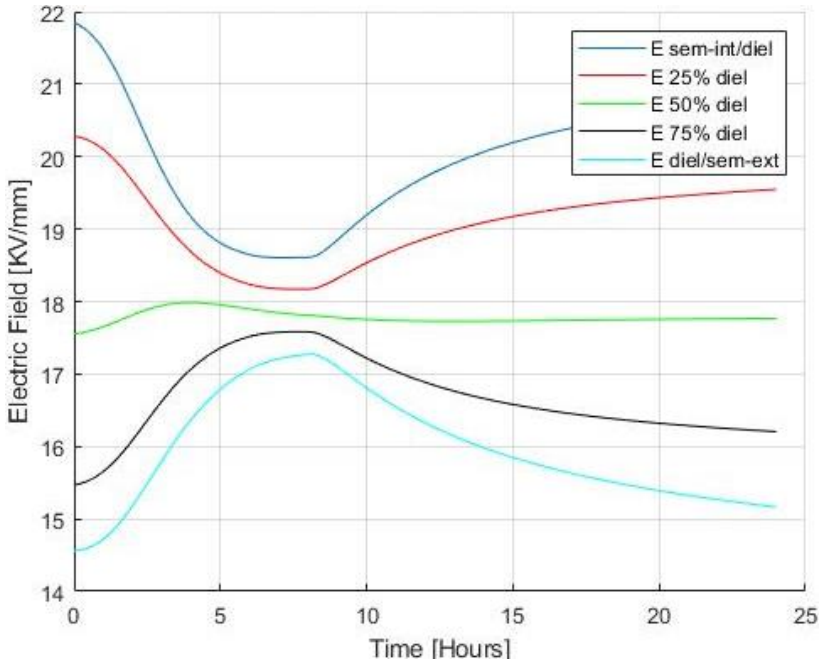

Figure 4.2 – Transient exact electric field during the 1'st cycle of the 24-hour Load Cycles period (LC) under the rated voltage U_o at 5 points of the insulation of the sample cable for a_L, b_L.

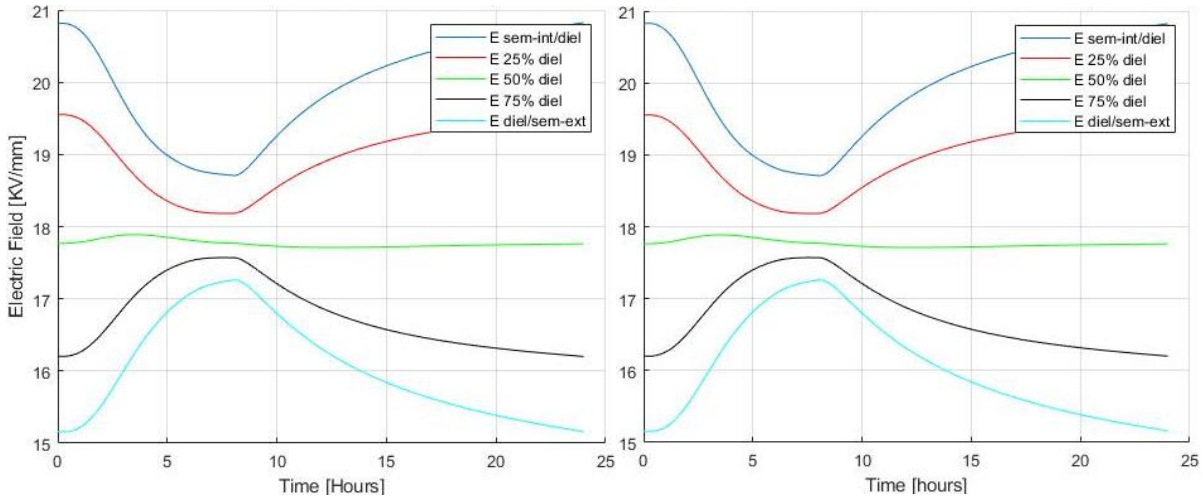

Figure 4.3 – Transient exact electric field during the 2'nd (a) and the 3'rd (b) cycles of the 24-hour Load Cycles period (LC) under the rated voltage U_o at 5 points of the insulation of the sample cable for a_L, b_L.

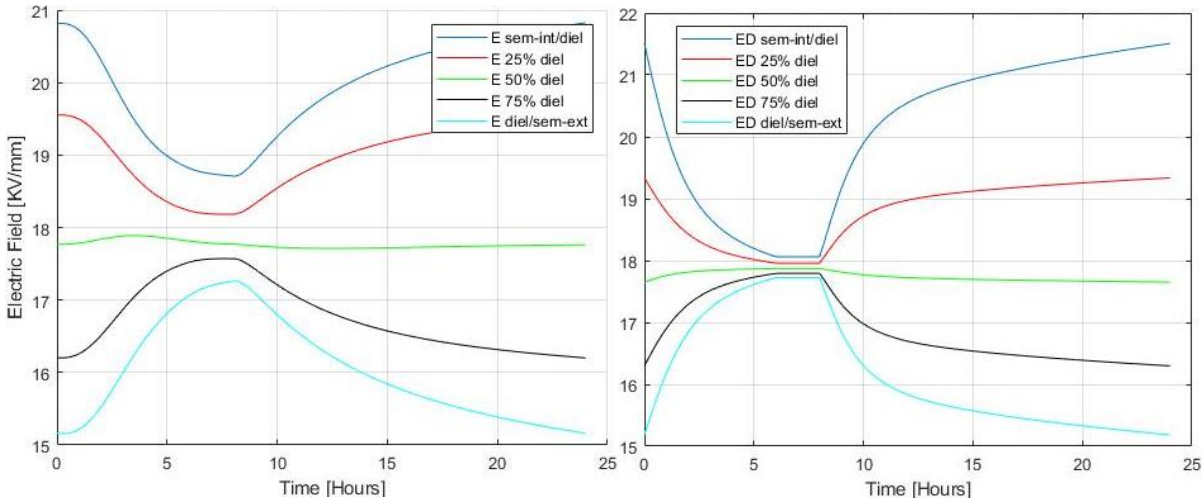

Figure 4.4 – comparison between exact (a) and approximated (b) transient electric field during the 24-hour Load Cycles period (LC) under the rated voltage U_o at 5 points of the insulation of the sample cable for a_L, b_L.

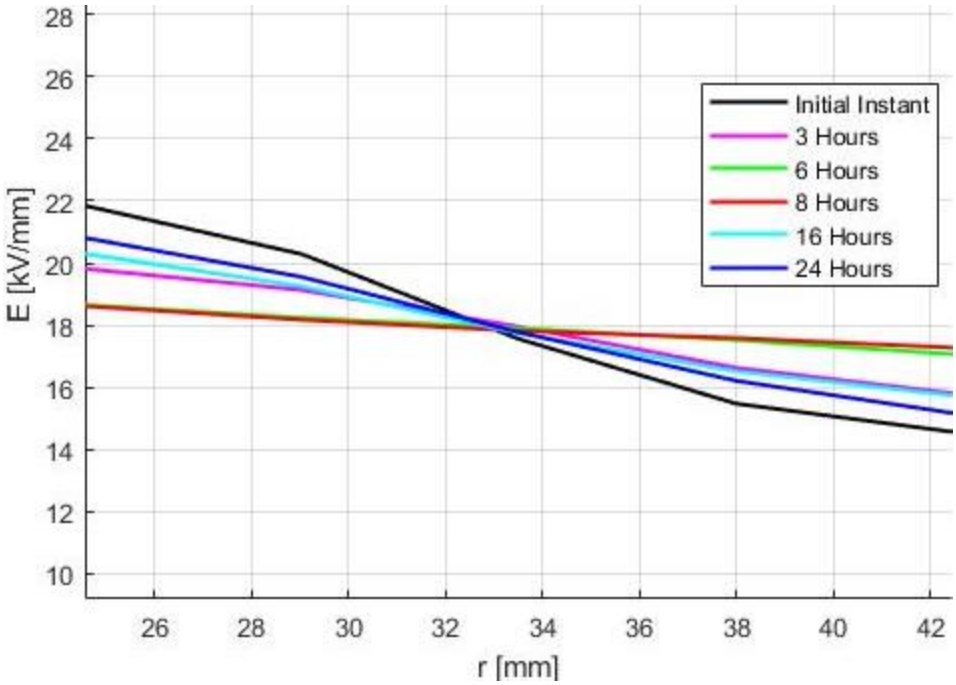

Figure 4.5 – Transient exact electric field profile during the 1'st cycle of the 24-hour Load Cycles period (LC) under the rated voltage U_o at 5 points of the insulation of the sample cable for a_L, b_L.

- **48-hour Load Cycles**

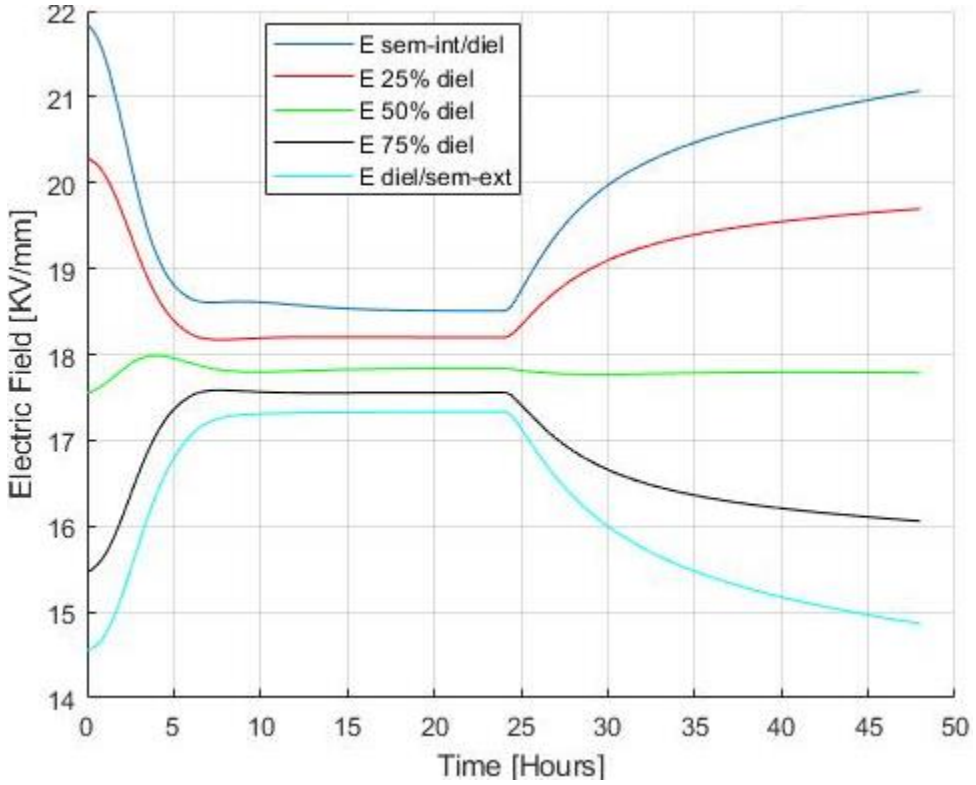

Figure 4.6 – Transient exact electric field during the 1'st cycle of the 48-hour Load Cycles period (LC) under the rated voltage U_o at 5 points of the insulation of the sample cable for a_L, b_L.

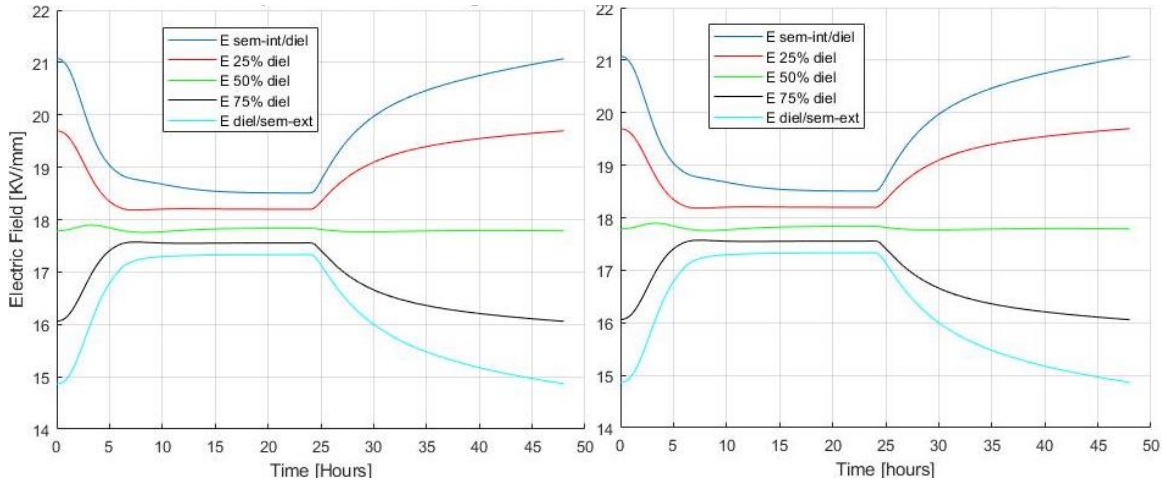

Figure 4.7 – Transient exact electric field during the 2'nd (a) and the 3'rd (b) cycles of the 48-hour Load Cycles period (LC) under the rated voltage U_o at 5 points of the insulation of the sample cable for a_L, b_L.

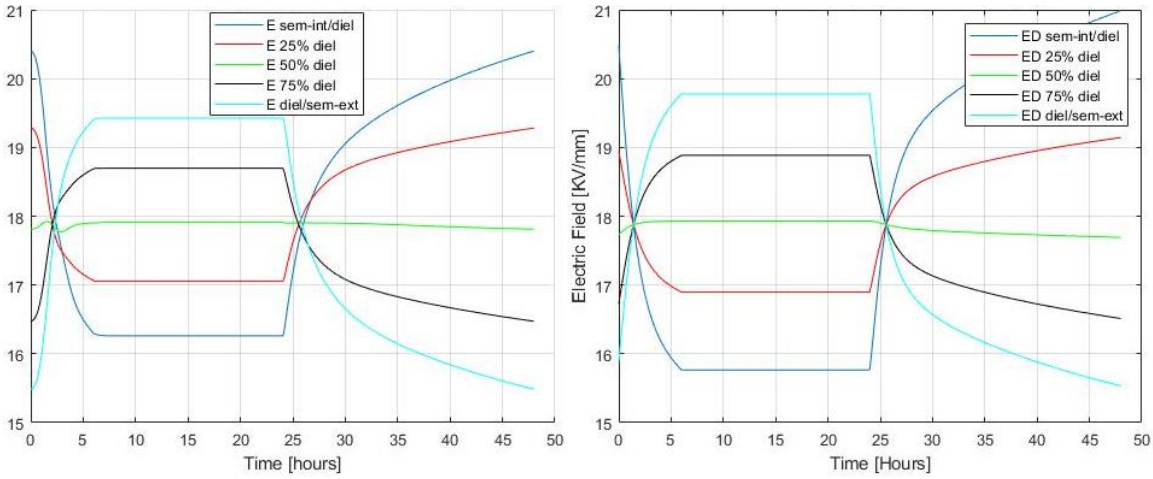

Figure 4.8 – comparison between exact (a) and approximated (b) transient electric field during the 48-hour Load Cycles period (LC) under the rated voltage U_o at 5 points of the insulation of the sample cable for a_L, b_L.

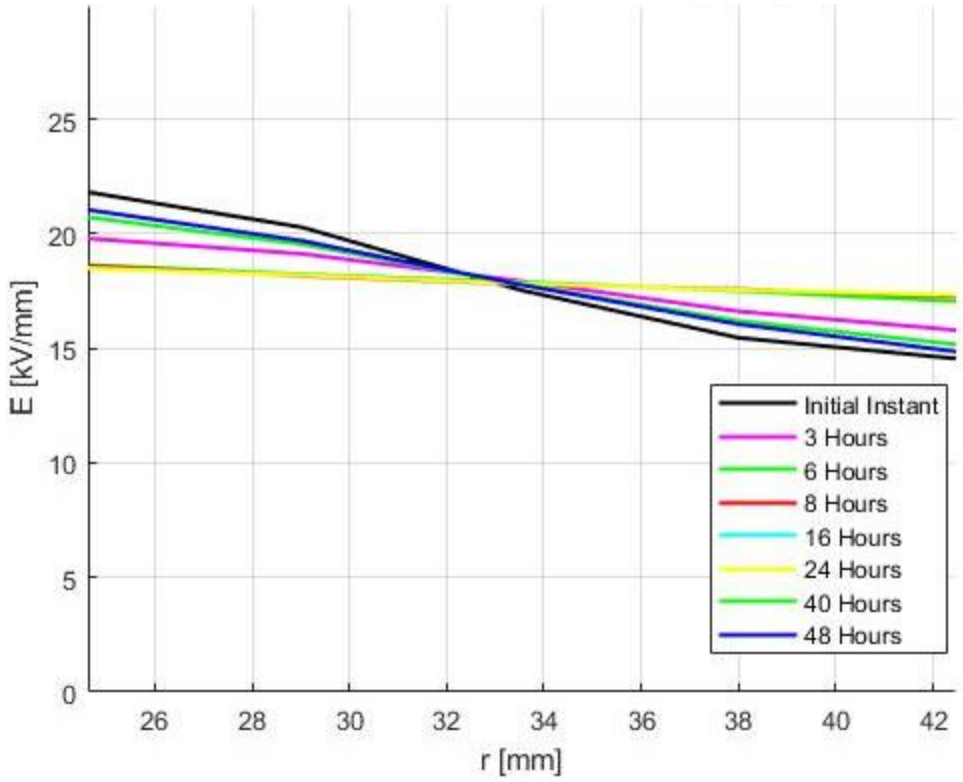

Figure 4.9 – Transient exact electric field profile during the 1'st cycle of the 48-hour Load Cycles period (LC) under the rated voltage U_o at 5 points of the insulation of the sample cable for a_L, b_L.

2) Test under the Type Test conditions U =1.85 U_o:

- **24-hour Load Cycles**

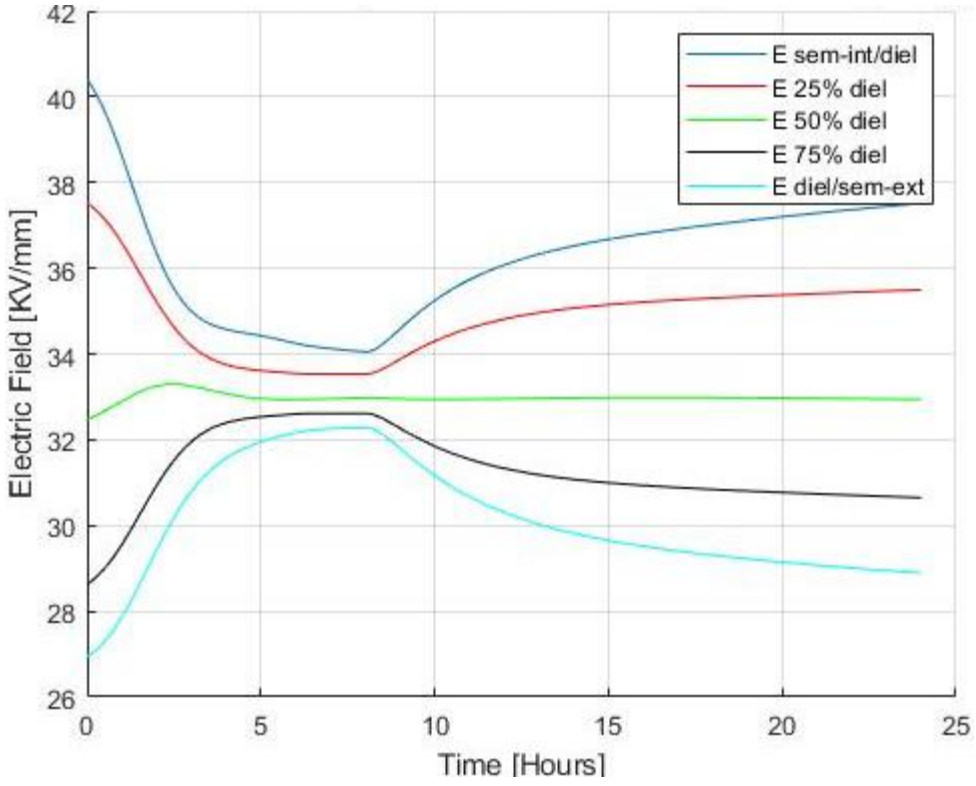

Figure 4.10– Transient exact electric field during the 1'st cycle of the 24-hour Load Cycles period (LC) under the Type Test conditions at 5 points of the insulation of the sample cable for a_L, b_L.

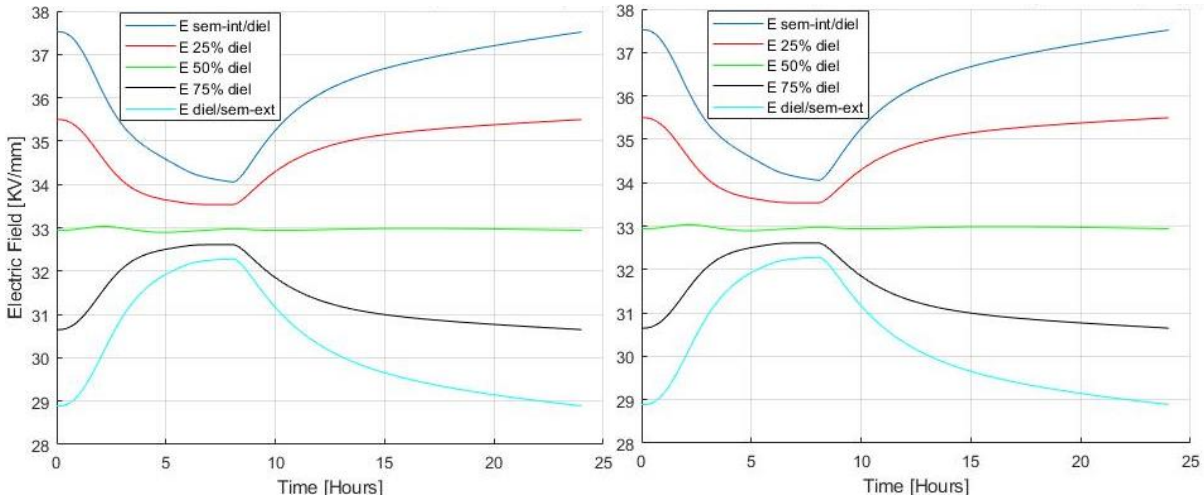

Figure 4.11 – Transient exact electric field during the 2'nd (a) and the 3'rd (b) cycles of the 24-hour Load Cycles period (LC) under the Type Test conditions at 5 points of the insulation of the sample cable for a_L, b_L.

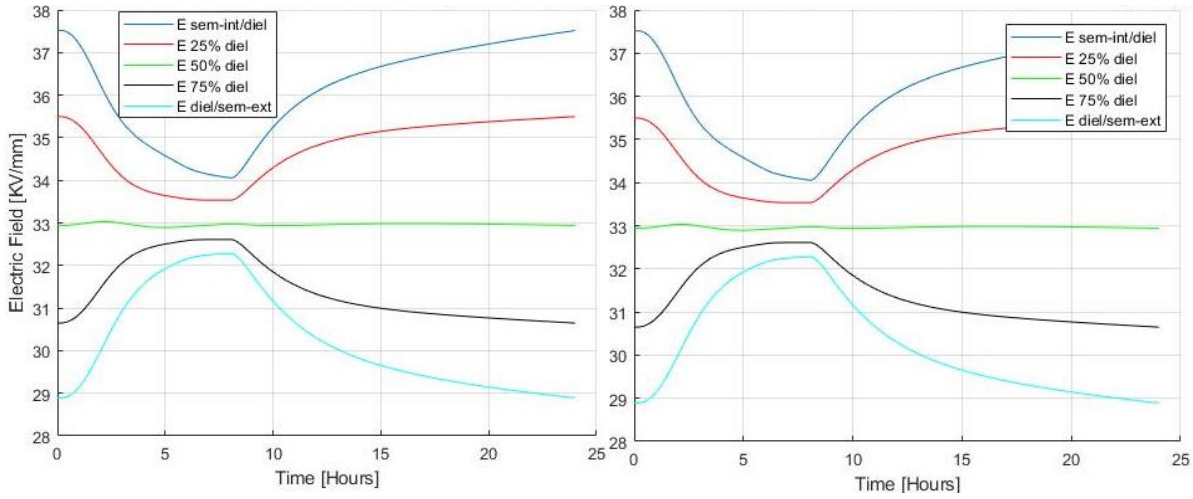

Figure 4.12 – Transient exact electric field during the 4'th (a) and the 5'th (b) cycles of the 24-hour Load Cycles period (LC) under the Type Test conditions at 5 points of the insulation of the sample cable for a_L, b_L.

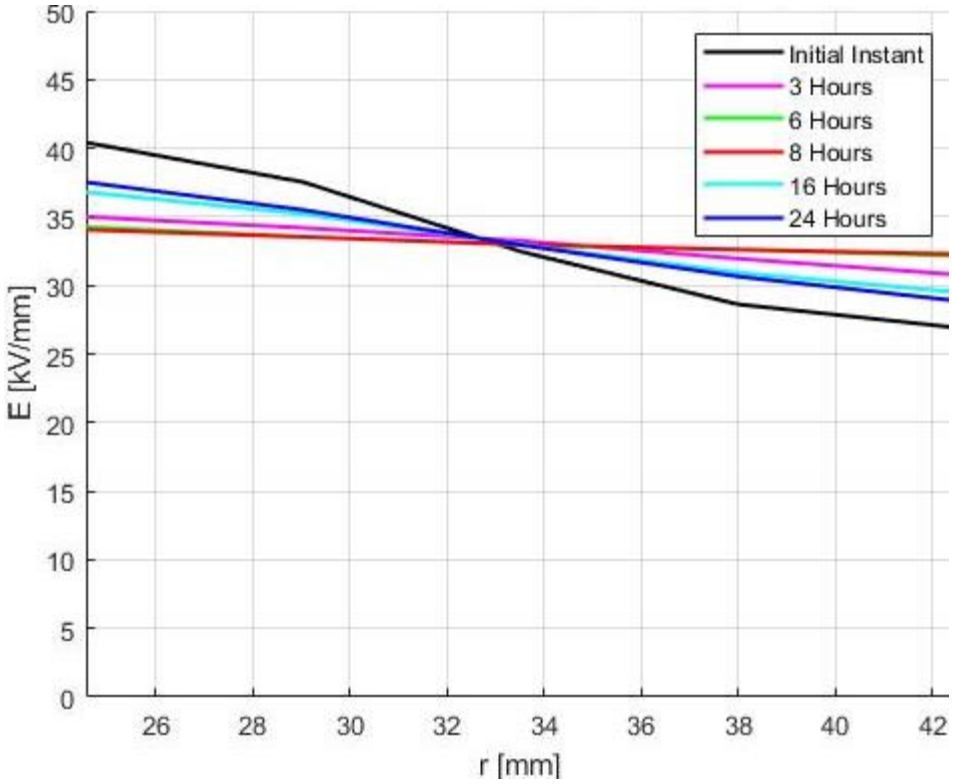

Figure 4.13 – Transient exact electric field profile during the 1'st cycle of the 24-hour Load Cycles period (LC) under the Type Test conditions at 5 points of the insulation of the sample cable for a_L, b_L.

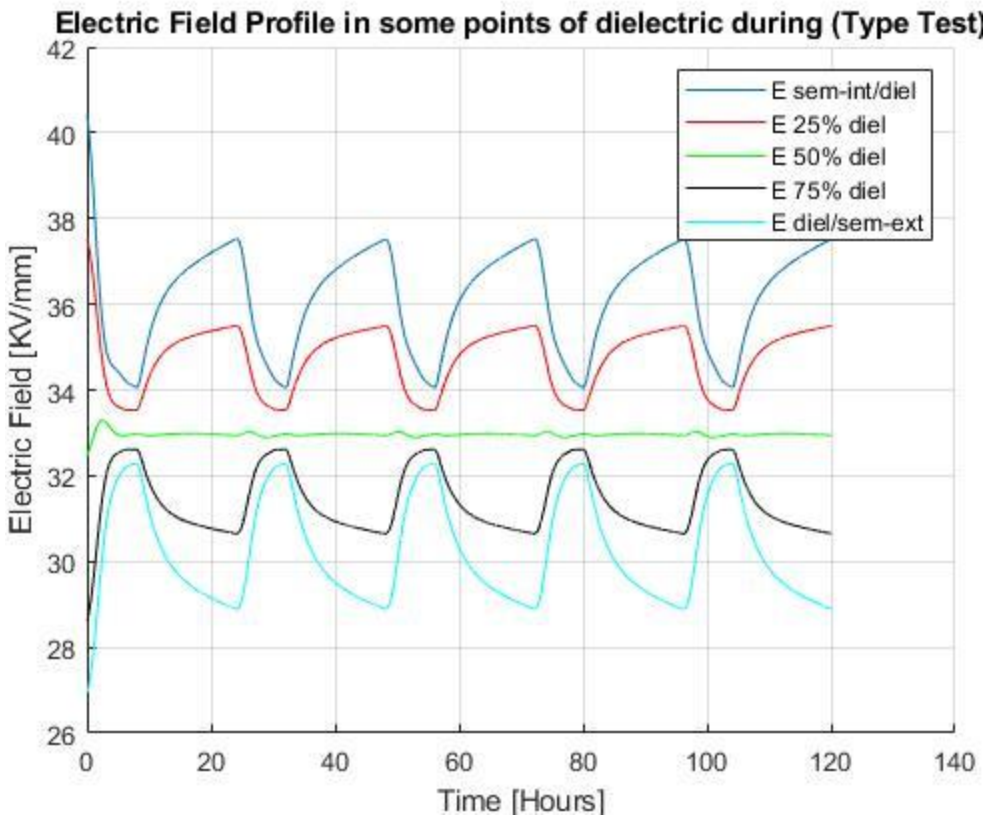

Figure 4.14 – Transient exact electric field profile during the first 5 cycles of the 24-hour Load Cycles period (LC) under the Type Test conditions at 5 points of the insulation of the sample cable for a_L, b_L.

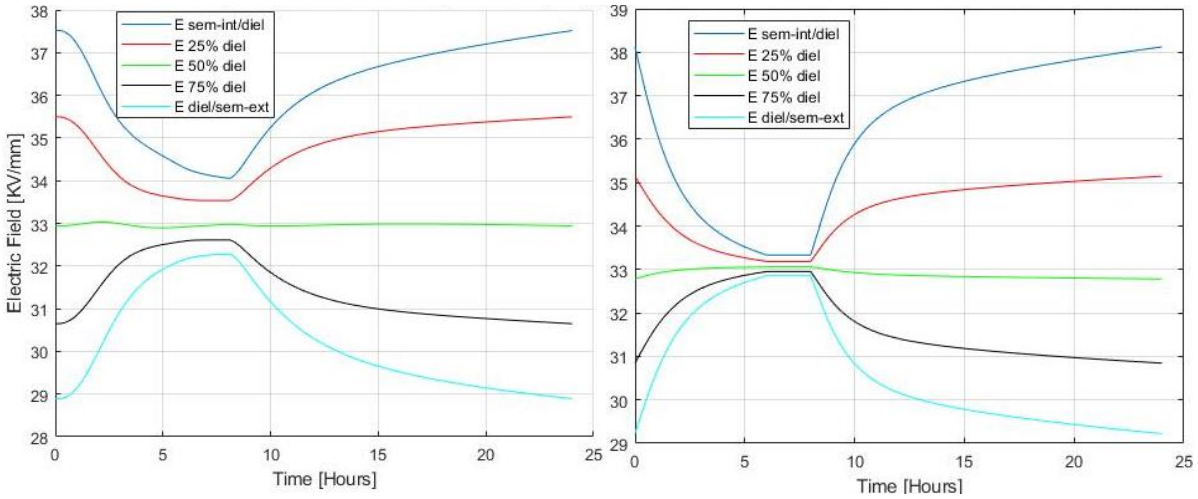

Figure 4.15 – comparison between exact (a) and approximated (b) transient electric field during the 24-hour Load Cycles period (LC) under the Type Test conditions at 5 points of the insulation of the sample cable for a_L, b_L.

- **48-hour Load Cycles**

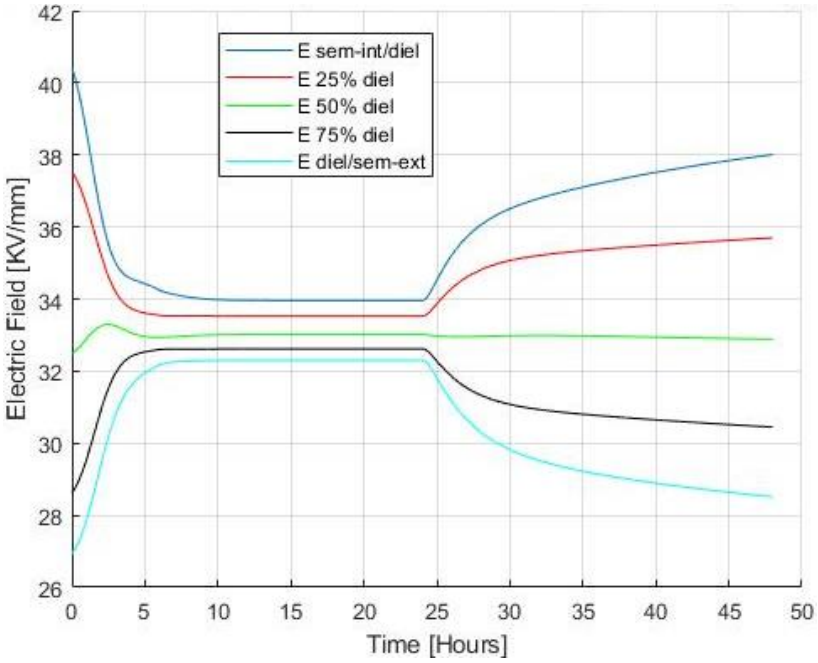

Figure 4.16 – Transient exact electric field during the 1'st cycle of the 24-hour Load Cycles period (LC) under the Type Test conditions at 5 points of the insulation of the sample cable for a_L, b_L.

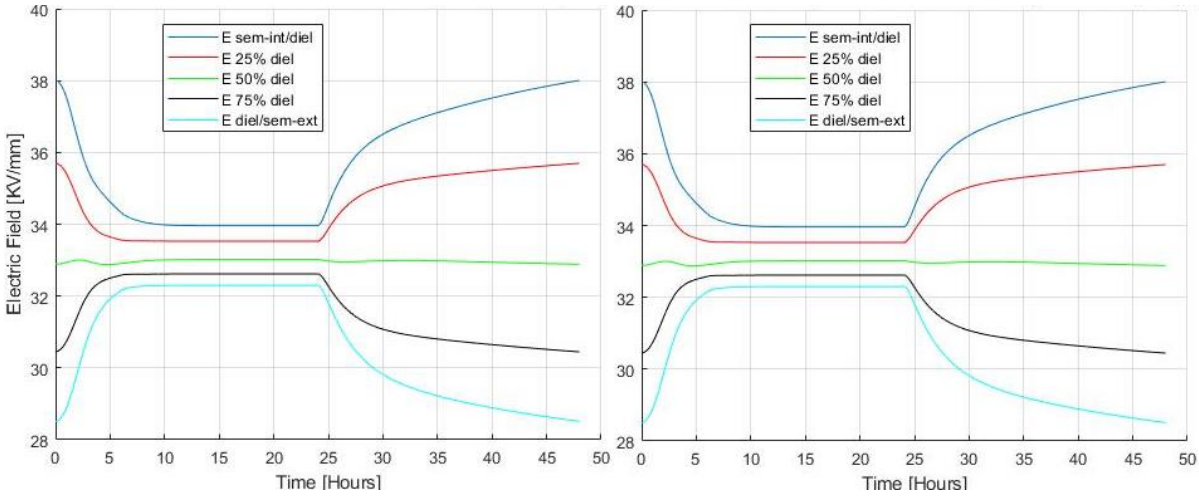

Figure 4.17 – Transient exact electric field during the 2'nd (a) and the 3'rd (b) cycles of the 24-hour Load Cycles period (LC) under the Type Test conditions at 5 points of the insulation of the sample cable for a_L, b_L.

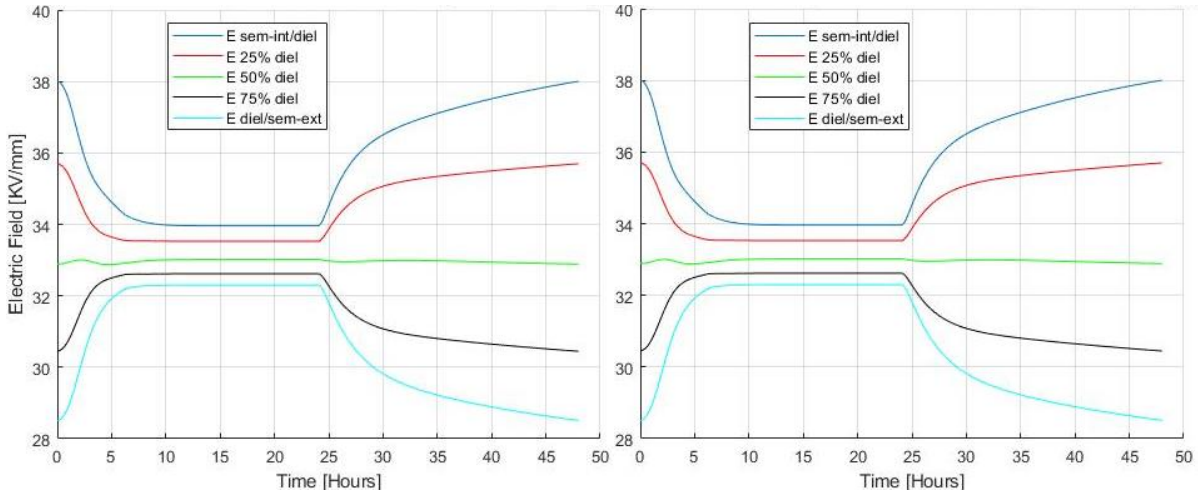

Figure 4.18 – Transient exact electric field during the 4'th (a) and the 5'th (b) cycles of the 24-hour Load Cycles period (LC) under the Type Test conditions at 5 points of the insulation of the sample cable for a_L, b_L.

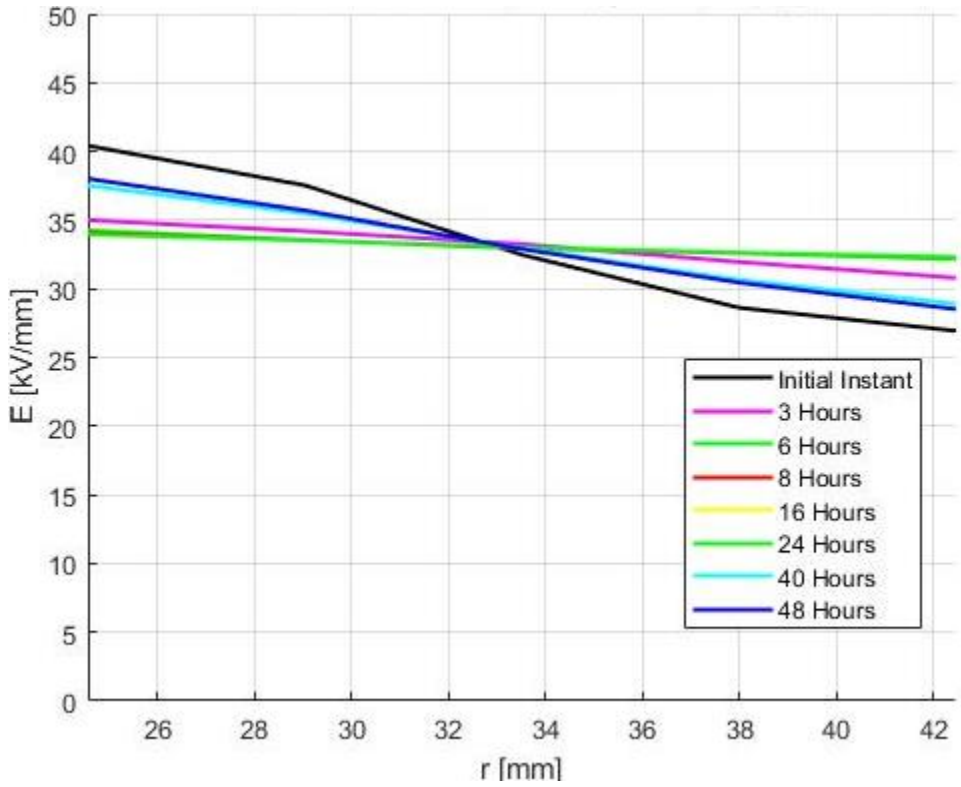

Figure 4.19 – Transient exact electric field profile during the 1'st cycle of the 24-hour Load Cycles period (LC) under the Type Test conditions at 5 points of the insulation of the sample cable for a_L, b_L.

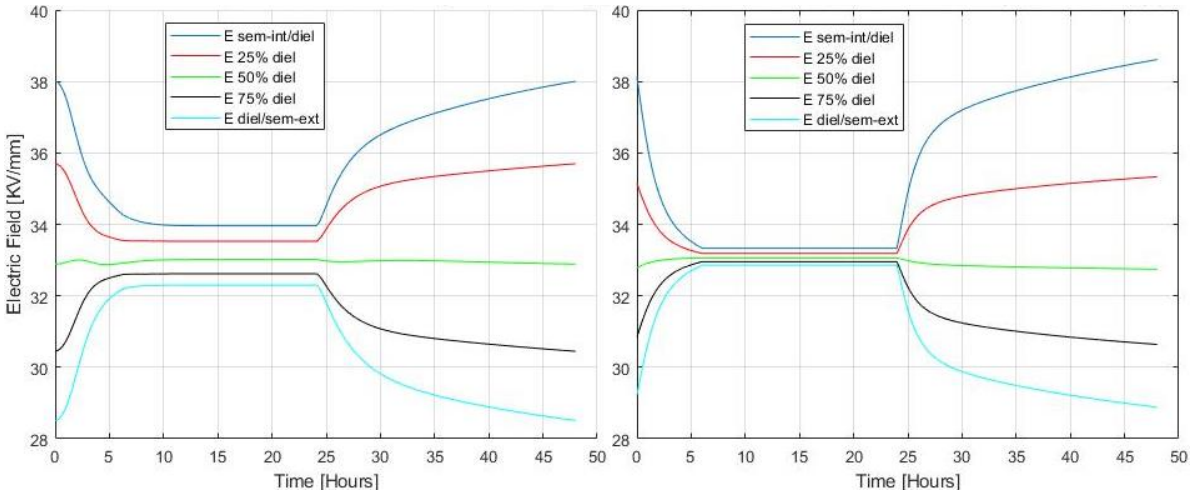

Figure 4.20 – comparison between exact (a) and approximated (b) transient electric field during the 24-hour Load Cycles period (LC) under the Type Test conditions at 5 points of the insulation of the sample cable for a_L, b_L.

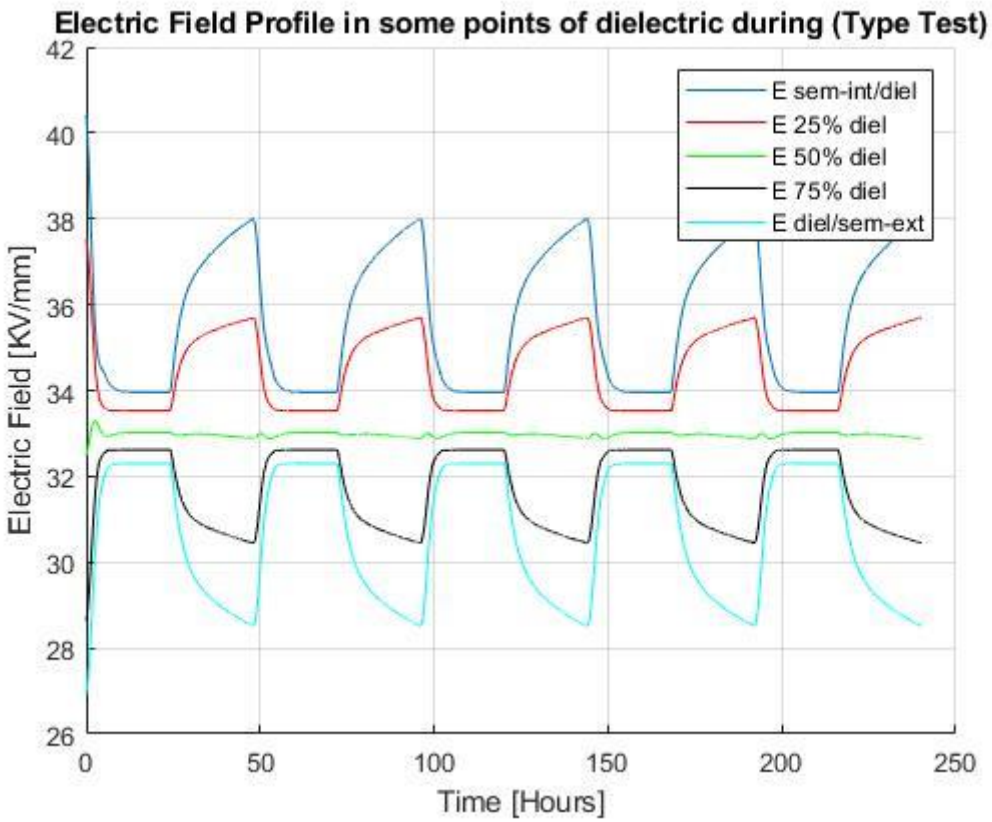

Figure 4.21 – Transient exact electric field profile during the first 5 cycles of the 48-hour Load Cycles period (LC) under the Type Test conditions at 5 points of the insulation of the sample cable for a_L, b_L.

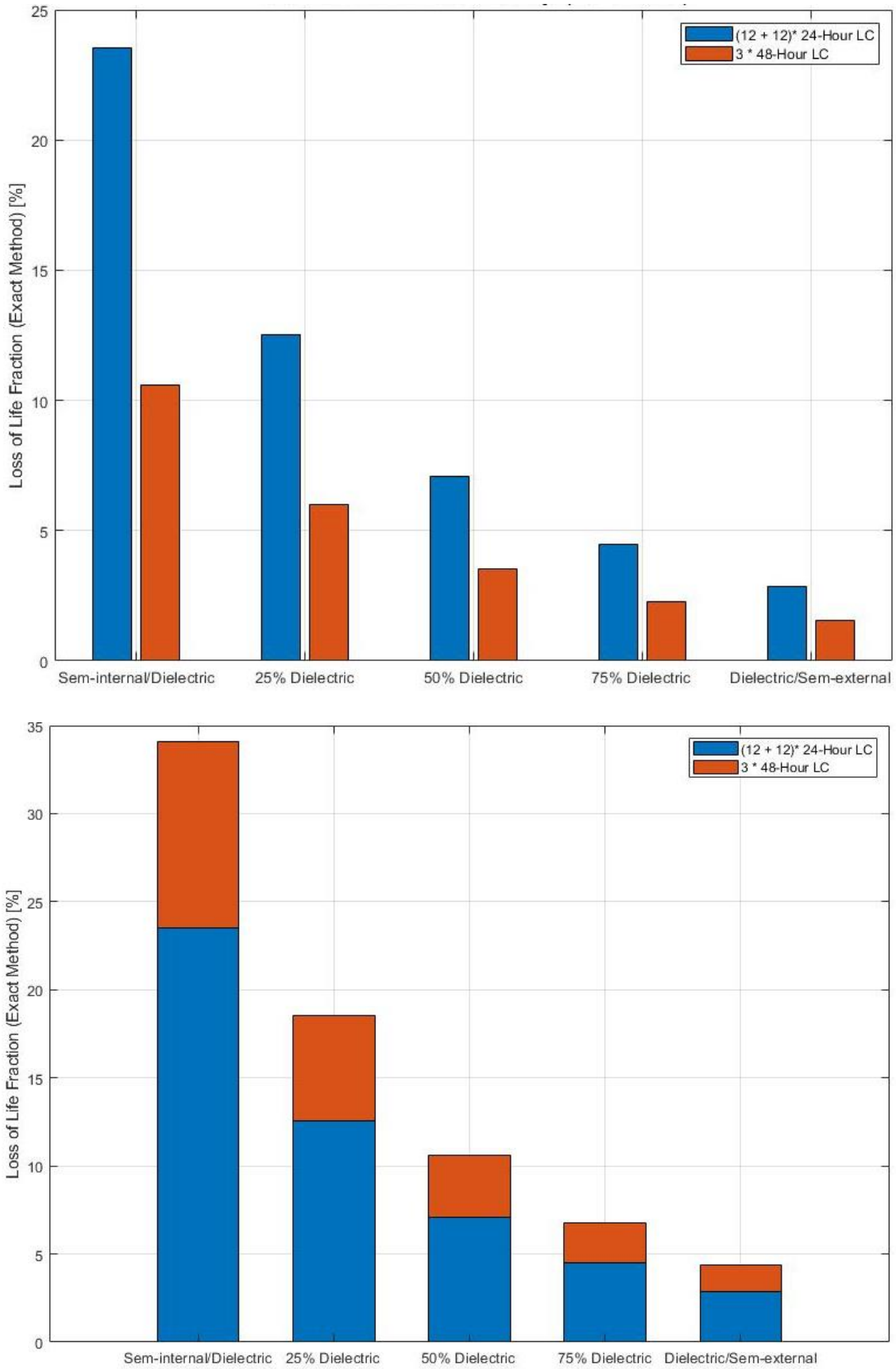

Figure 4.22 – Exact loss-of-life fractions during 12 + 12 cycles of 24-hour Load Cycle (LC) and 3 cycles of 48 hours Load Cycle (LC) under the Type Test conditions at 5 points of the insulation of the sample cable for a_L, b_L.

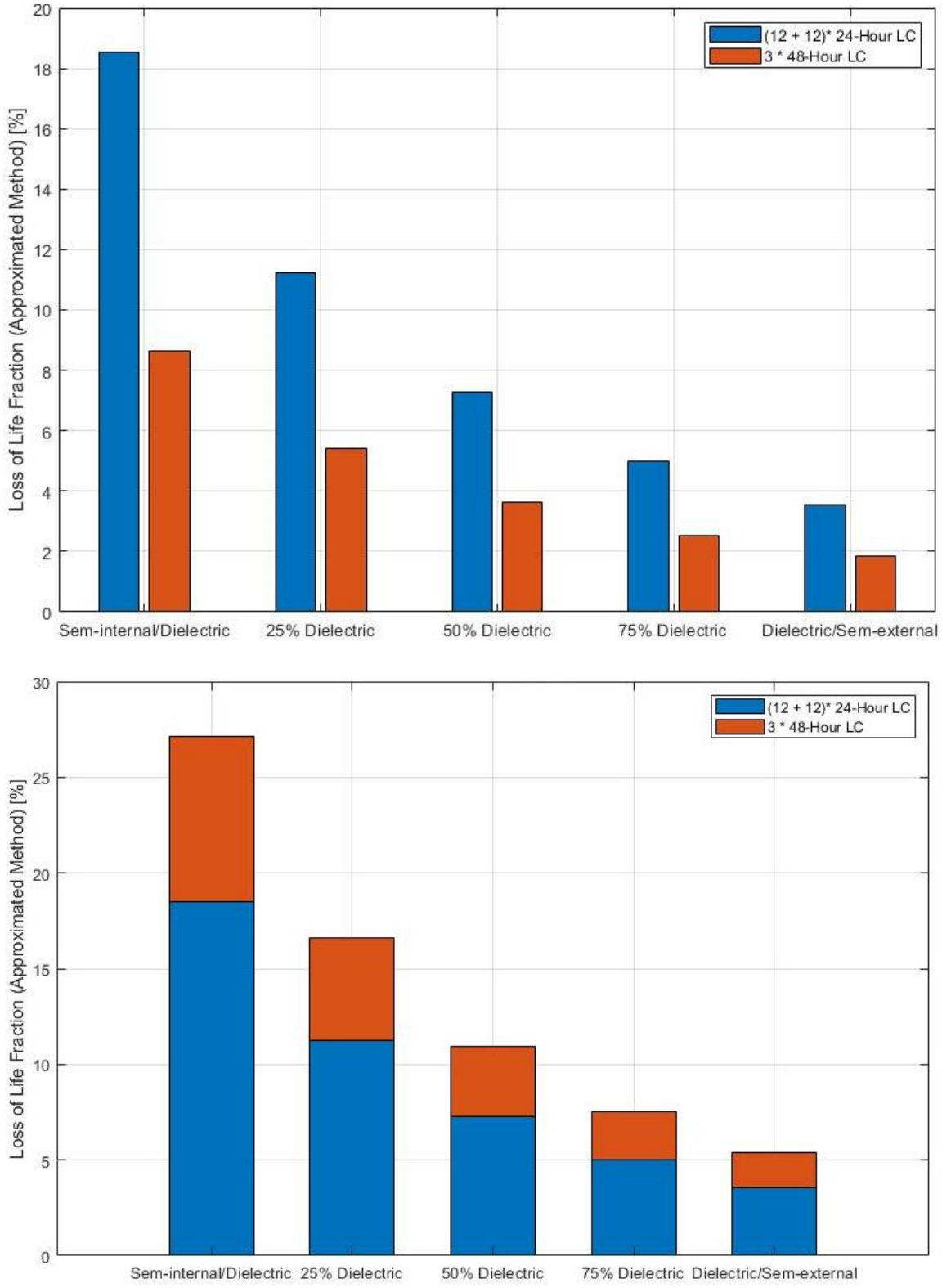

Figure 4.23 – Approximated loss-of-life fractions during 12+12 cycles of 24-hour Load Cycles (LC) and 3 cycles of 48-hour Load Cycles (LC) under the Type Test conditions at 5 points of the insulation of the sample cable for a_L, b_L

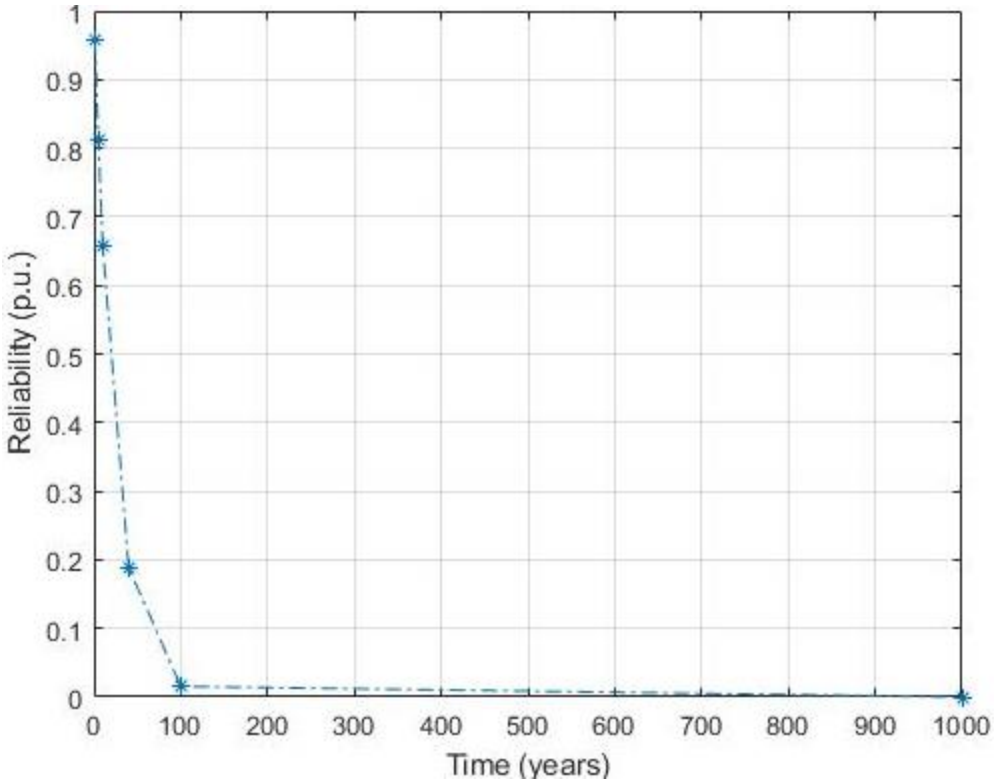

Figure 4.24 – Exact reliability during 12 + 12 cycles of 24-hour Load Cycles (LC) and 3 cycles of 48-hour Load Cycles (LC) under the Type Test conditions of the insulation of the sample cable for a_L, b_L.

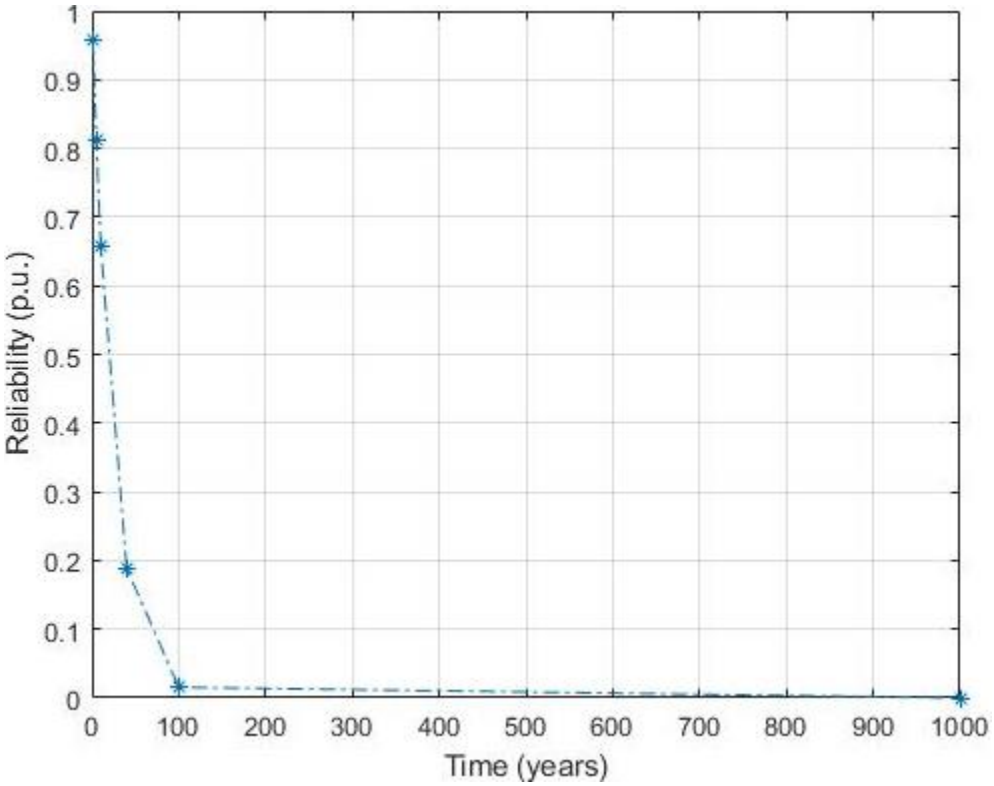

Figure 4.25 – Approximated reliability during 12 + 12 cycles of 24-hour Load Cycles (LC) and 3 cycles of 48-hour Load Cycles (LC) under the Type Test conditions of the insulation of the sample cable for a_L, b_L.

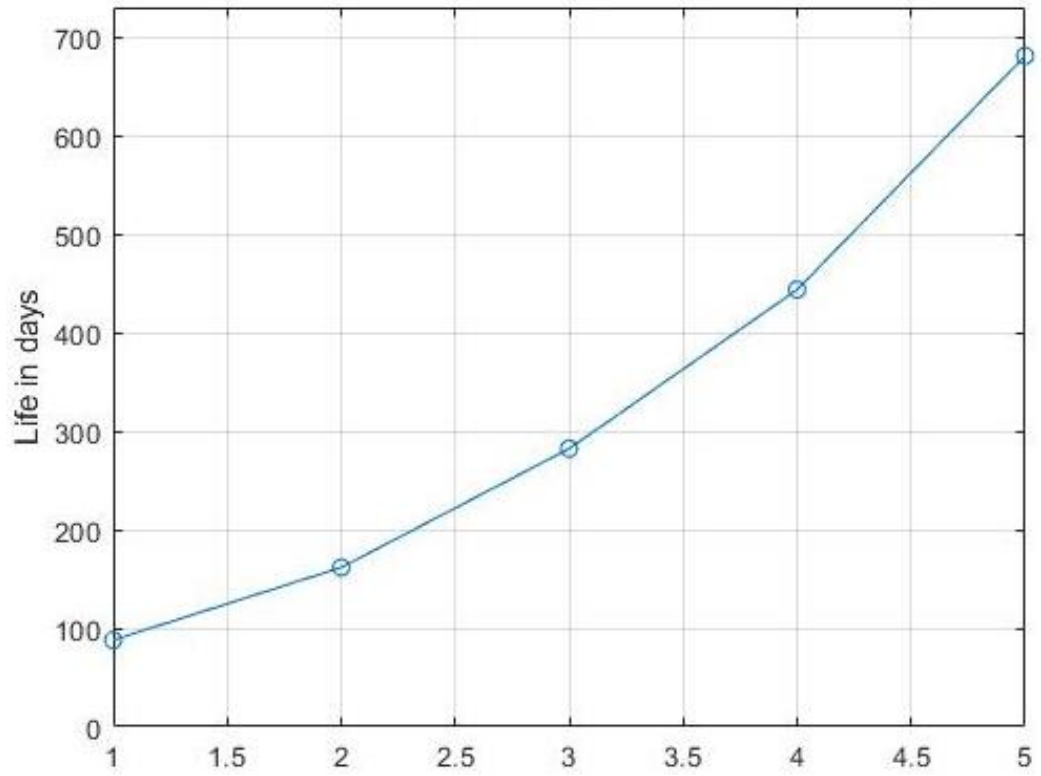

Figure 4.26 – Exact life during 12 + 12 cycles of 24-hour Load Cycles (LC) and 3 cycles of 48-hour Load Cycles (LC) under the Type Test conditions at 5 points of the insulation of the sample cable for a_L, b_L.

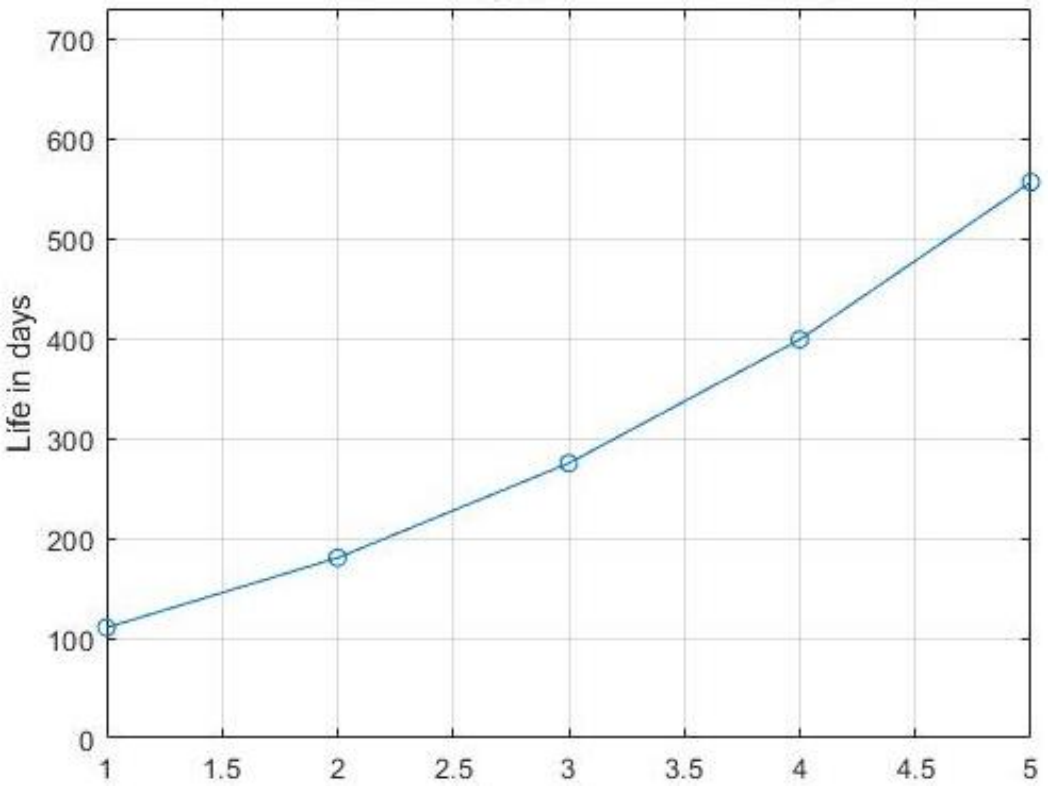

Figure 4.27 – Approximated life during 12 + 12 cycles of 24-hour Load Cycles (LC) and 3 cycles of 48-hour Load Cycles (LC) under the Type Test conditions at 5 points of the insulation of the sample cable for a_L, b_L.

Results in the case of medium values of *a* and *b*:

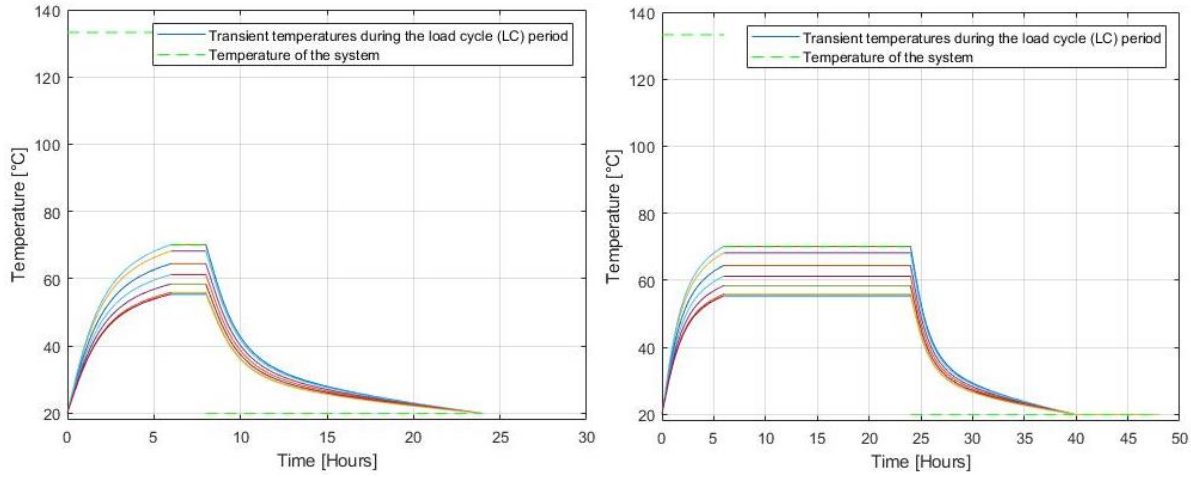

Figure 4.28- Thermal profiles of 24-hour and 48-hour Load Cycles

1) Test under the rated voltage U_o:

- **24-hour Load Cycles**

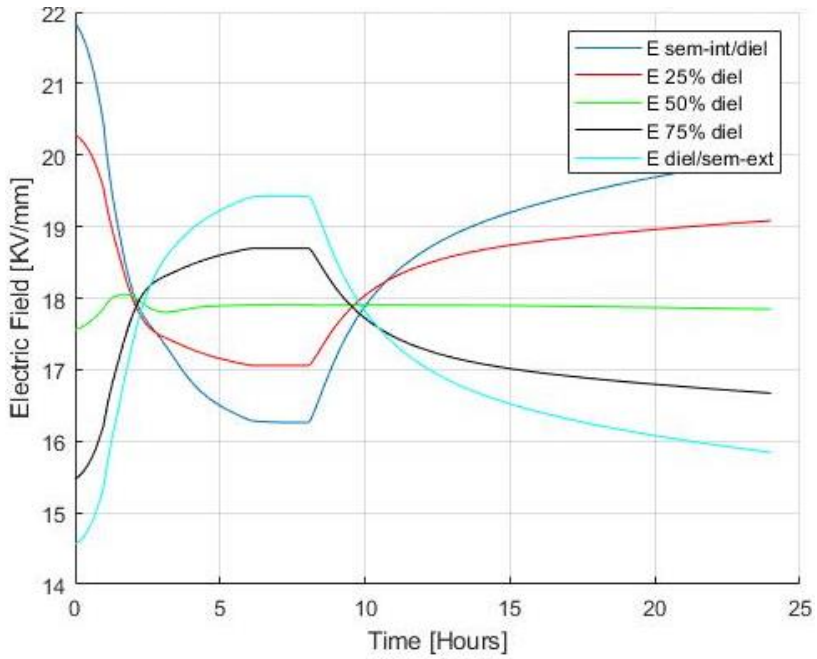

Figure 4.29 – Transient exact electric field during the 1'st cycle of the 24-hour Load Cycles period (LC) under the rated voltage U_o at 5 points of the insulation of the sample cable for a_M, b_M.

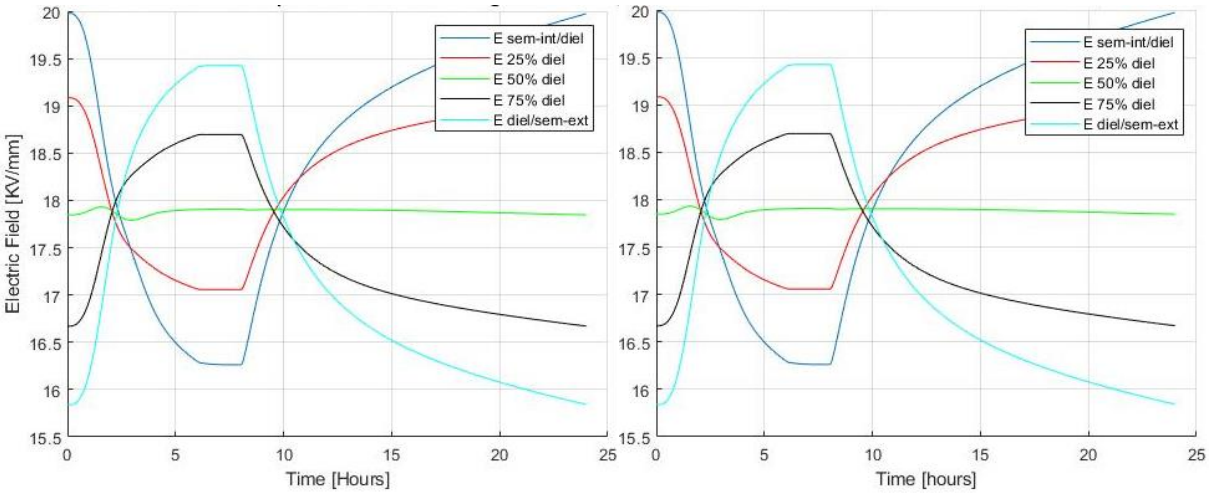

Figure 4.30 – Transient exact electric field during the 2'nd (a) and the 3'rd (b) cycles of the 24-hour Load Cycles period (LC) under the rated voltage U_o at 5 points of the insulation of the sample cable for a_M, b_M.

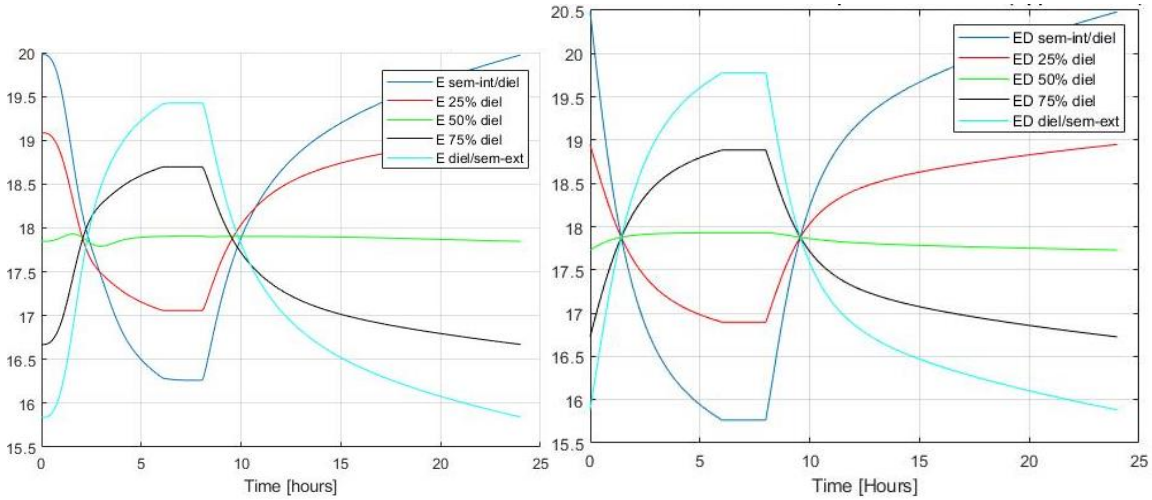

Figure 4.31 – comparison between exact (a) and approximated (b) transient electric field during the 24-hour Load Cycles period (LC) under the rated voltage U_o at 5 points of the insulation of the sample cable for a_M, b_M.

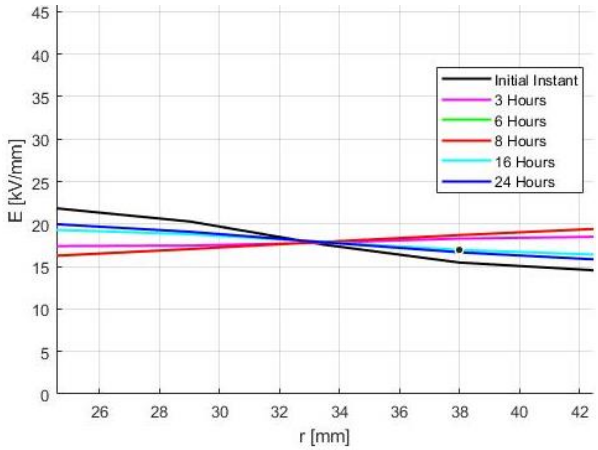

Figure 4.32 – Transient exact electric field profile during the 1'st cycle of the 24-hour Load Cycles period (LC) under the rated voltage U_o at 5 points of the insulation of the sample cable for a_M, b_M.

- **48-hour Load Cycles**

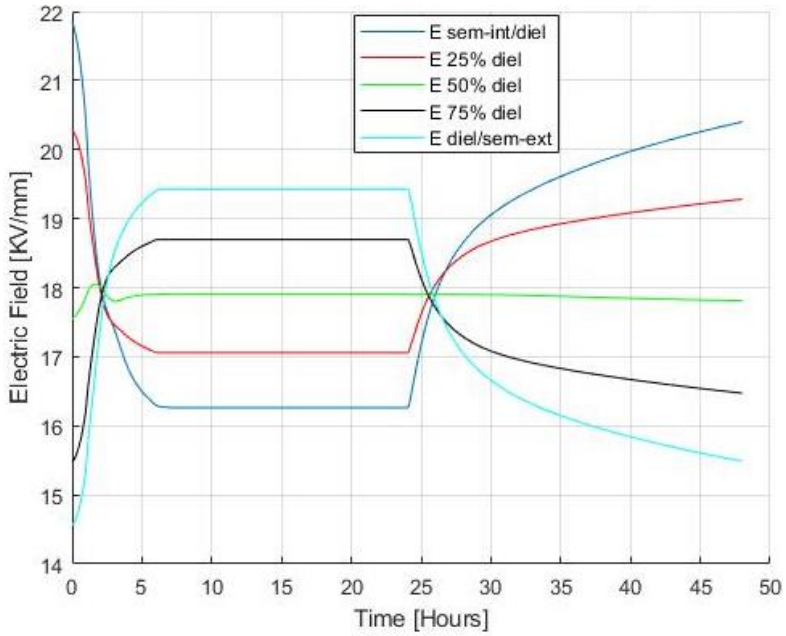

Figure 4.33 – Transient exact electric field during the 1'st cycle of the 48-hour Load Cycles period (LC) under the rated voltage U_o at 5 points of the insulation of the sample cable for a_M, b_M.

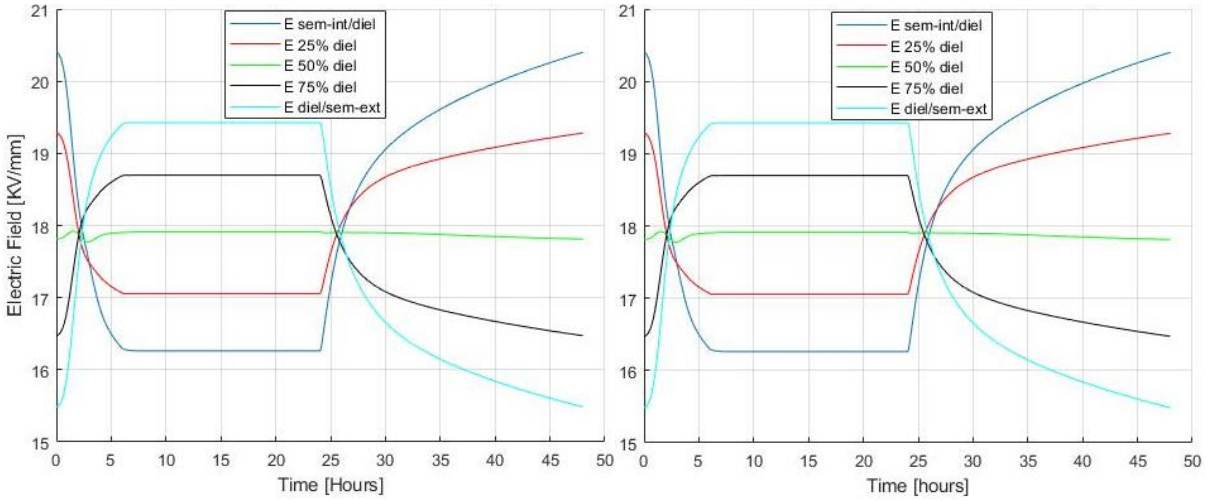

Figure 4.34 – Transient exact electric field during the 2'nd (a) and the 3'rd (b) cycles of the 48-hour Load Cycles period (LC) under the rated voltage U_o at 5 points of the insulation of the sample cable for a_M, b_M.

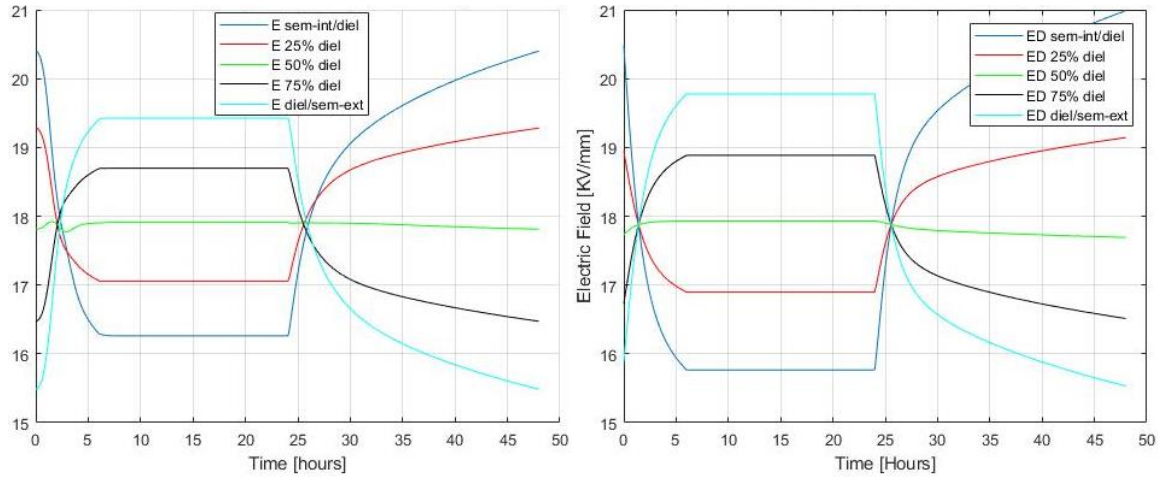

Figure 4.35 – comparison between exact (a) and approximated (b) transient electric field during the 48-hour Load Cycles period (LC) under the rated voltage U_o at 5 points of the insulation of the sample cable for a_M, b_M.

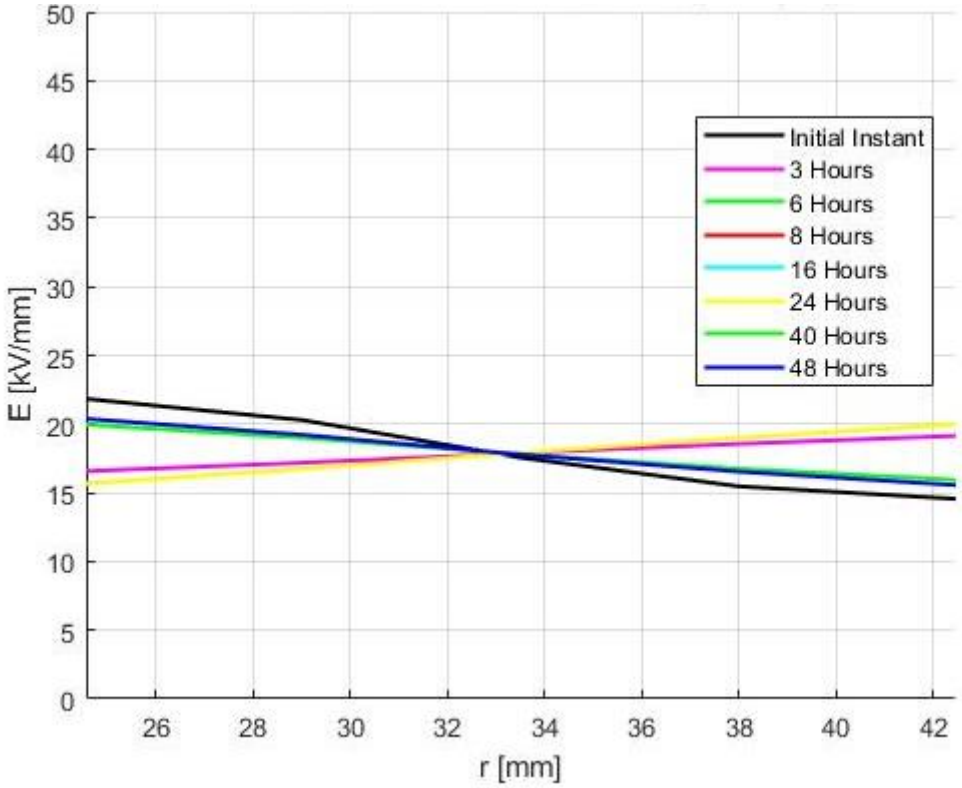

Figure 4.36 – Transient exact electric field profile during the 1'st cycle of the 48-hour Load Cycles period (LC) under the rated voltage U_o at 5 points of the insulation of the sample cable for a_M, b_M.

2) Test under the Type Test conditions U =1.85 U_o:

- **24-hour Load Cycles**

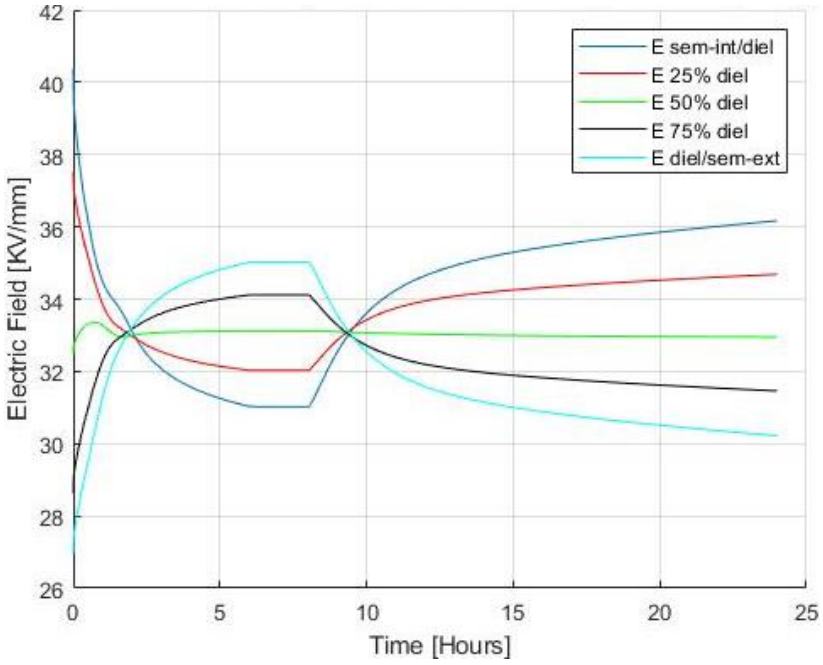

Figure 4.37 – Transient exact electric field during the 1'st cycle of the 24-hour Load Cycles period (LC) under the Type Test conditions at 5 points of the insulation of the sample cable for a_M, b_M.

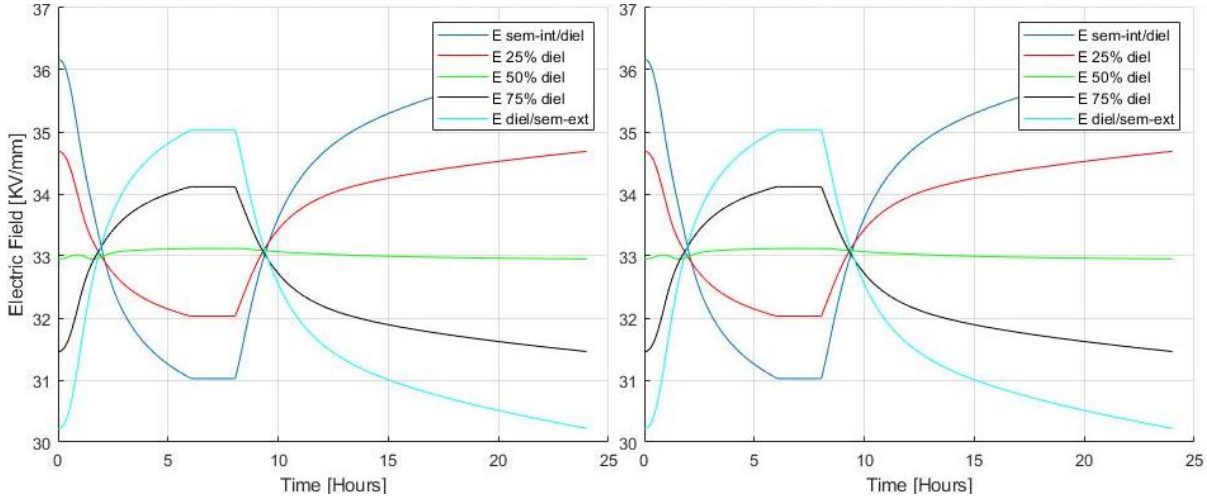

Figure 4.38 – Transient exact electric field during the 2'nd (a) and the 3'rd (b) cycles of the 24-hour Load Cycles period (LC) under the Type Test conditions at 5 points of the insulation of the sample cable for a_M, b_M.

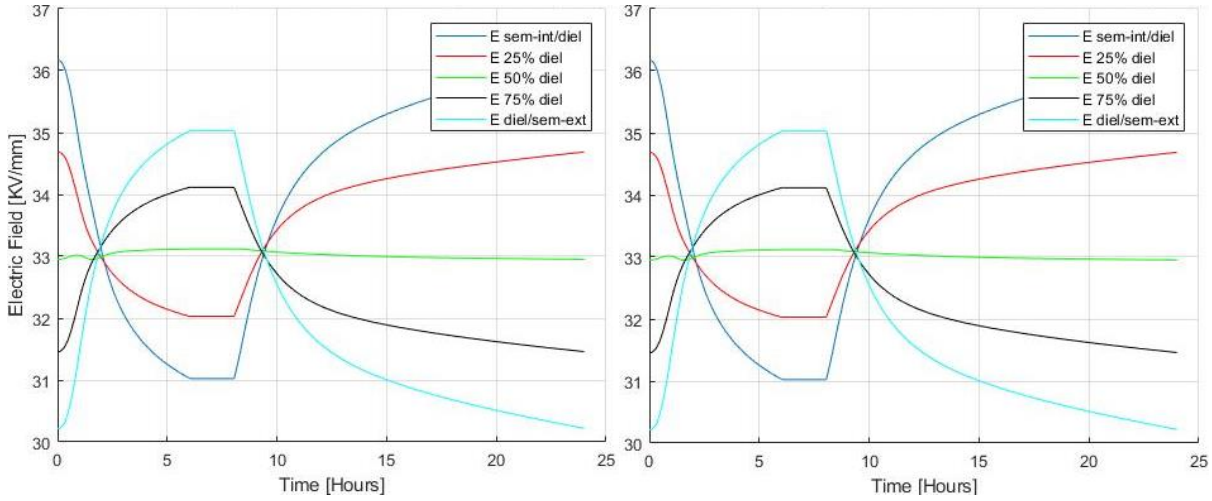

Figure 4.39 – Transient exact electric field during the 4'th (a) and the 5'th (b) cycles of the 24-hour Load Cycles period (LC) under the Type Test conditions at 5 points of the insulation of the sample cable for a_M, b_M.

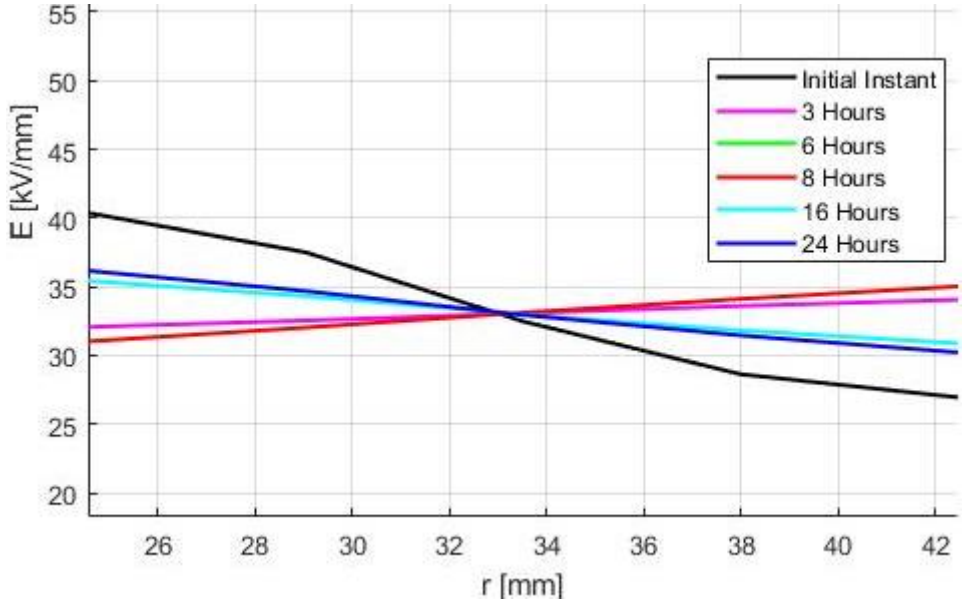

Figure 4.40 – Transient exact electric field profile during the 1'st cycle of the 24-hour Load Cycles period (LC) under the Type Test conditions at 5 points of the insulation of the sample cable for a_M, b_M.

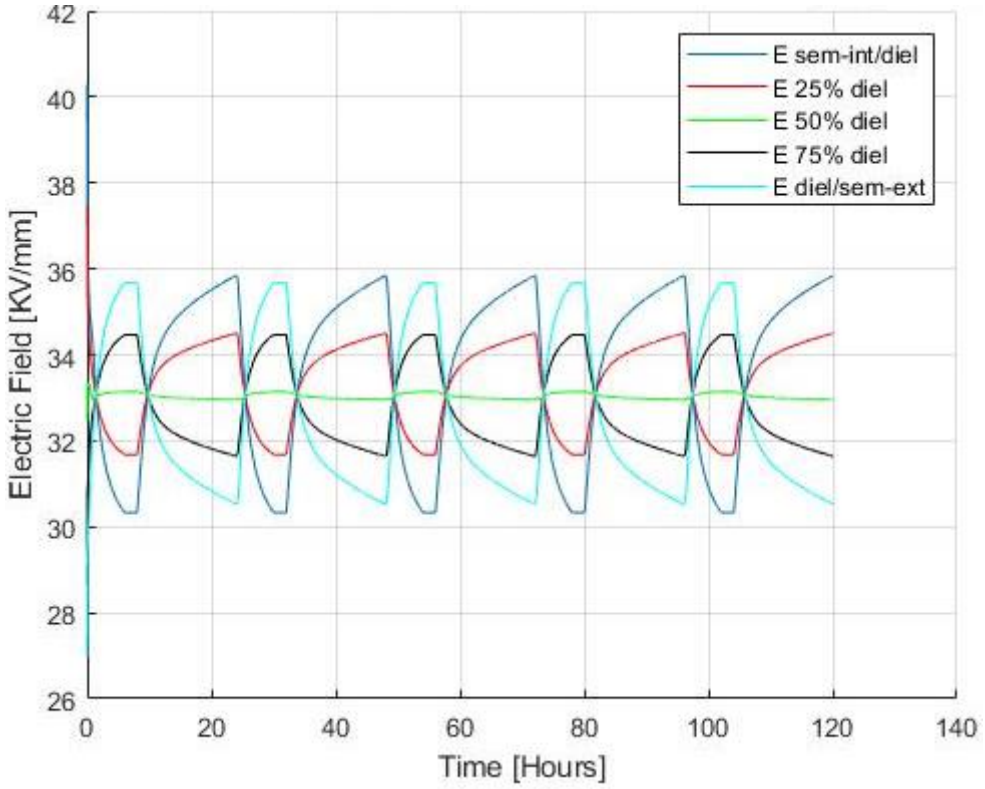

Figure 4.41 – Transient exact electric field profile during the first 5 cycles of the 24-hour Load Cycles period (LC) under the Type Test conditions at 5 points of the insulation of the sample cable for a_M, b_M.

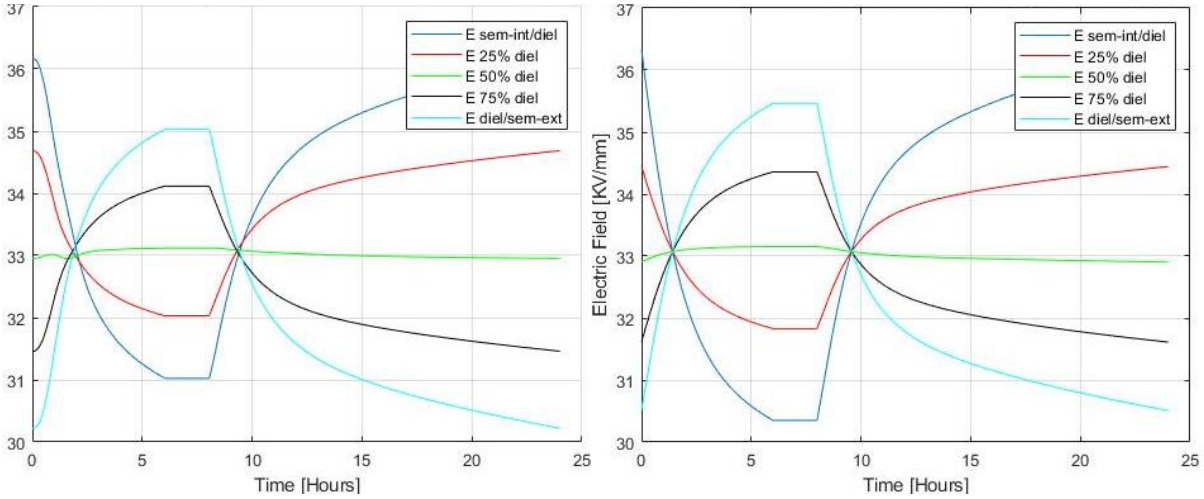

Figure 4.42 – comparison between exact (a) and approximated (b) transient electric field during the 24-hour Load Cycles period (LC) under the Type Test conditions at 5 points of the insulation of the sample cable for a_M, b_M.

- **48-hour Load Cycles**

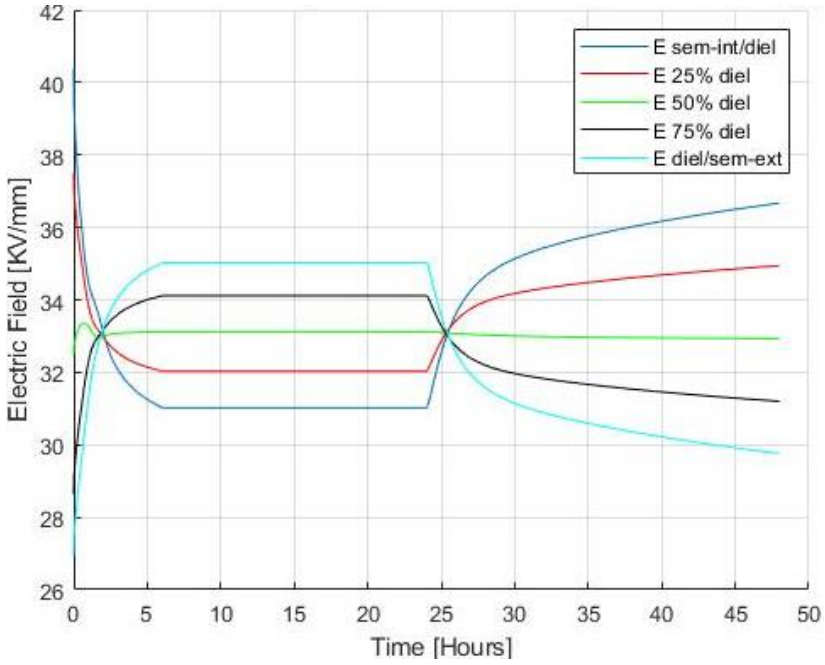

Figure 4.43 – Transient exact electric field during the 1'st cycle of the 24-hour Load Cycles period (LC) under the Type Test conditions at 5 points of the insulation of the sample cable for a_M, b_M.

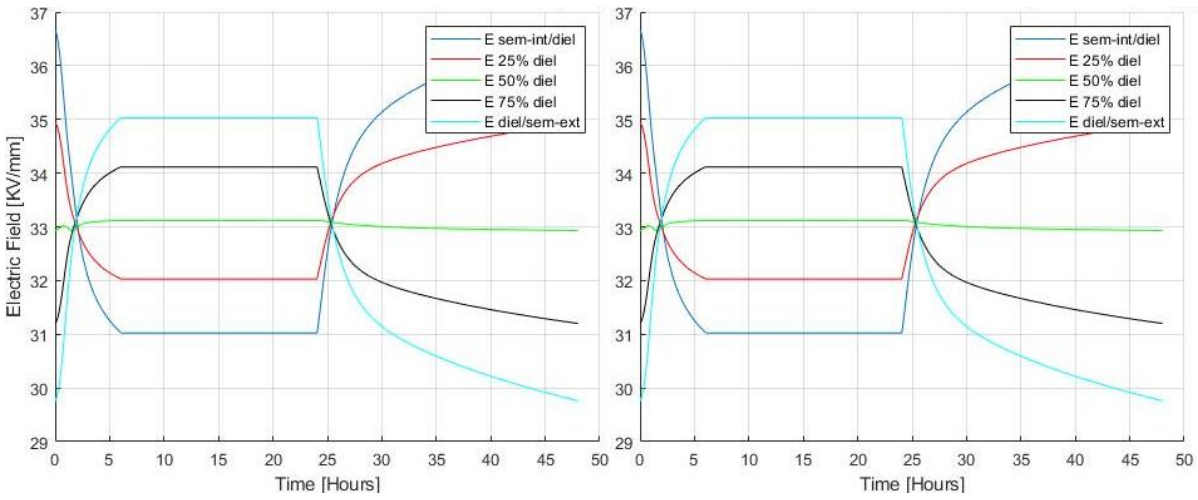

Figure 4.44 – Transient exact electric field during the 2'nd (a) and the 3'rd (b) cycles of the 24-hour Load Cycles period (LC) under the Type Test conditions at 5 points of the insulation of the sample cable for a_M, b_M.

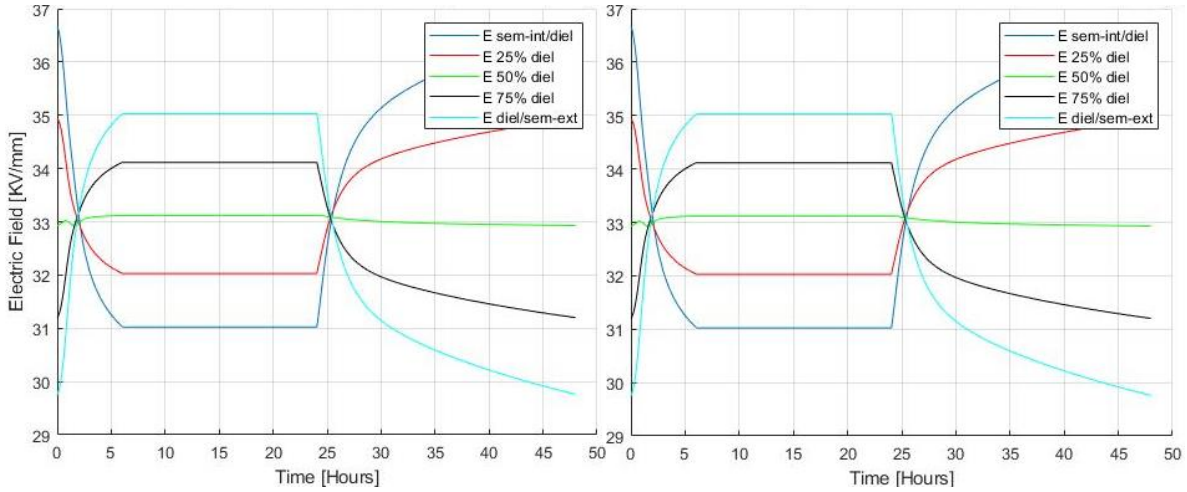

Figure 4.45 – Transient exact electric field during the 4'th (a) and the 5'th (b) cycles of the 24-hour Load Cycles period (LC) under the Type Test conditions at 5 points of the insulation of the sample cable for a_M, b_M.

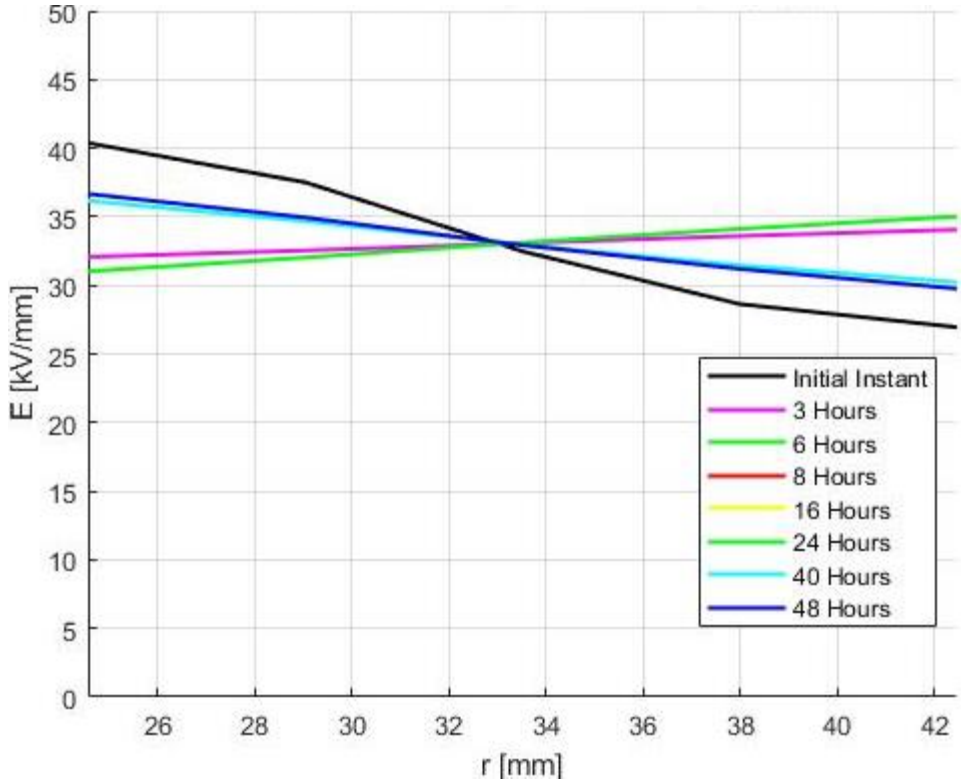

Figure 4.46 – Transient exact electric field profile during the 1'st cycle of the 24-hour Load Cycles period (LC) under the Type Test conditions at 5 points of the insulation of the sample cable for a_M, b_M.

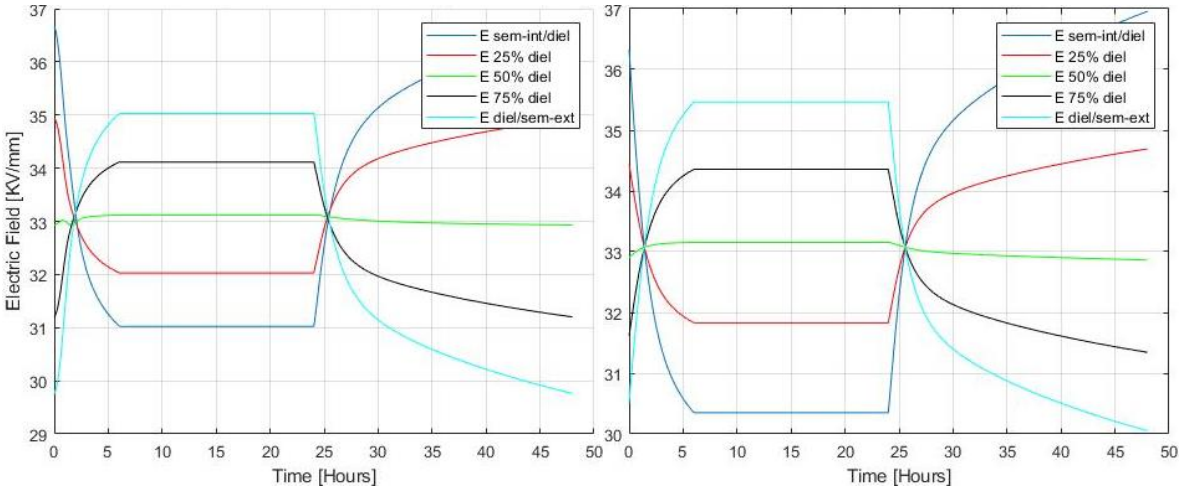

Figure 4.47 – comparison between exact (a) and approximated (b) transient electric field during the 24-hour Load Cycles period (LC) under the Type Test conditions at 5 points of the insulation of the sample cable for a_M, b_M.

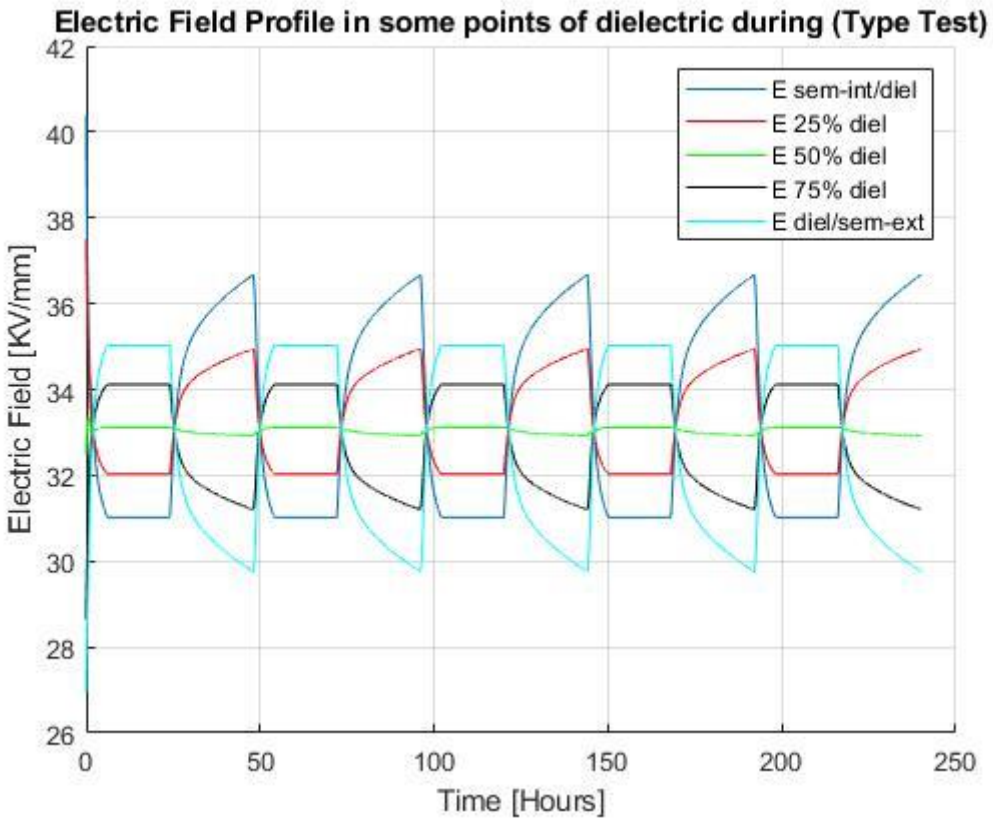

Figure 4.48 – Transient exact electric field profile during the first 5 cycles of the 48-hour Load Cycles period (LC) under the Type Test conditions at 5 points of the insulation of the sample cable for a_M, b_M.

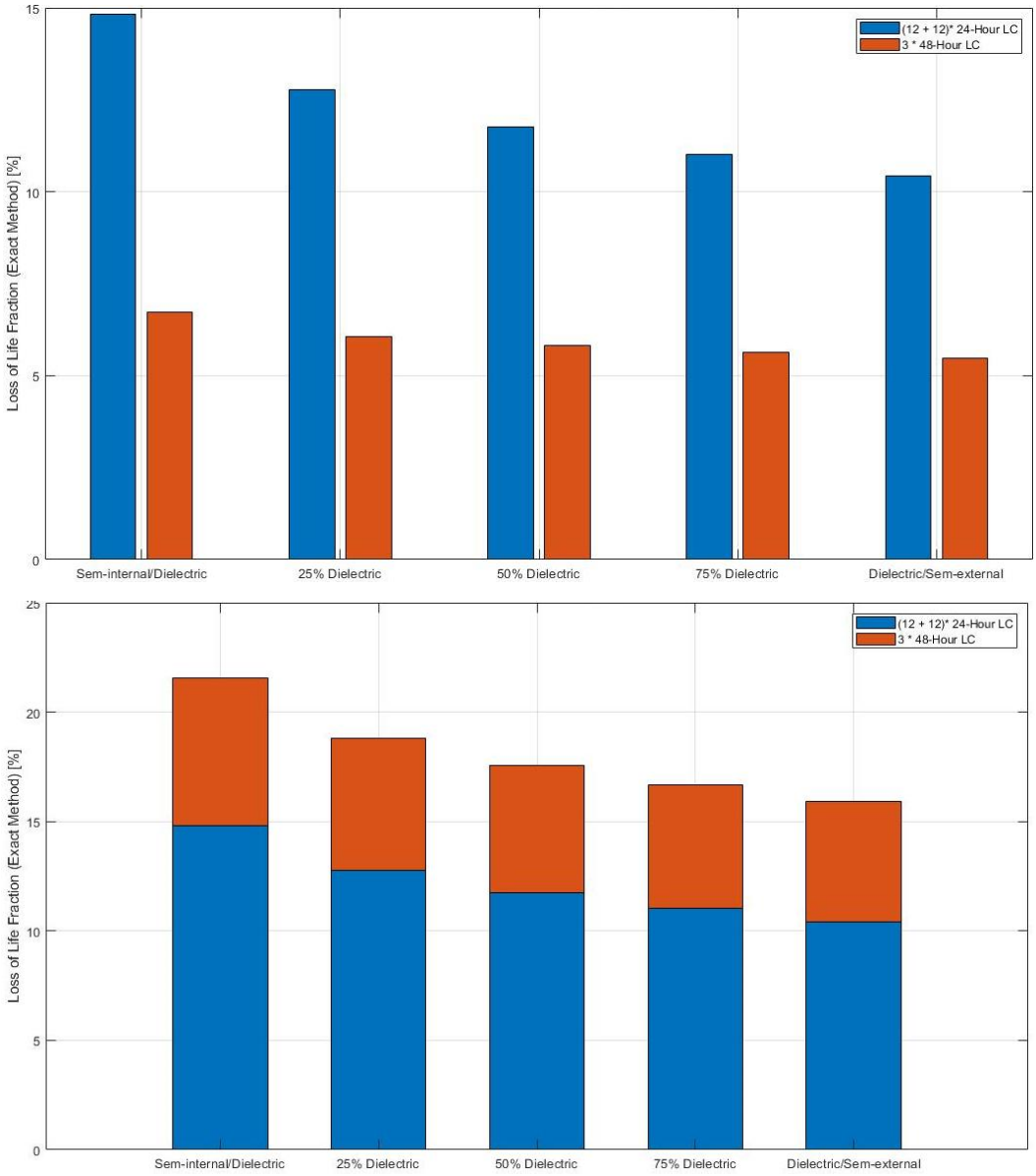

Figure 4.49 – Exact loss-of-life fractions during 12 + 12 cycles of 24-hour Load Cycle (LC) and 3 cycles of 48 hours Load Cycle (LC) under the Type Test conditions at 5 points of the insulation of the sample cable for a_M, b_M.

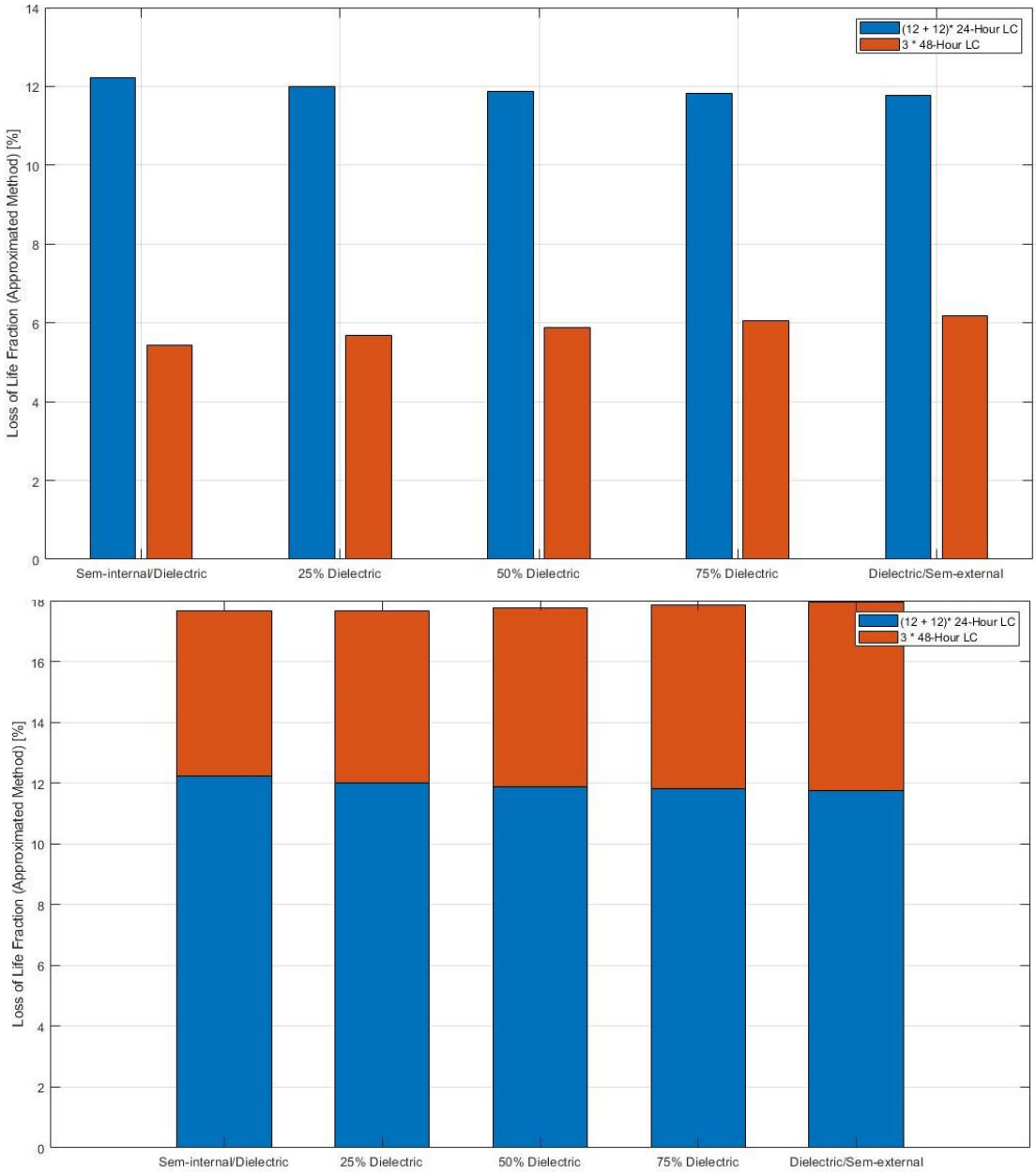

Figure 4.50 – Approximated loss-of-life fractions during 12+12 cycles of 24-hour Load Cycles (LC) and 3 cycles of 48-hour Load Cycles (LC) under the Type Test conditions at 5 points of the insulation of the sample cable for a_M, b_M

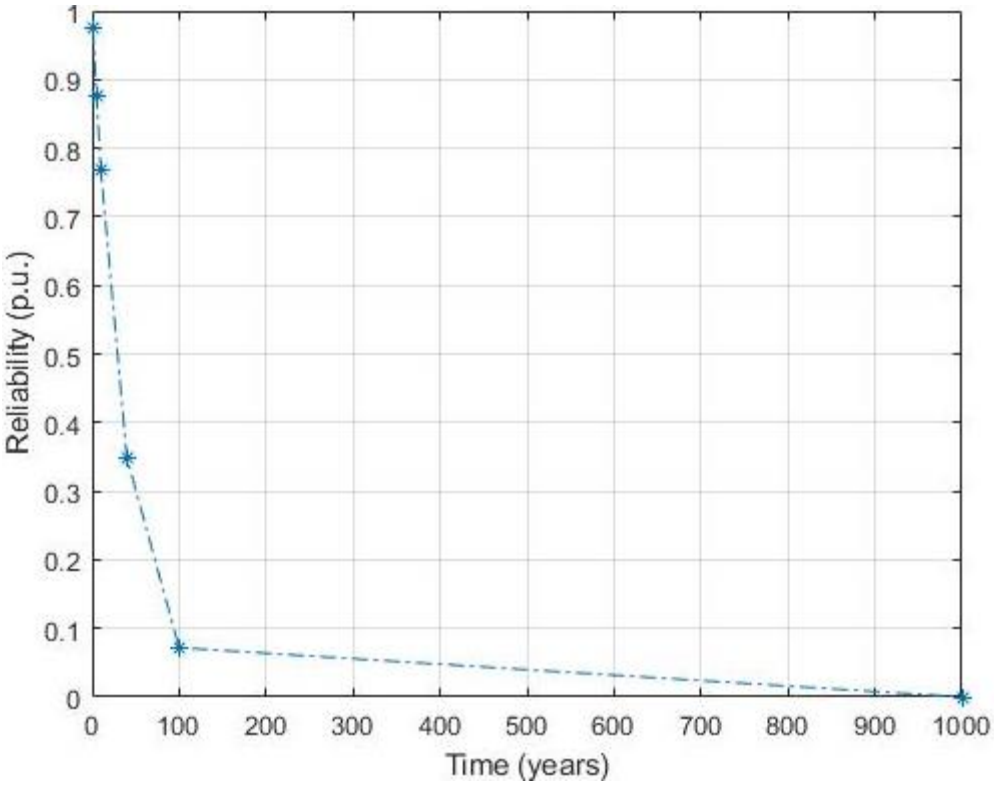

Figure 4.51 – Exact reliability during 12 + 12 cycles of 24-hour Load Cycles (LC) and 3 cycles of 48-hour Load Cycles (LC) under the Type Test conditions of the insulation of the sample cable for a_M, b_M.

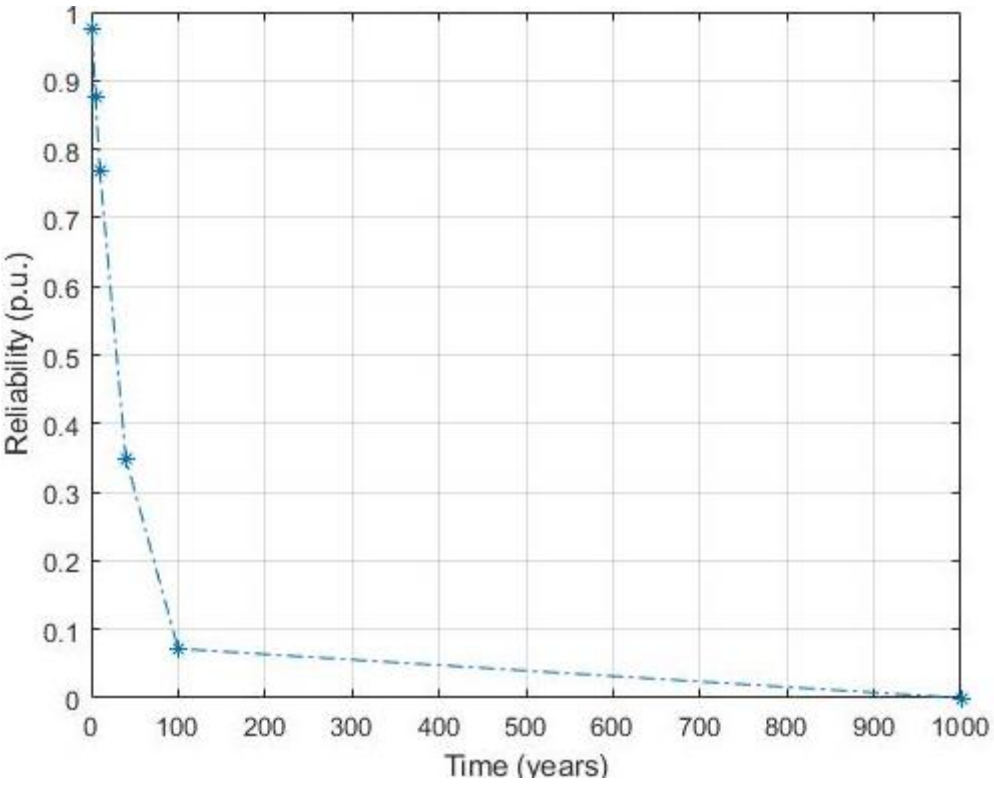

Figure 4.52 – Approximated reliability during 12 + 12 cycles of 24-hour Load Cycles (LC) and 3 cycles of 48-hour Load Cycles (LC) under the Type Test conditions of the insulation of the sample cable for a_M, b_M.

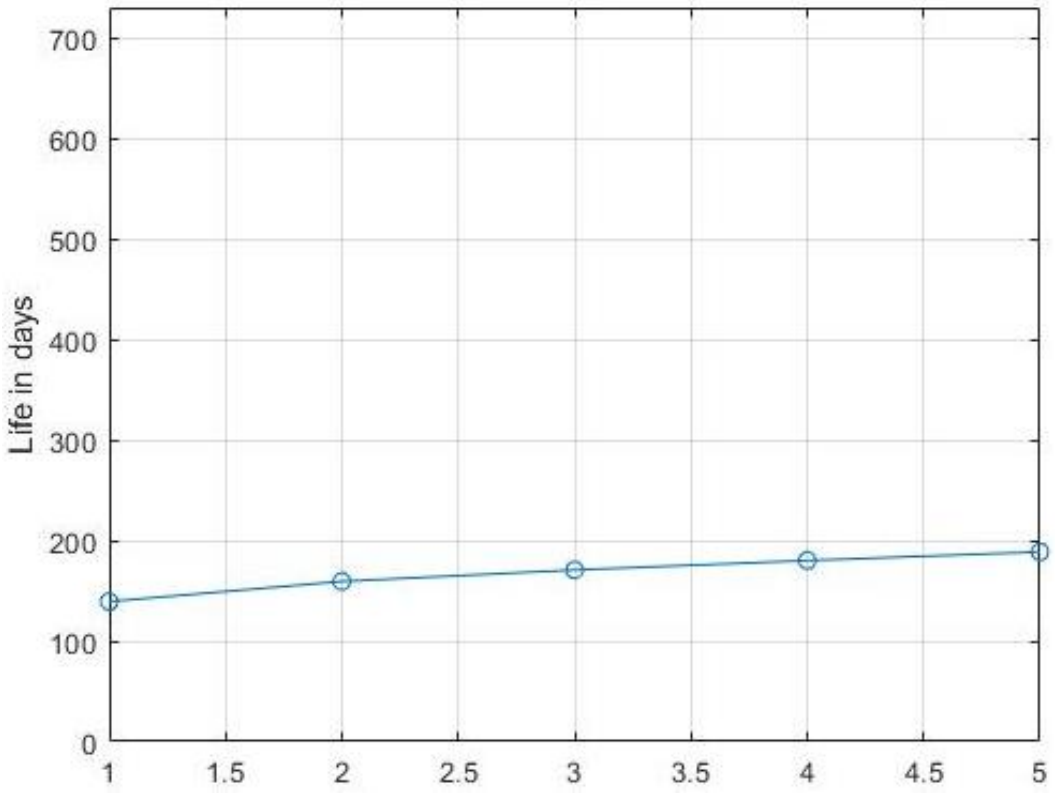

Figure 4.53 – Exact life during 12 + 12 cycles of 24-hour Load Cycles (LC) and 3 cycles of 48-hour Load Cycles (LC) under the Type Test conditions at 5 points of the insulation of the sample cable for a_M, b_M.

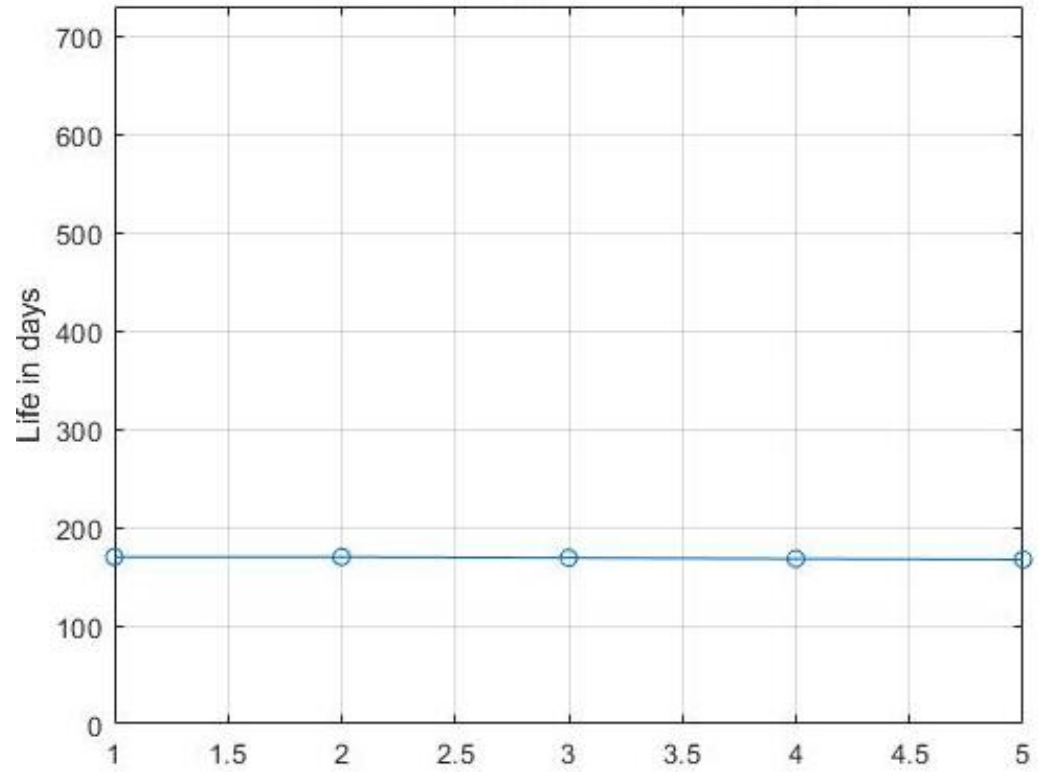

Figure 4.54 – Approximated life during 12 + 12 cycles of 24-hour Load Cycles (LC) and 3 cycles of 48-hour Load Cycles (LC) under the Type Test conditions at 5 points of the insulation of the sample cable for a_M, b_M.

Results in the case of high values of *a* and *b*:

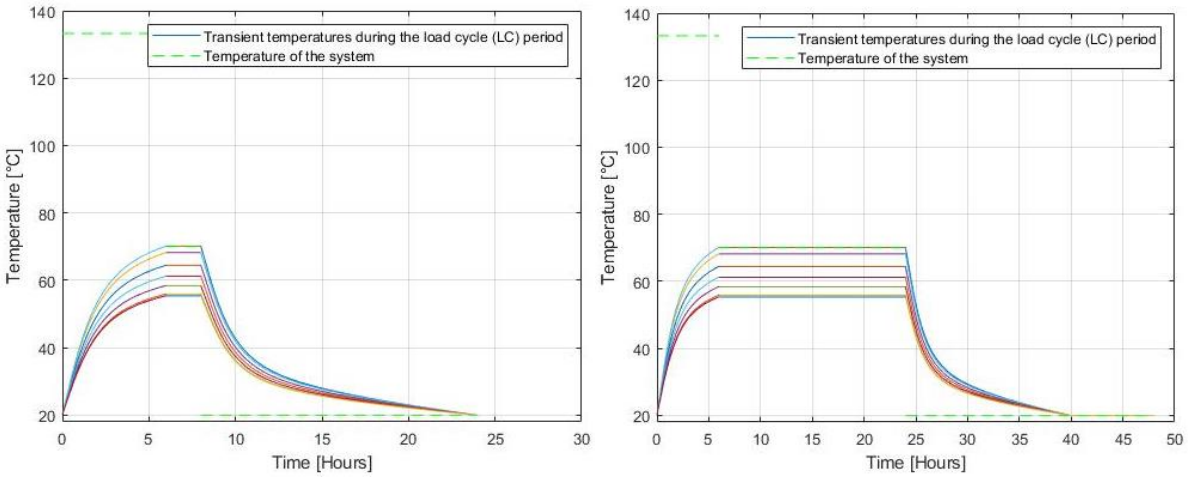

Figure 4.55 - Thermal profiles of 24-hour and 48-hour Load Cycles

1) Test under the rated voltage U_o:

- **24-hour Load Cycles**

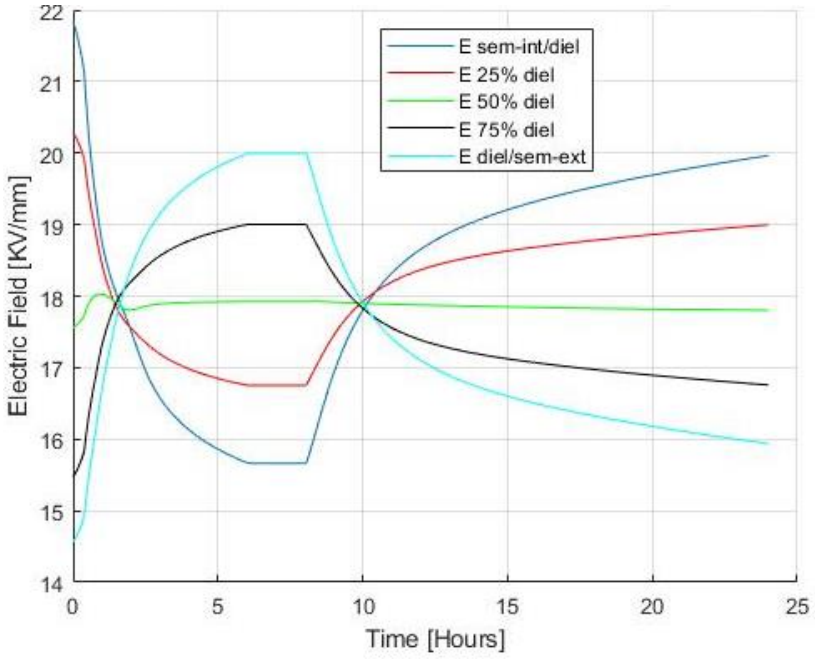

Figure 4.56 – Transient exact electric field during the 1'st cycle of the 24-hour Load Cycles period (LC) under the rated voltage U_o at 5 points of the insulation of the sample cable for a_H, b_H.

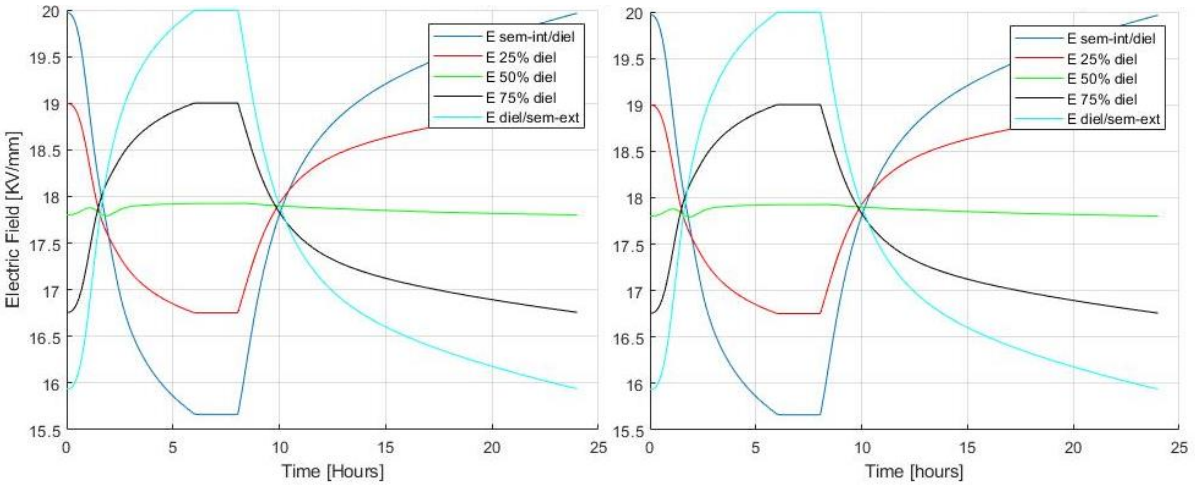

Figure 4.57 – Transient exact electric field during the 2'nd (a) and the 3'rd (b) cycles of the 24-hour Load Cycles period (LC) under the rated voltage U_o at 5 points of the insulation of the sample cable for a_H, b_H.

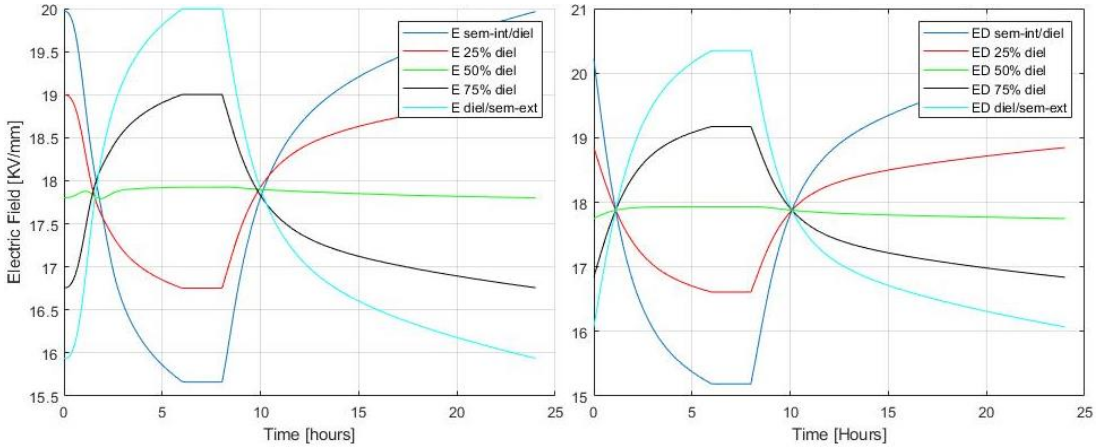

Figure 4.58 – comparison between exact (a) and approximated (b) transient electric field during the 24-hour Load Cycles period (LC) under the rated voltage U_o at 5 points of the insulation of the sample cable for a_H, b_H.

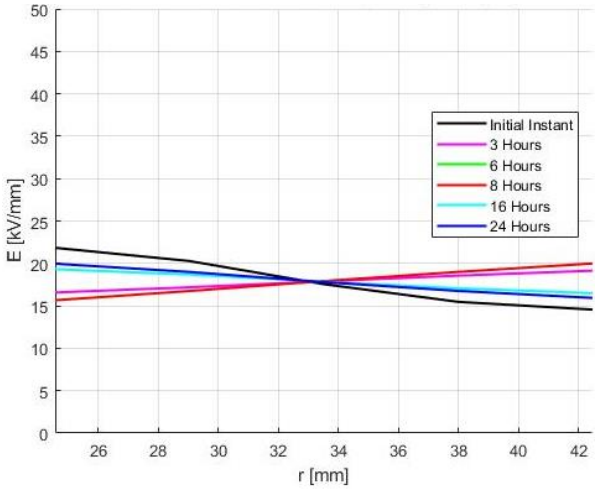

Figure 4.59 – Transient exact electric field profile during the 1'st cycle of the 24-hour Load Cycles period (LC) under the rated voltage U_o at 5 points of the insulation of the sample cable for a_H, b_H.

- **48-hour Load Cycles**

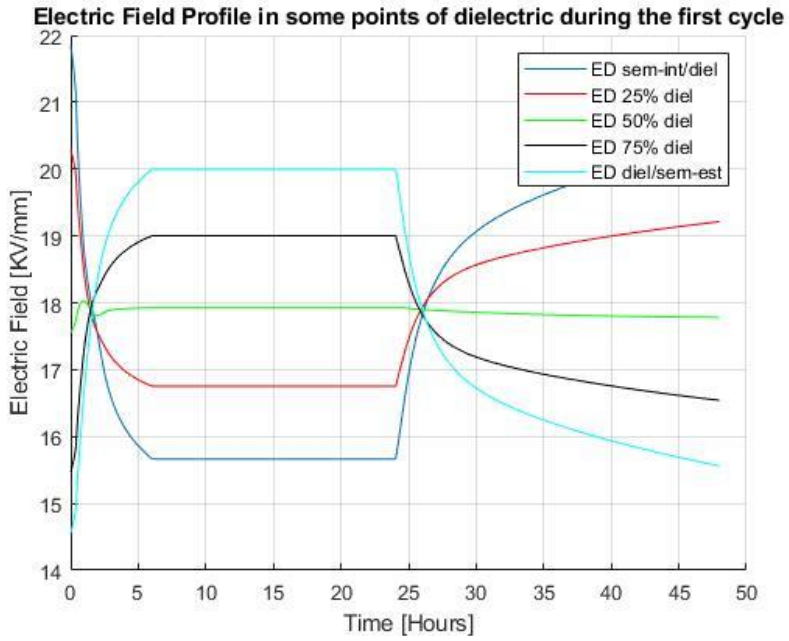

Figure 4.60 – Transient exact electric field during the 1'st cycle of the 48-hour Load Cycles period (LC) under the rated voltage U_o at 5 points of the insulation of the sample cable for a_H, b_H.

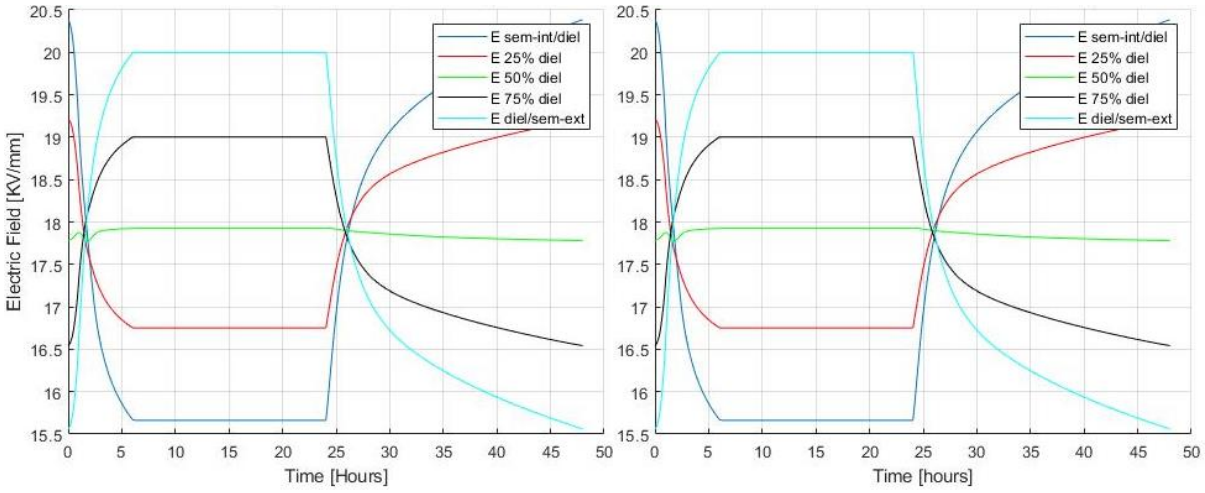

Figure 4.61 – Transient exact electric field during the 2'nd (a) and the 3'rd (b) cycles of the 48-hour Load Cycles period (LC) under the rated voltage U_o at 5 points of the insulation of the sample cable for a_H, b_H.

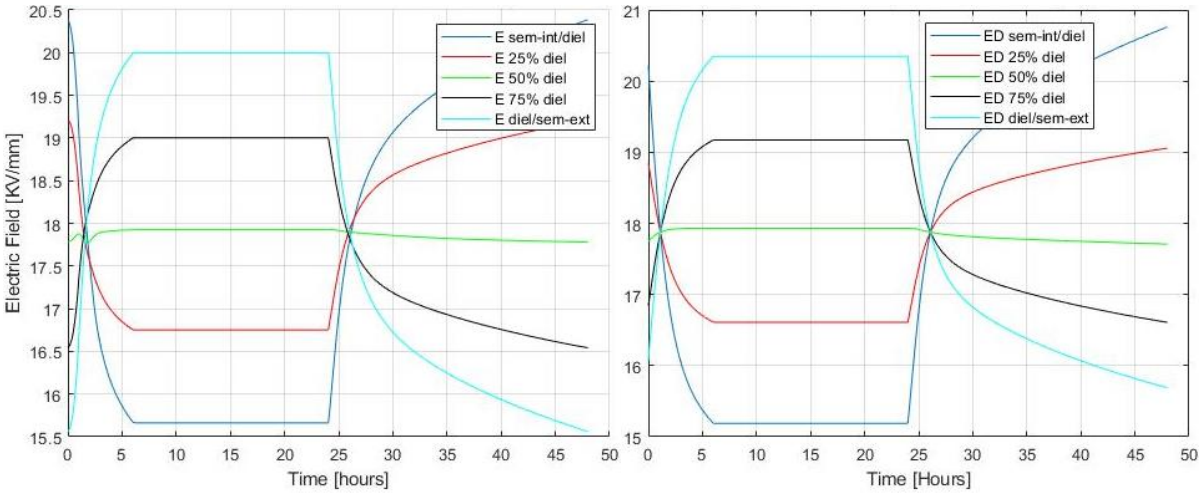

Figure 4.62 – comparison between exact (a) and approximated (b) transient electric field during the 48-hour Load Cycles period (LC) under the rated voltage U_o at 5 points of the insulation of the sample cable for a_H, b_H.

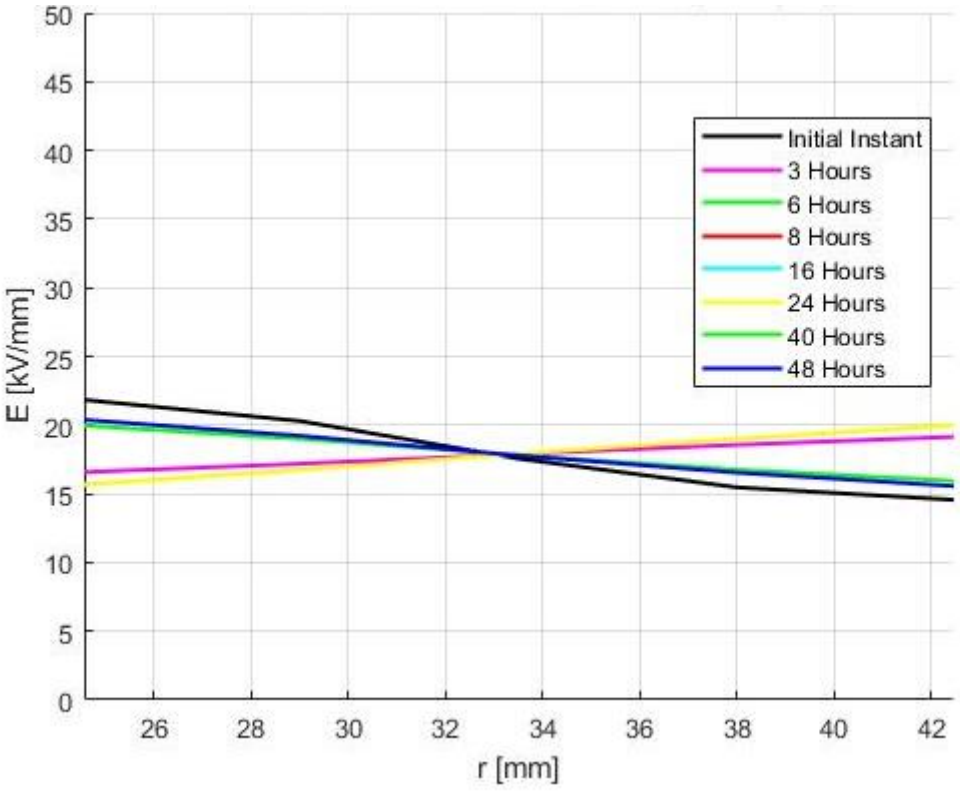

Figure 4.63 – Transient exact electric field profile during the 1'st cycle of the 48-hour Load Cycles period (LC) under the rated voltage U_o at 5 points of the insulation of the sample cable for a_H, b_H.

2) Test under the Type Test conditions U =1.85 U_o:

- **24-hour Load Cycles**

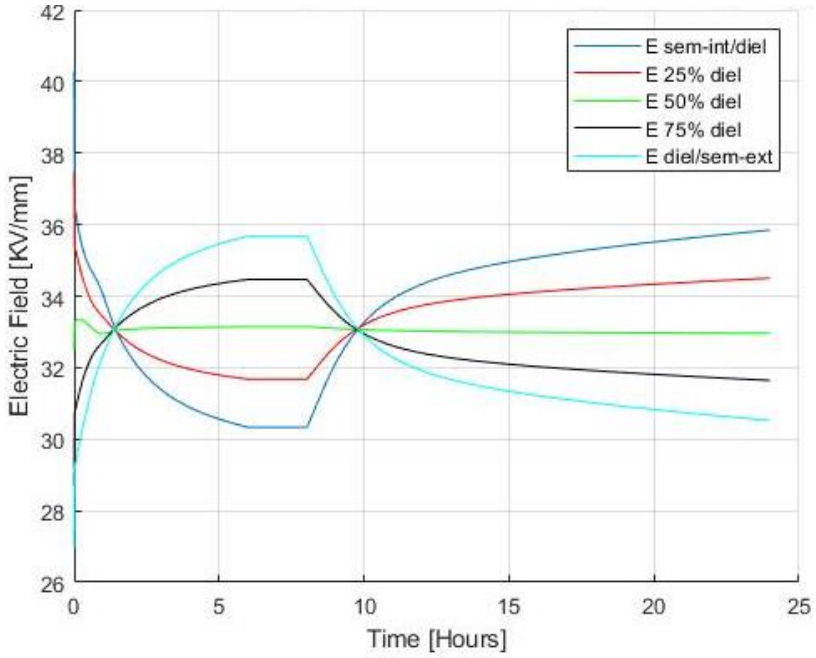

Figure 4.64 – Transient exact electric field during the 1'st cycle of the 24-hour Load Cycles period (LC) under the Type Test conditions at 5 points of the insulation of the sample cable for a_H, b_H.

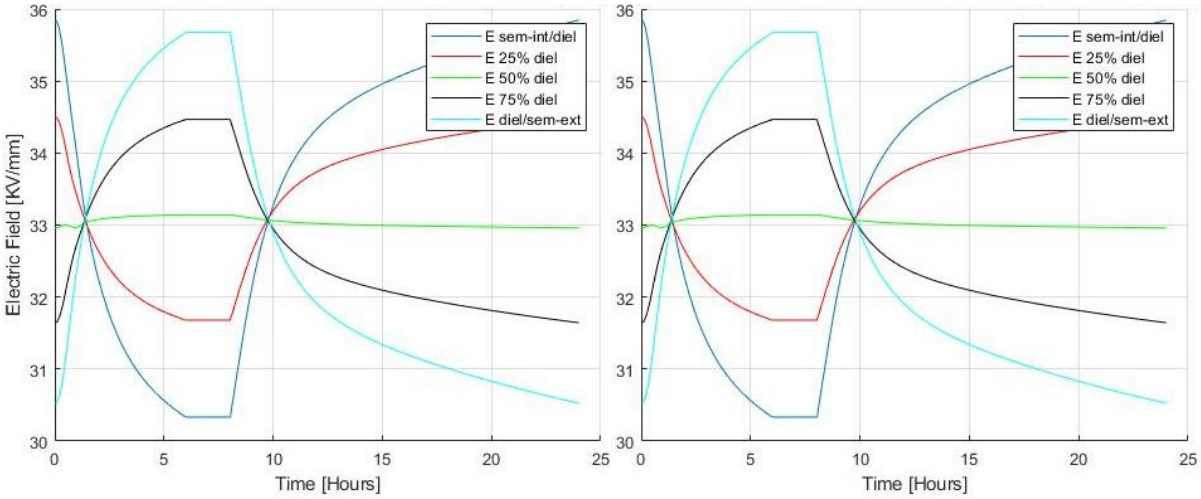

Figure 4.65 – Transient exact electric field during the 2'nd (a) and the 3'rd (b) cycles of the 24-hour Load Cycles period (LC) under the Type Test conditions at 5 points of the insulation of the sample cable for a_H, b_H.

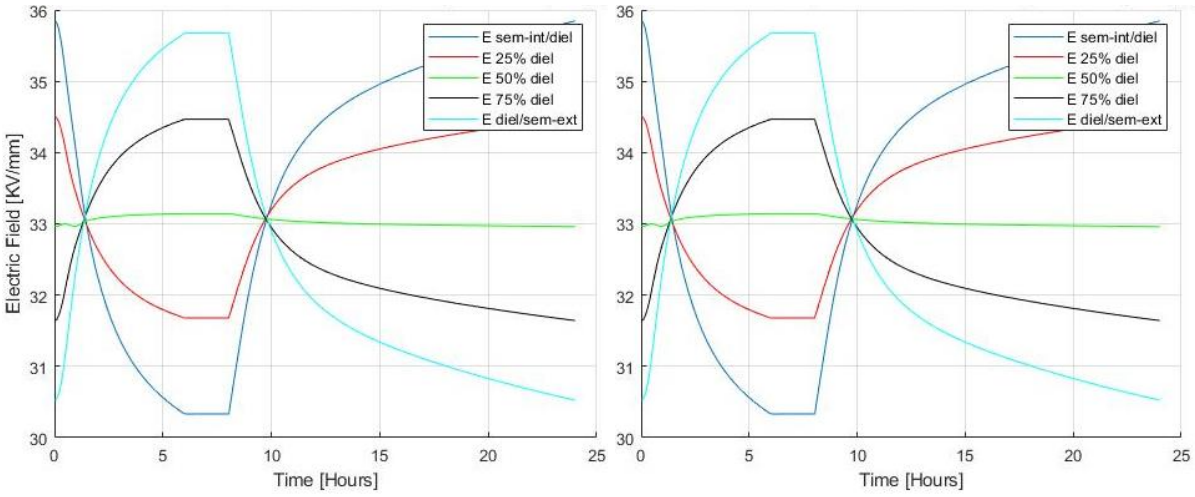

Figure 4.66 – Transient exact electric field during the 4'th (a) and the 5'th (b) cycles of the 24-hour Load Cycles period (LC) under the Type Test conditions at 5 points of the insulation of the sample cable for a_H, b_H.

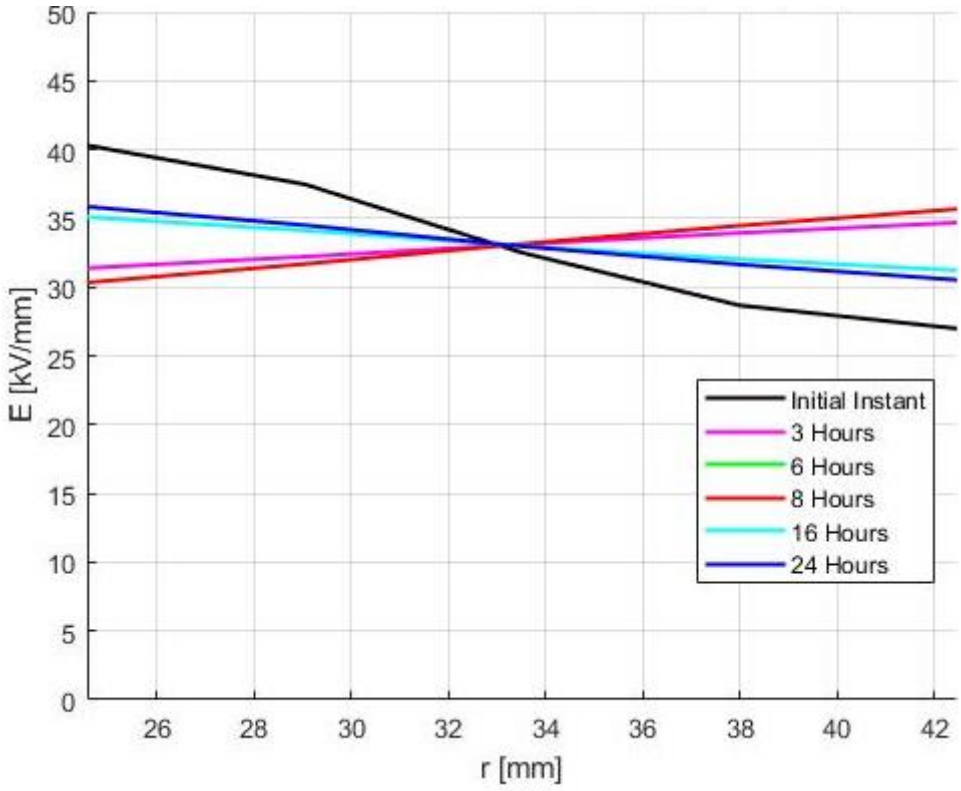

Figure 4.67 – Transient exact electric field profile during the 1'st cycle of the 24-hour Load Cycles period (LC) under the Type Test conditions at 5 points of the insulation of the sample cable for a_H, b_H.

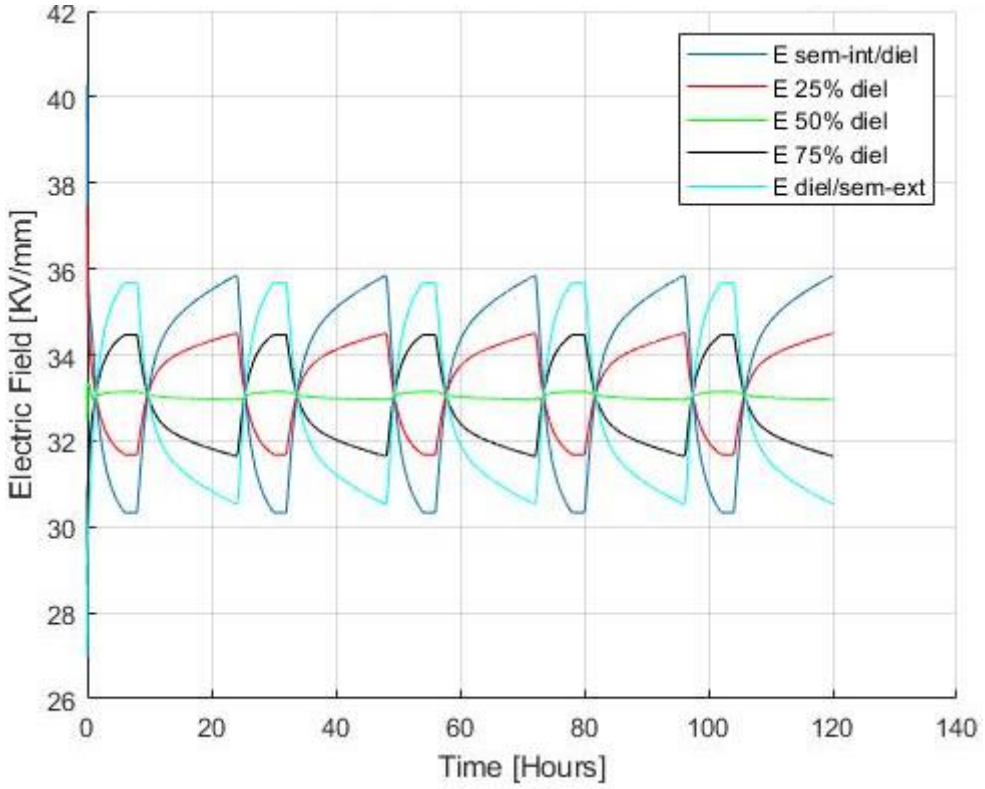

Figure 4.68 – Transient exact electric field profile during the first 5 cycles of the 24-hour Load Cycles period (LC) under the Type Test conditions at 5 points of the insulation of the sample cable for a_H, b_H.

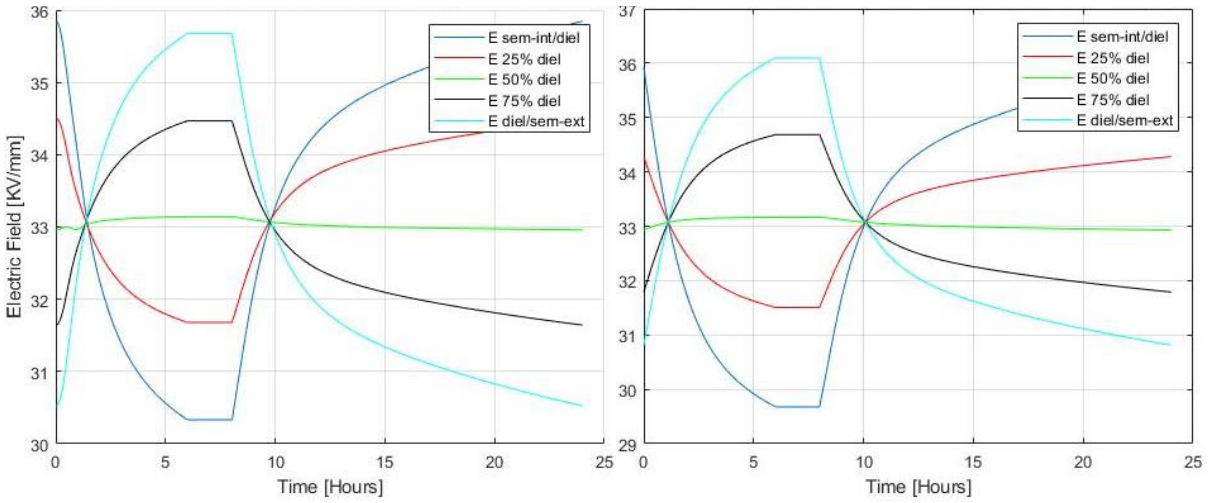

Figure 4.69 – comparison between exact (a) and approximated (b) transient electric field during the 24-hour Load Cycles period (LC) under the Type Test conditions at 5 points of the insulation of the sample cable for a_H, b_H.

- **48-hour Load Cycles**

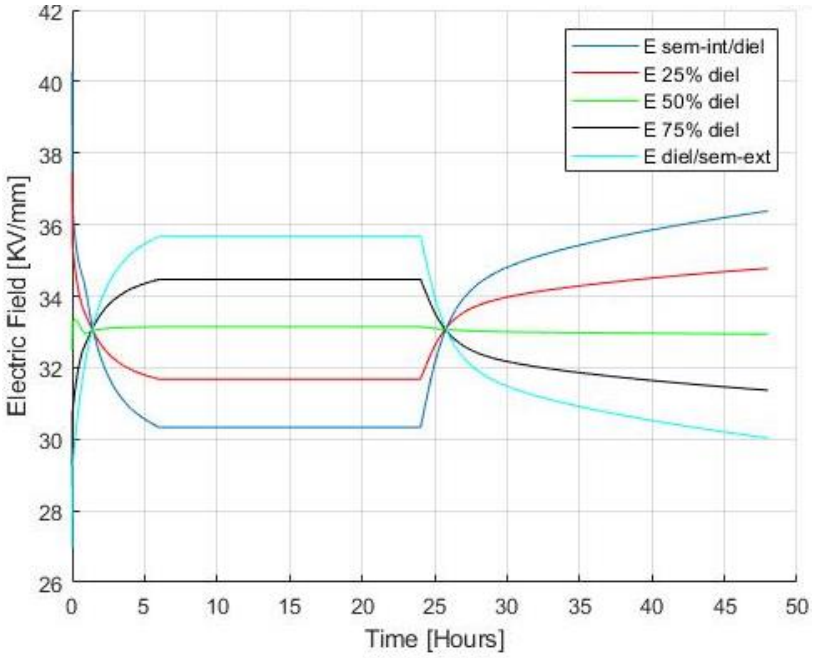

Figure 4.70 – Transient exact electric field during the 1'st cycle of the 48-hour Load Cycles period (LC) under the Type Test conditions at 5 points of the insulation of the sample cable for a_H, b_H.

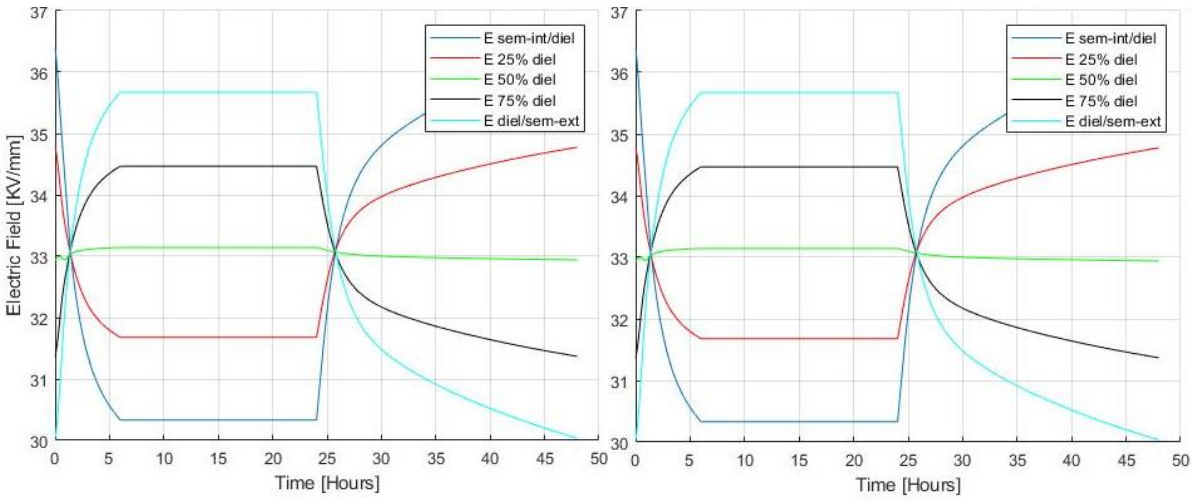

Figure 4.71 – Transient exact electric field during the 2'nd (a) and the 3'rd (b) cycles of the 48-hour Load Cycles period (LC) under the Type Test conditions at 5 points of the insulation of the sample cable for a_H, b_H.

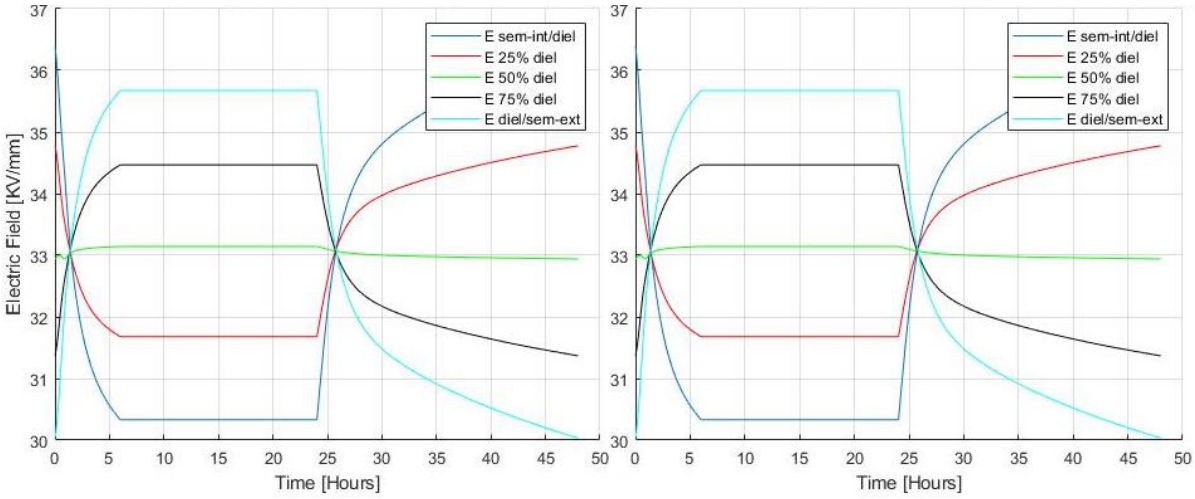

Figure 4.72 – Transient exact electric field during the 4'th (a) and the 5'th (b) cycles of the 48-hour Load Cycles period (LC) under the Type Test conditions at 5 points of the insulation of the sample cable for a_H, b_H.

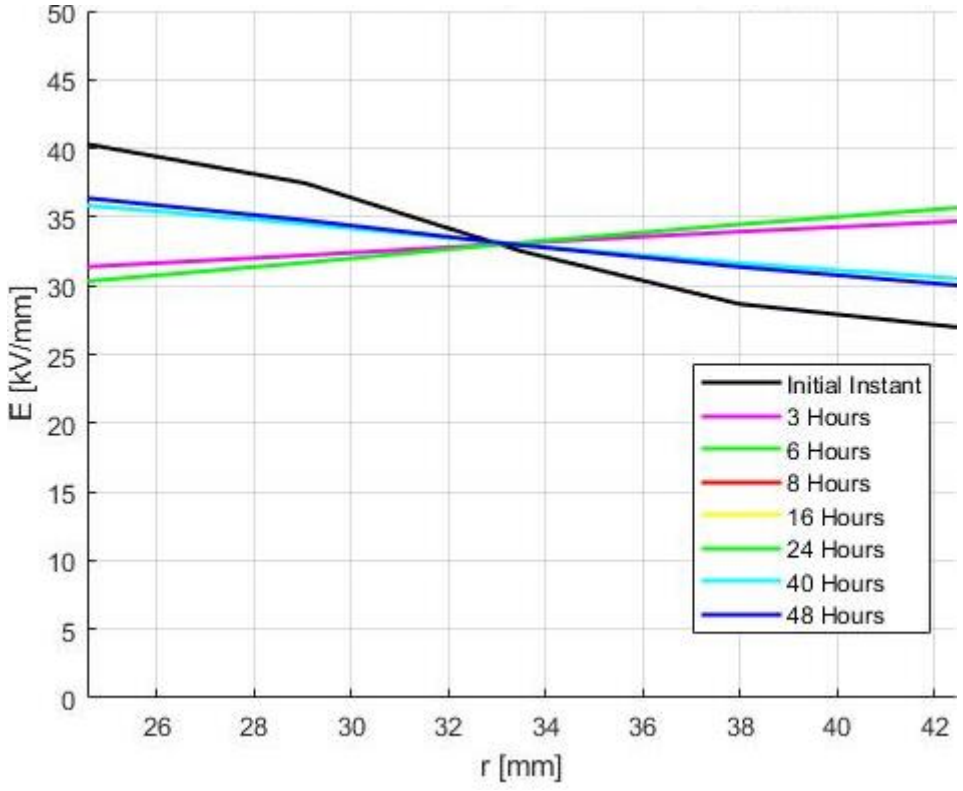

Figure 4.73 – Transient exact electric field profile during the 1'st cycle of the 48-hour Load Cycles period (LC) under the Type Test conditions at 5 points of the insulation of the sample cable for a_H, b_H.

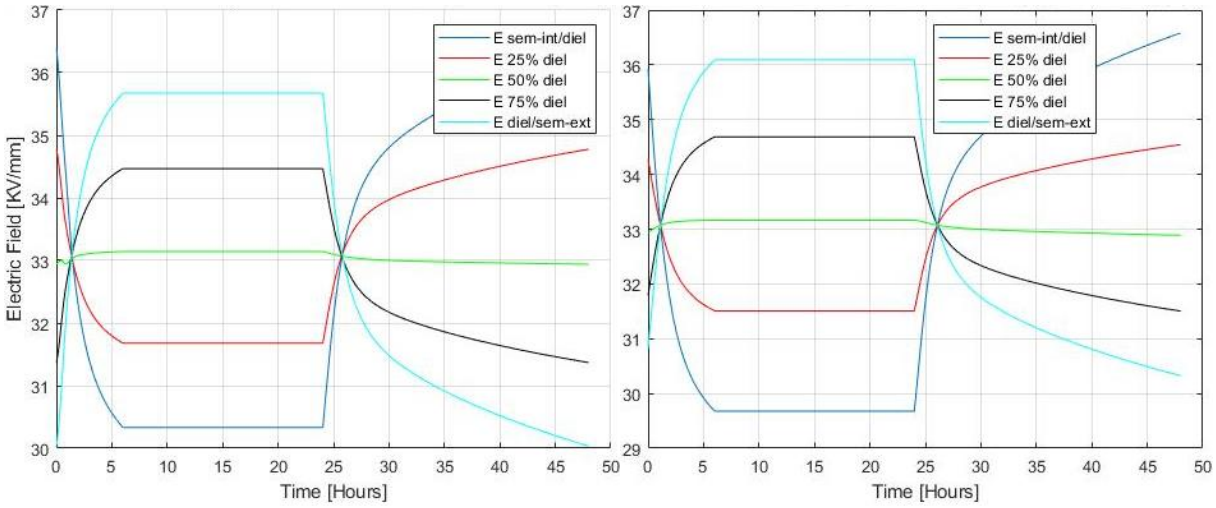

Figure 4.74 – comparison between exact (a) and approximated (b) transient electric field during the 48-hour Load Cycles period (LC) under the Type Test conditions at 5 points of the insulation of the sample cable for a_H, b_H.

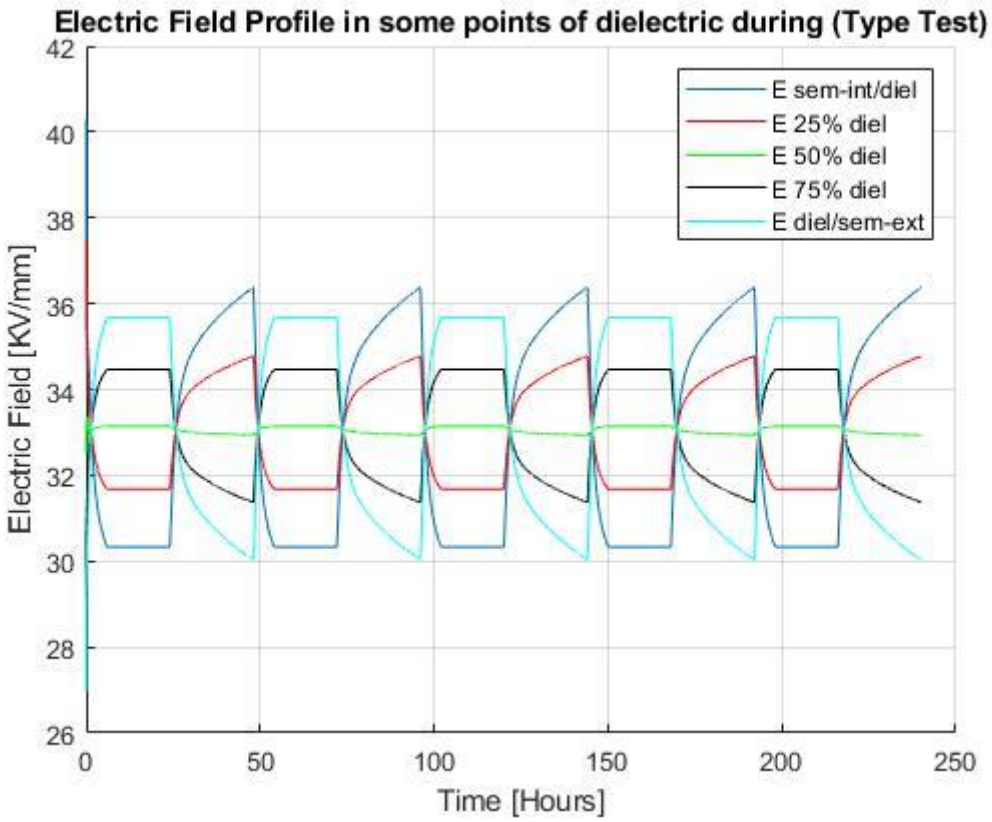

Figure 4.75 – Transient exact electric field profile during the first 5 cycles of the 48-hour Load Cycles period (LC) under the Type Test conditions at 5 points of the insulation of the sample cable for a_H, b_H.

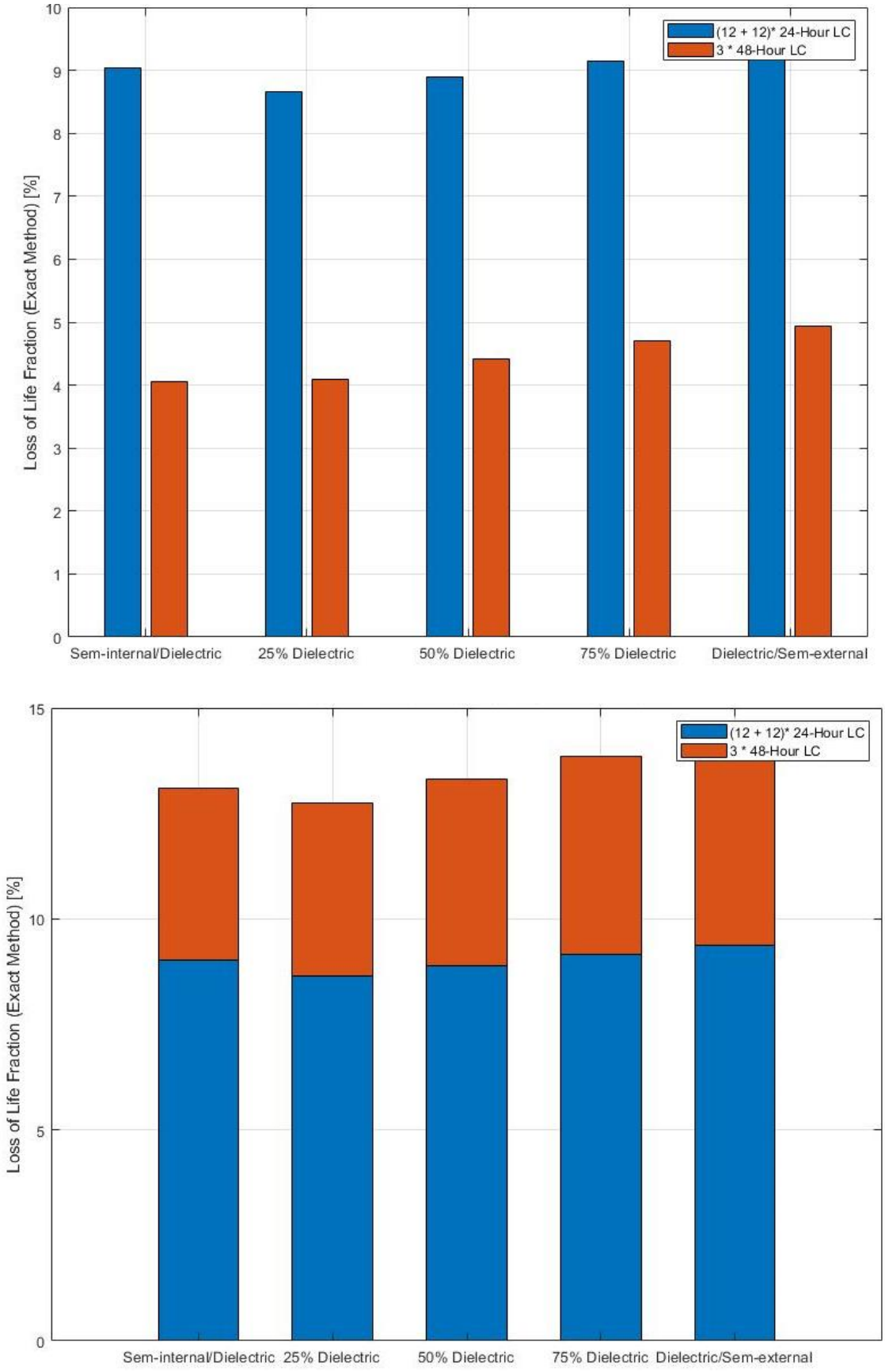

Figure 4.76 – Exact loss-of-life fractions during 12 + 12 cycles of 24-hour Load Cycle (LC) and 3 cycles of 48 hours Load Cycle (LC) under the Type Test conditions at 5 points of the insulation of the sample cable for a_H, b_H.

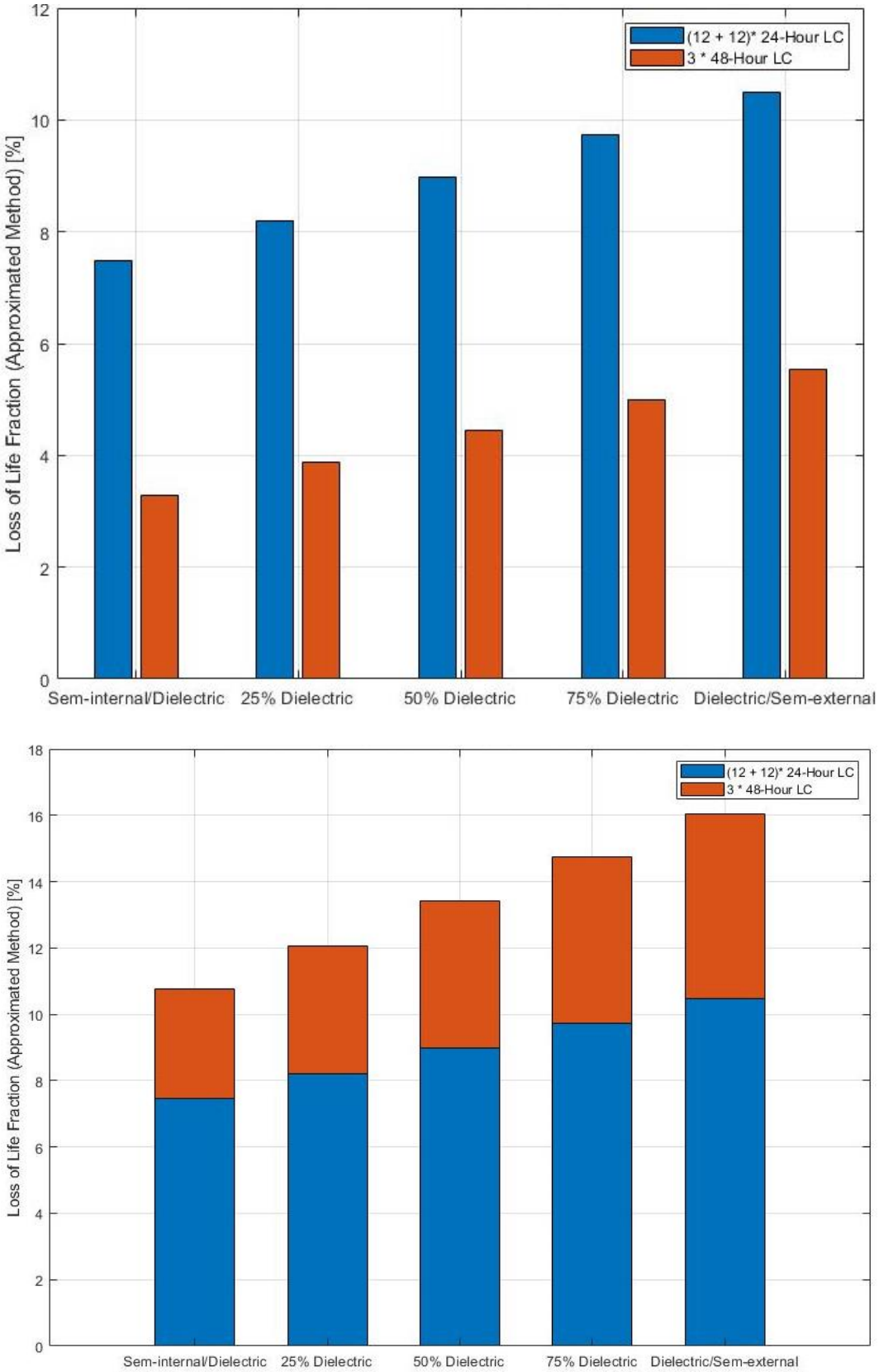

Figure 4.77– Approximated loss-of-life fractions during 12+12 cycles of 24-hour Load Cycles (LC) and 3 cycles of 48-hour Load Cycles (LC) under the Type Test conditions at 5 points of the insulation of the sample cable for a_H, b_H

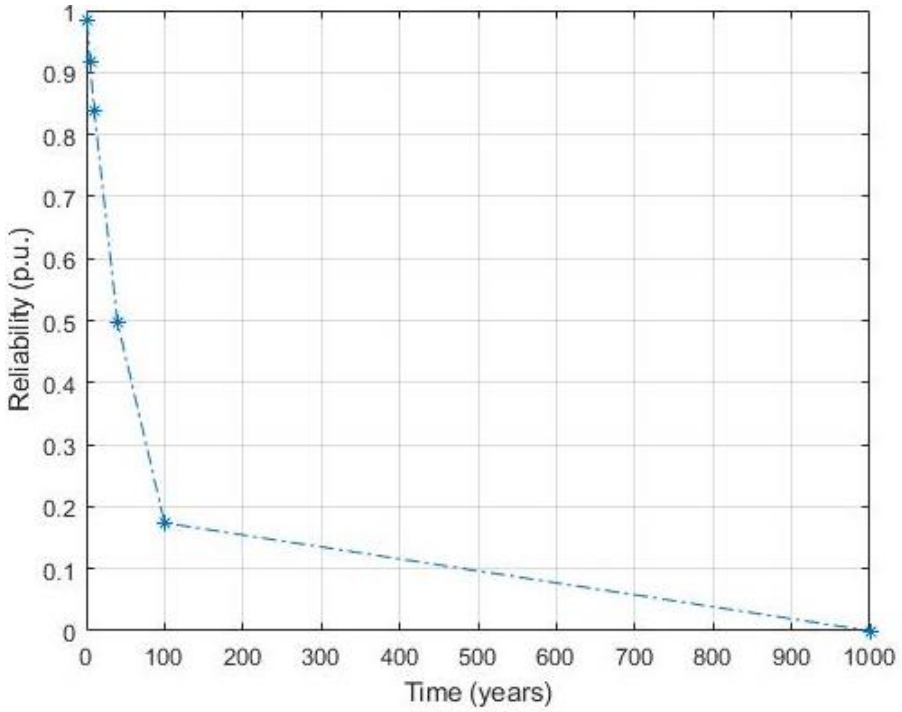

Figure 4.78 – Exact reliability during 12 + 12 cycles of 24-hour Load Cycles (LC) and 3 cycles of 48-hour Load Cycles (LC) under the Type Test conditions of the insulation of the sample cable for a_H, b_H.

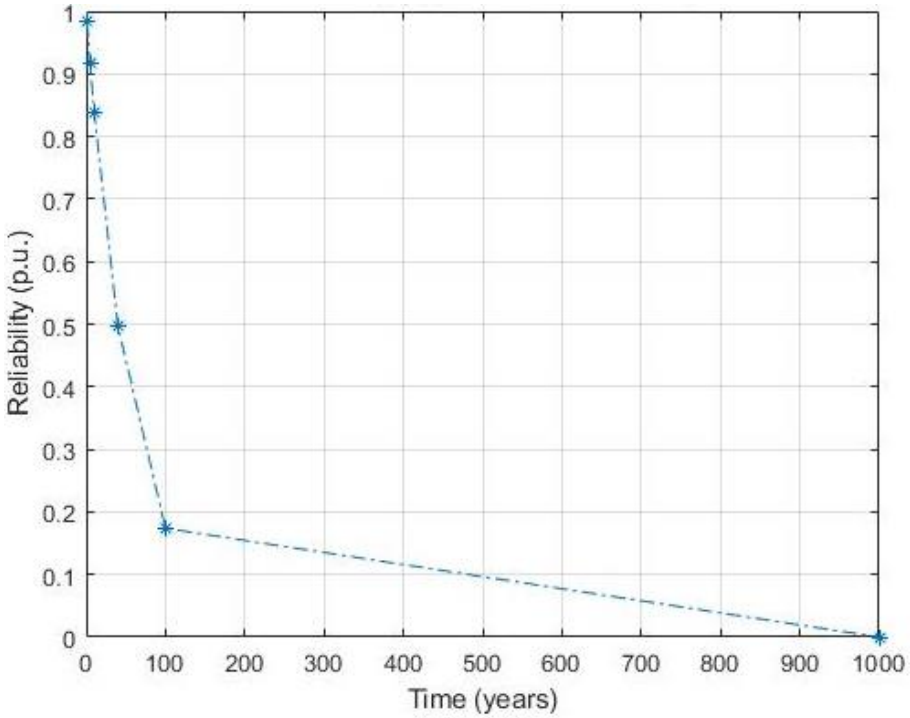

Figure 4.79 – Approximated reliability during 12 + 12 cycles of 24-hour Load Cycles (LC) and 3 cycles of 48-hour Load Cycles (LC) under the Type Test conditions of the insulation of the sample cable for a_H, b_H.

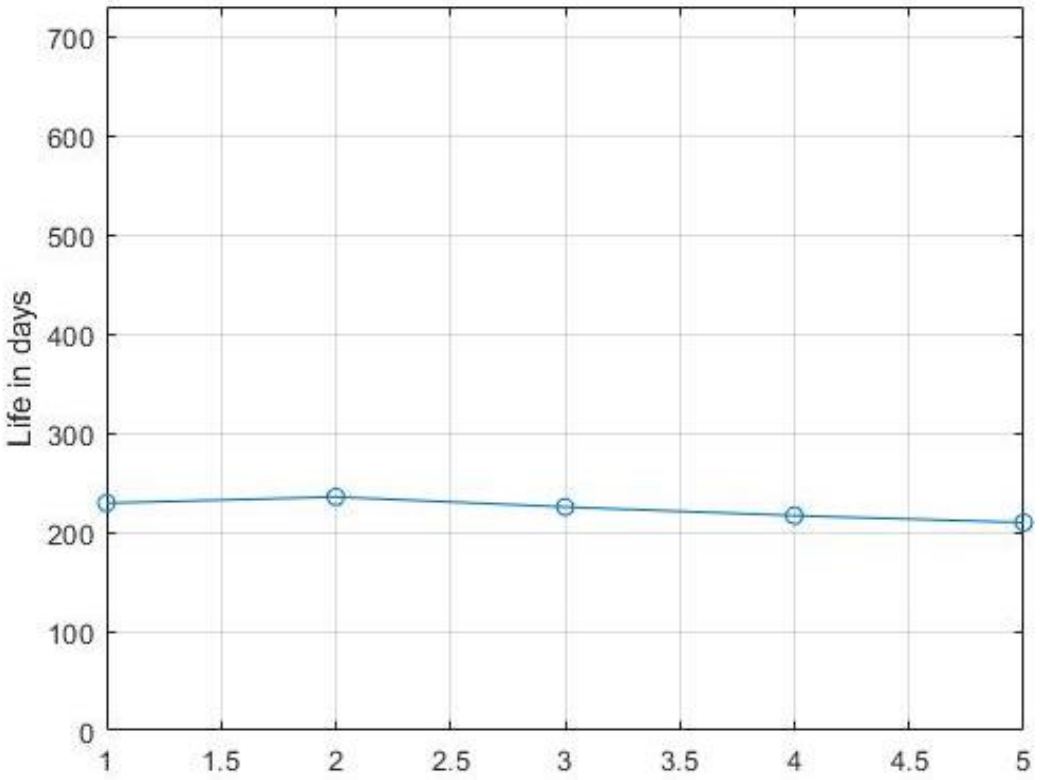

Figure 4.80– Exact life during 12 + 12 cycles of 24-hour Load Cycles (LC) and 3 cycles of 48-hour Load Cycles (LC) under the Type Test conditions at 5 points of the insulation of the sample cable for a_H, b_H.

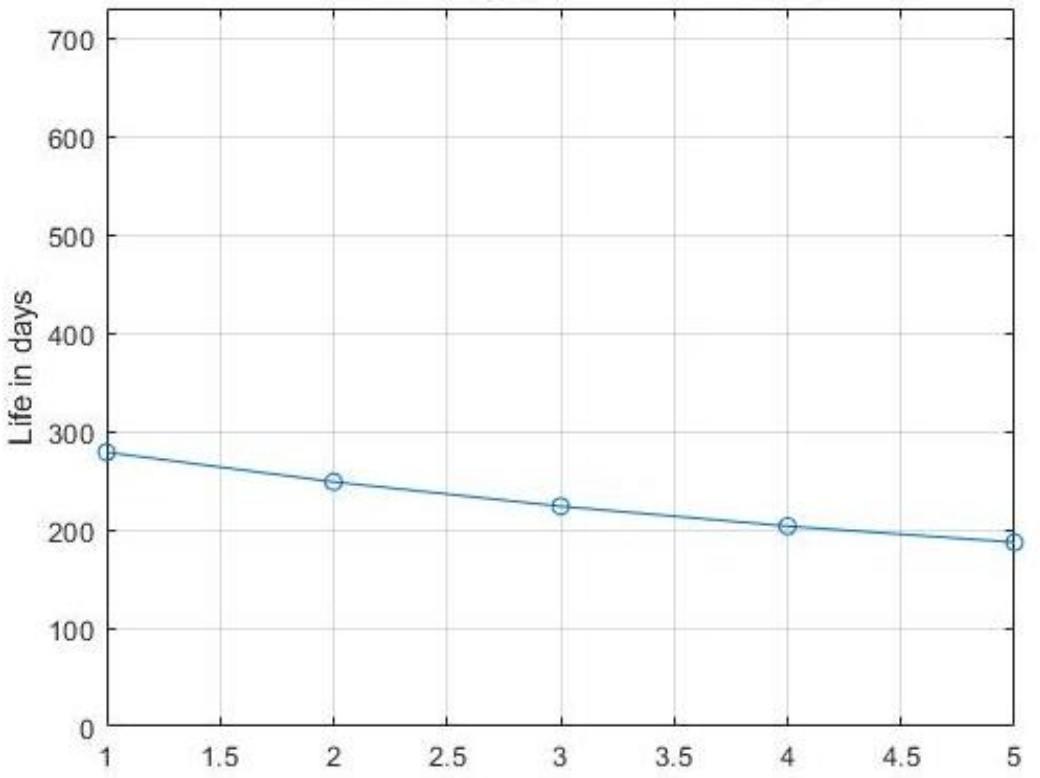

Figure 4.81 – Approximated life during 12 + 12 cycles of 24-hour Load Cycles (LC) and 3 cycles of 48-hour Load Cycles (LC) under the Type Test conditions at 5 points of the insulation of the sample cable for a_H, b_H.

Results in the case of very high values of *a* and *b*:

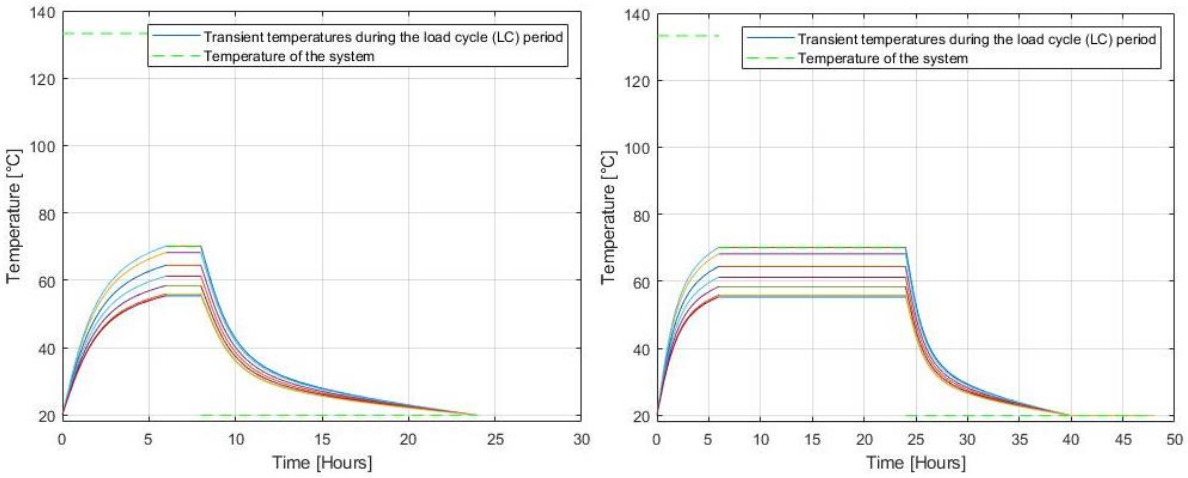

Figure 4.82 - Thermal profiles of 24-hour and 48-hour Load Cycles

3) Test under the rated voltage U_o:

- **24-hour Load Cycles**

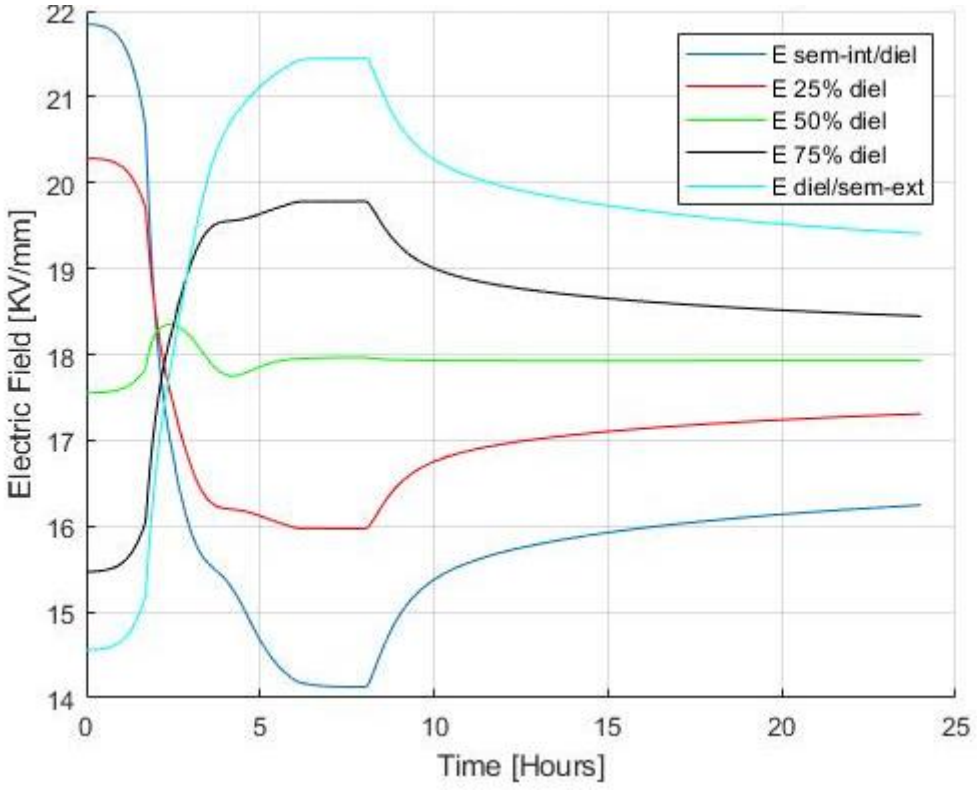

Figure 4.83 – Transient exact electric field during the 1'st cycle of the 24-hour Load Cycles period (LC) under the rated voltage U_o at 5 points of the insulation of the sample cable for a_{VH}, b_{VH}.

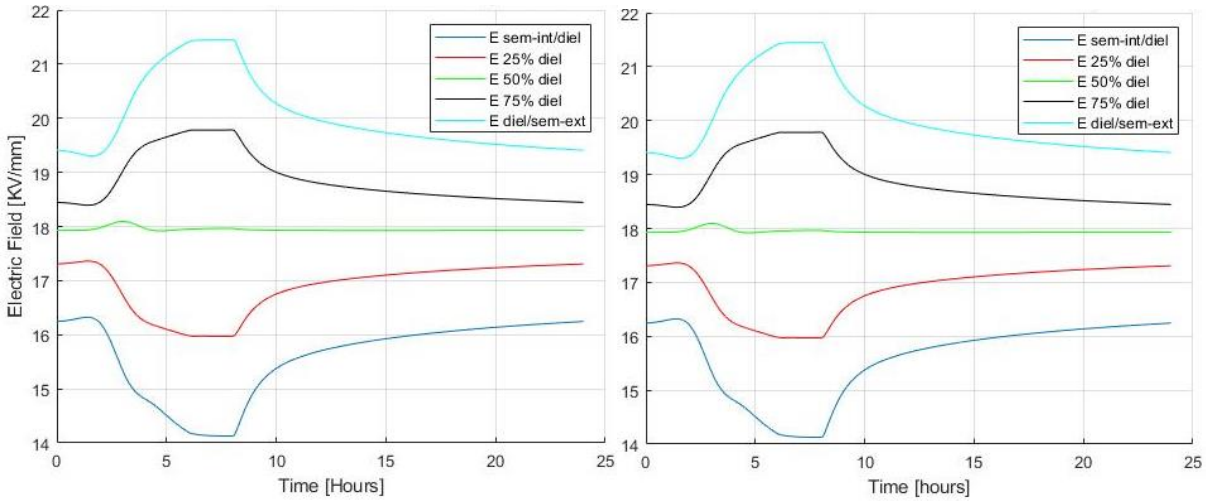

Figure 4.84 – Transient exact electric field during the 2'nd (a) and the 3'rd (b) cycles of the 24-hour Load Cycles period (LC) under the rated voltage U_o at 5 points of the insulation of the sample cable for a_{VH}, b_{VH}.

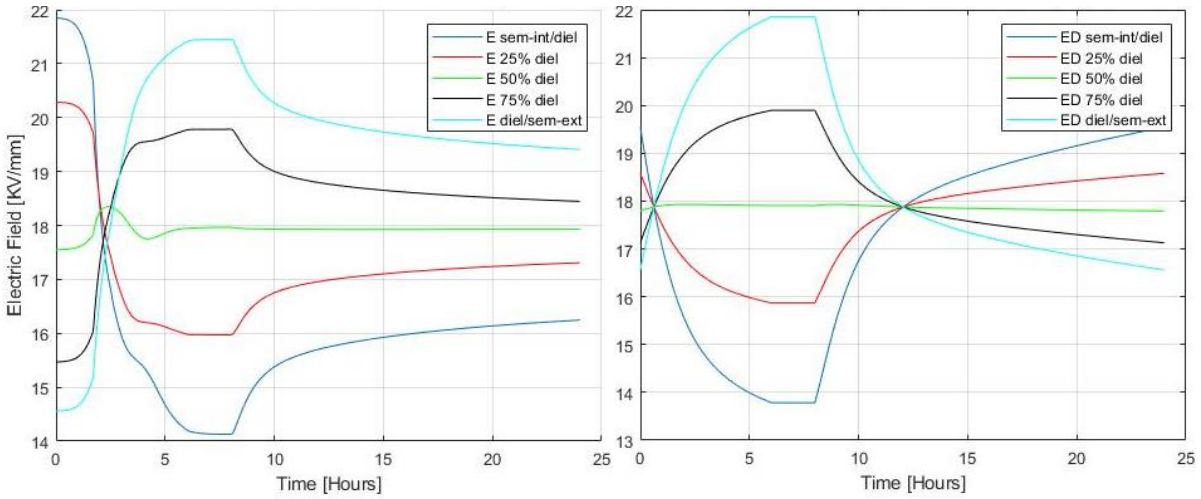

Figure 4.85 – comparison between exact (a) and approximated (b) transient electric field during the 24-hour Load Cycles period (LC) under the rated voltage U_o at 5 points of the insulation of the sample cable for a_{VH}, b_{VH}.

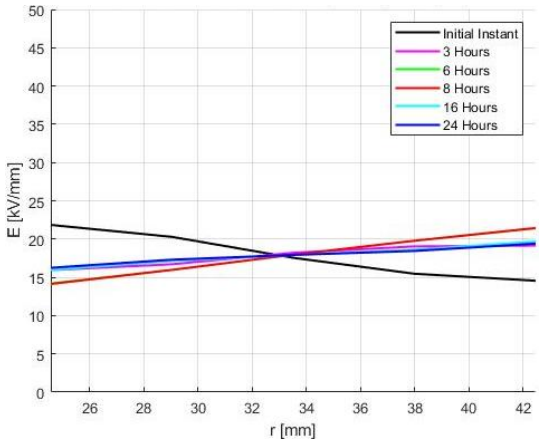

Figure 4.86 – Transient exact electric field profile during the 1'st cycle of the 24-hour Load Cycles period (LC) under the rated voltage U_o at 5 points of the insulation of the sample cable for a_{VH}, b_{VH}.

- **48-hour Load Cycles**

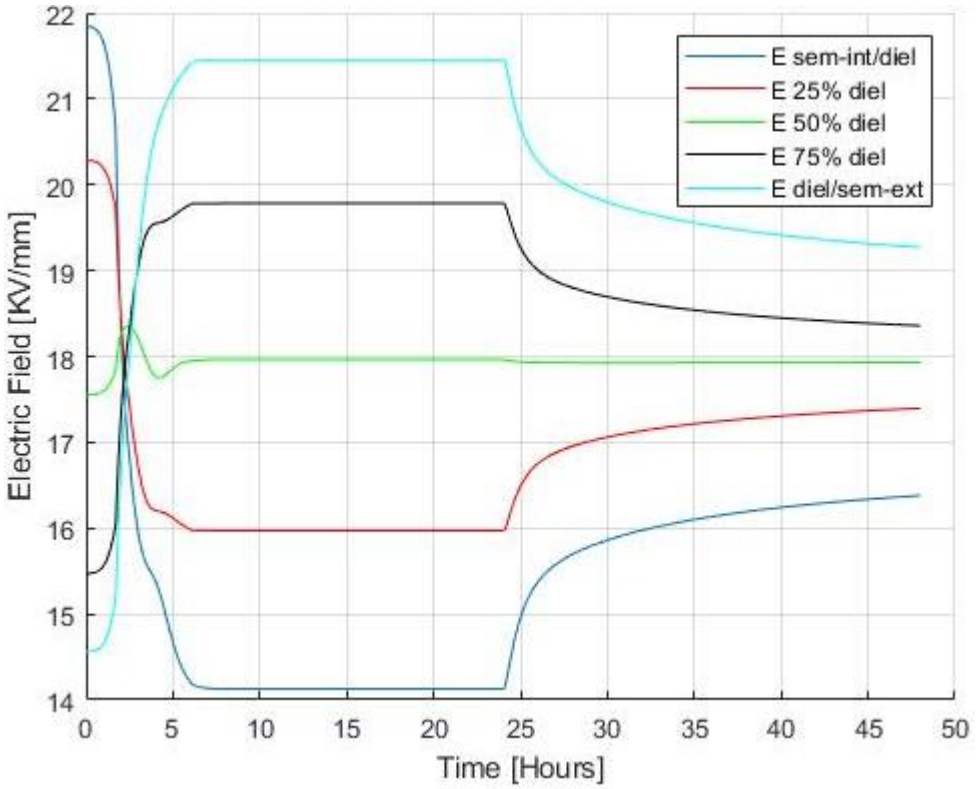

Figure 4.87– Transient exact electric field during the 1'st cycle of the 48-hour Load Cycles period (LC) under the rated voltage U_o at 5 points of the insulation of the sample cable for a_{VH}, b_{VH}.

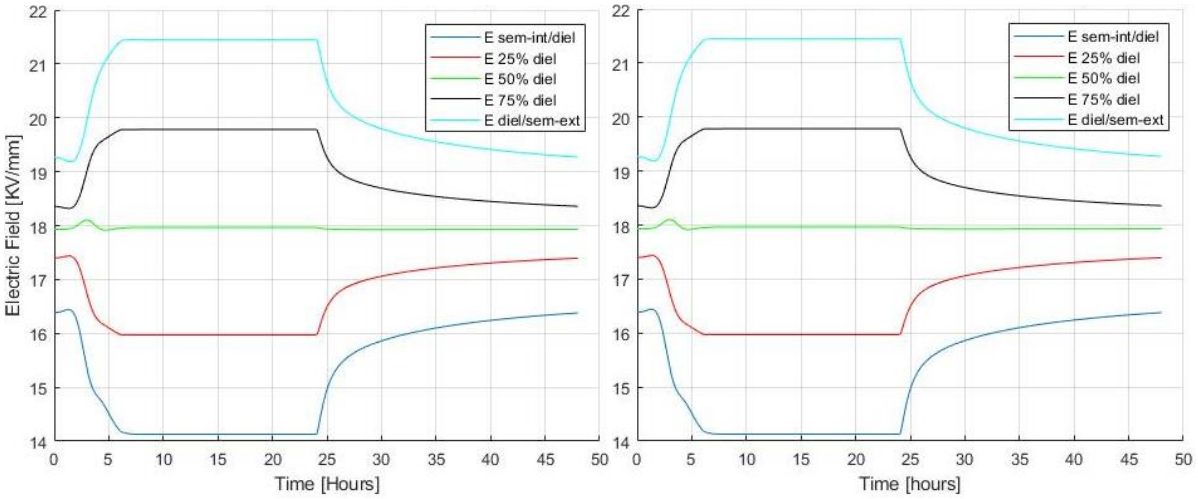

Figure 4.88– Transient exact electric field during the 2'nd (a) and the 3'rd (b) cycles of the 48-hour Load Cycles period (LC) under the rated voltage U_o at 5 points of the insulation of the sample cable for a_{VH}, b_{VH}.

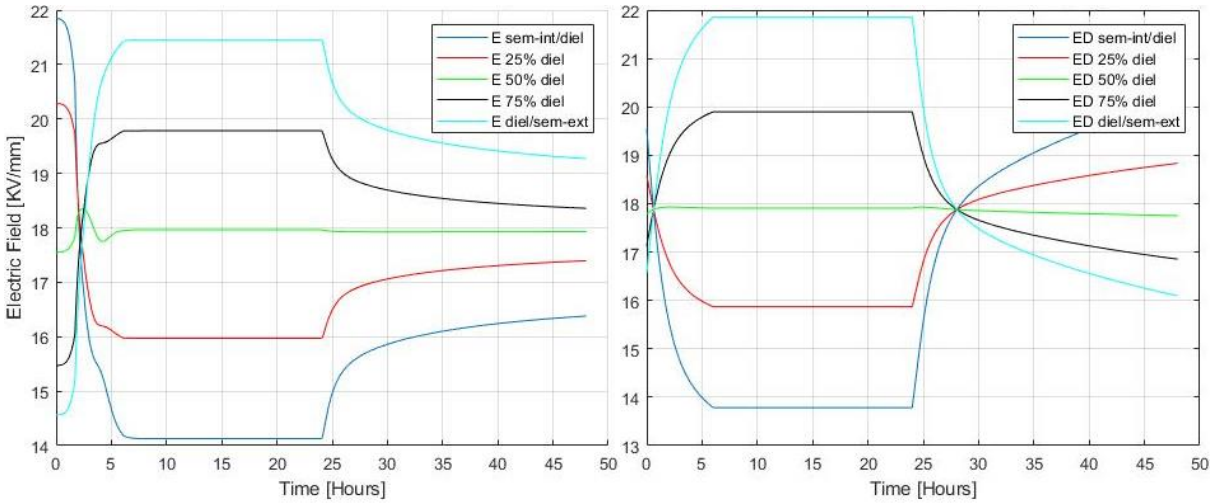

Figure 4.89 – comparison between exact (a) and approximated (b) transient electric field during the 48-hour Load Cycles period (LC) under the rated voltage U_o at 5 points of the insulation of the sample cable for a_{VH}, b_{VH}.

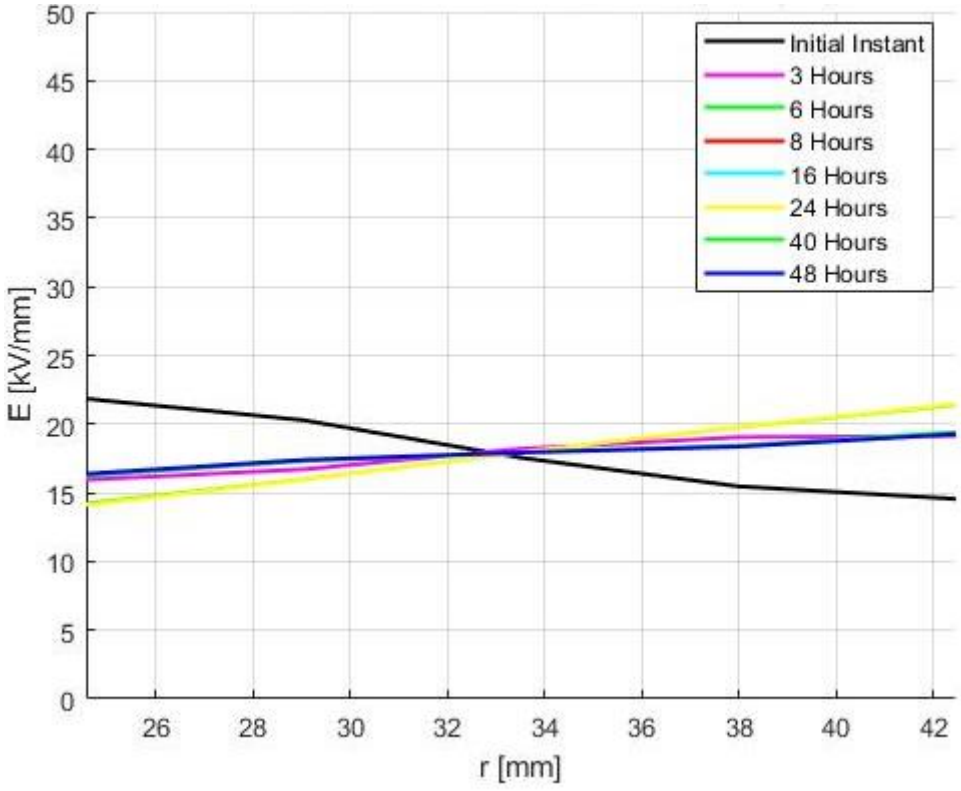

Figure 4.90 – Transient exact electric field profile during the 1'st cycle of the 48-hour Load Cycles period (LC) under the rated voltage U_o at 5 points of the insulation of the sample cable for a_{VH}, b_{VH}.

4) Test under the Type Test conditions U =1.85 U_o:

- **24-hour Load Cycles**

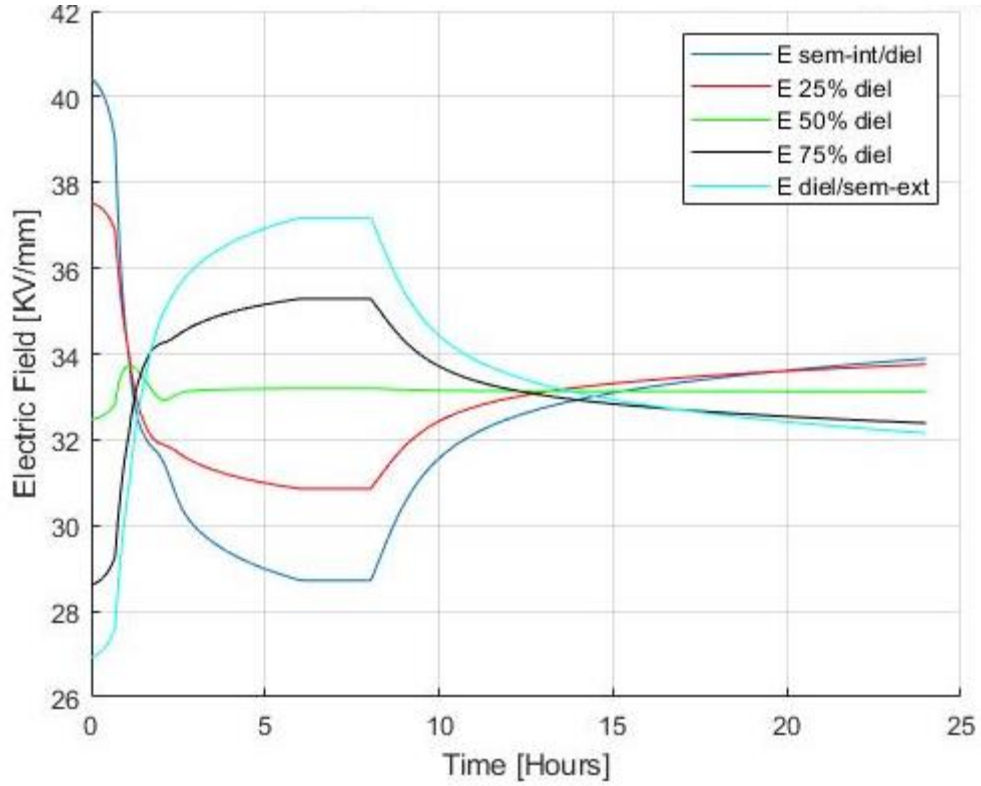

Figure 4.91 – Transient exact electric field during the 1'st cycle of the 24-hour Load Cycles period (LC) under the Type Test conditions at 5 points of the insulation of the sample cable for a_{VH}, b_{VH}.

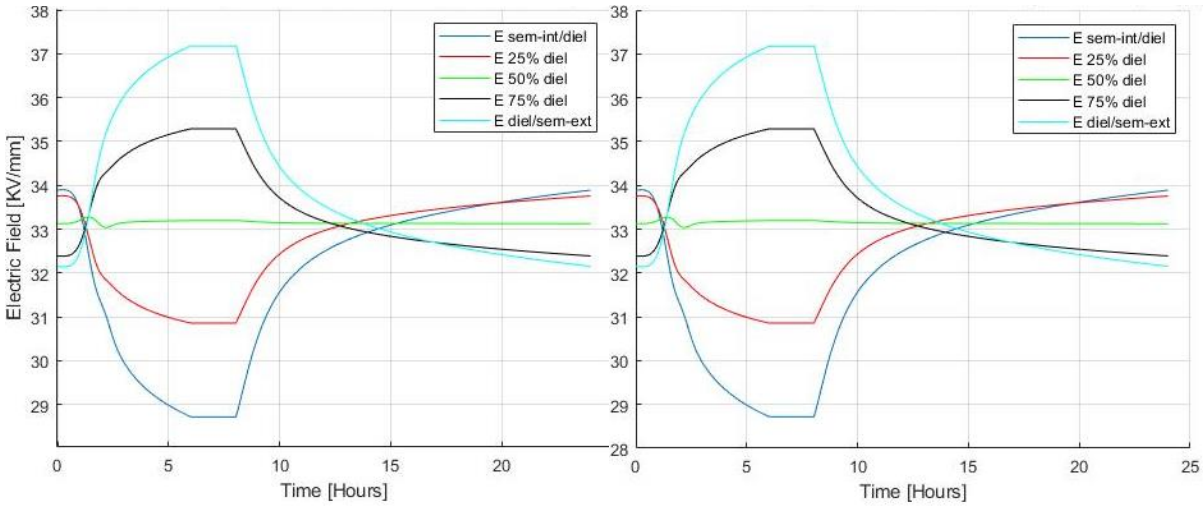

Figure 4.92 – Transient exact electric field during the 2'nd (a) and the 3'rd (b) cycles of the 24-hour Load Cycles period (LC) under the Type Test conditions at 5 points of the insulation of the sample cable for a_{VH}, b_{VH}.

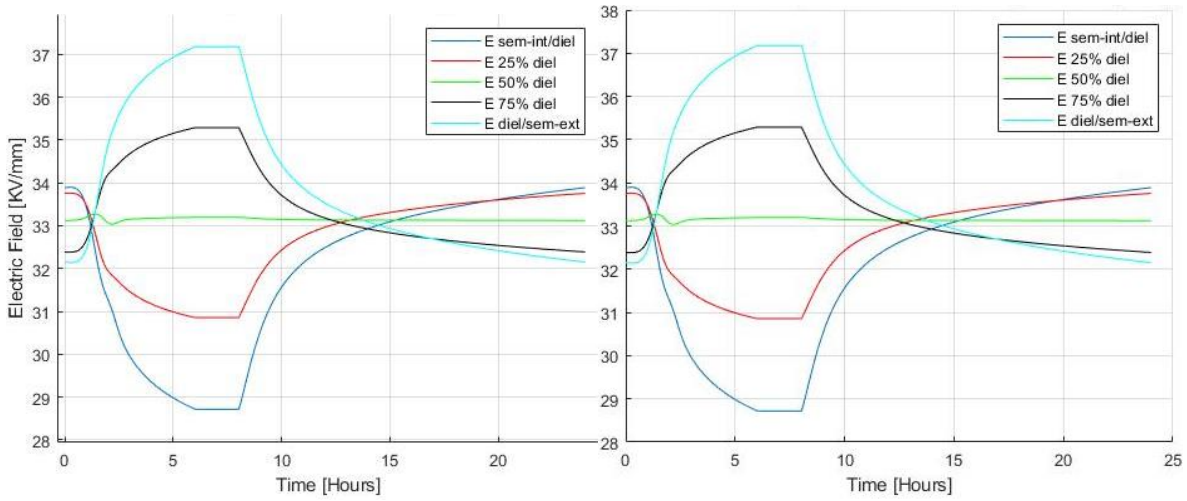

Figure 4.93– Transient exact electric field during the 4'th (a) and the 5'th (b) cycles of the 24-hour Load Cycles period (LC) under the Type Test conditions at 5 points of the insulation of the sample cable for a_{VH}, b_{VH}.

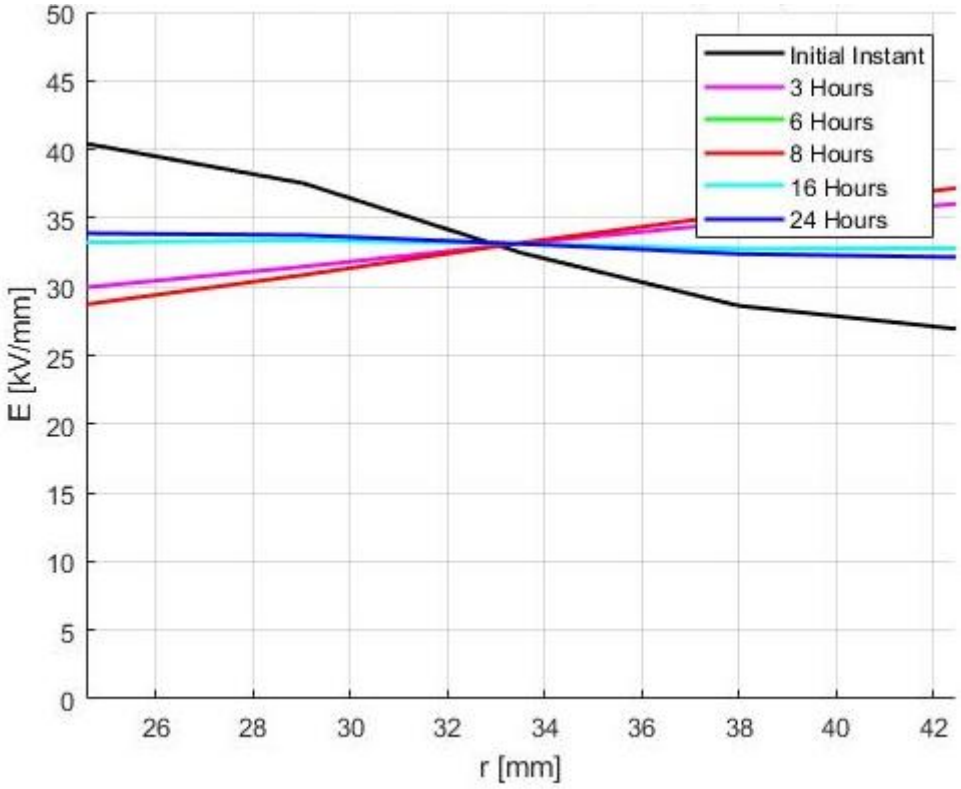

Figure 4.94 – Transient exact electric field profile during the 1'st cycle of the 24-hour Load Cycles period (LC) under the Type Test conditions at 5 points of the insulation of the sample cable for a_{VH}, b_{VH}.

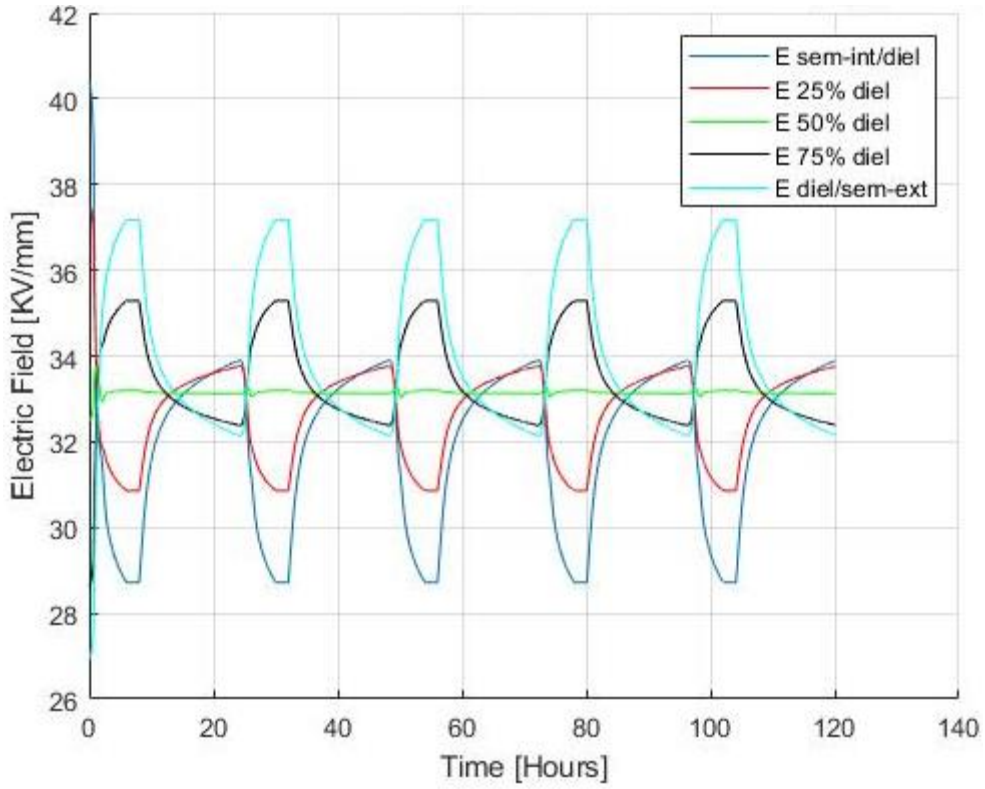

Figure 4.95 – Transient exact electric field profile during the first 5 cycles of the 24-hour Load Cycles period (LC) under the Type Test conditions at 5 points of the insulation of the sample cable for a_{VH}, b_{VH}.

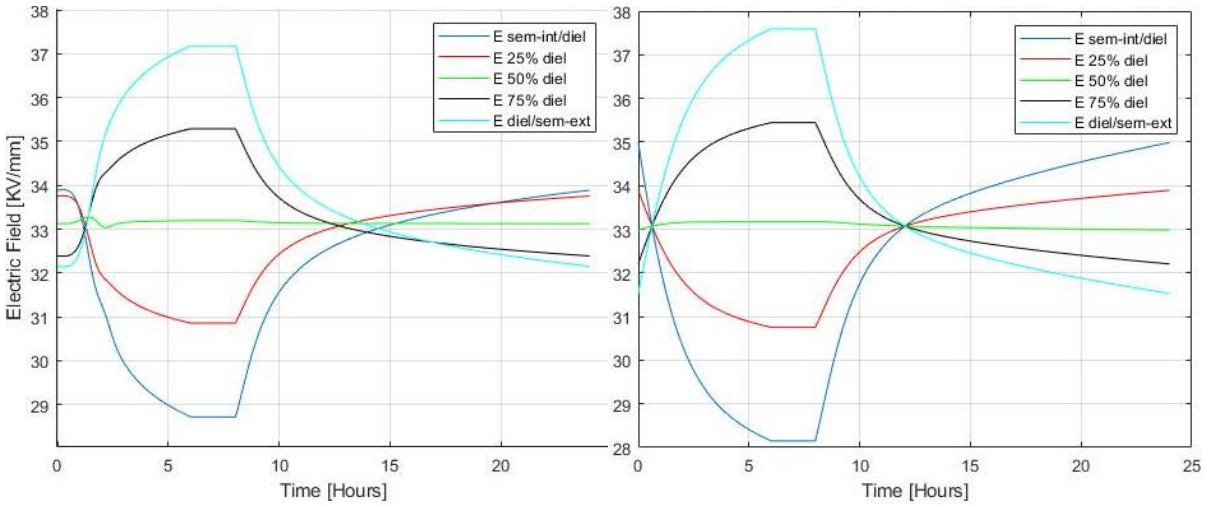

Figure 4.96– comparison between exact (a) and approximated (b) transient electric field during the 24-hour Load Cycles period (LC) under the Type Test conditions at 5 points of the insulation of the sample cable for a_{VH}, b_{VH}.

- **48-hour Load Cycles**

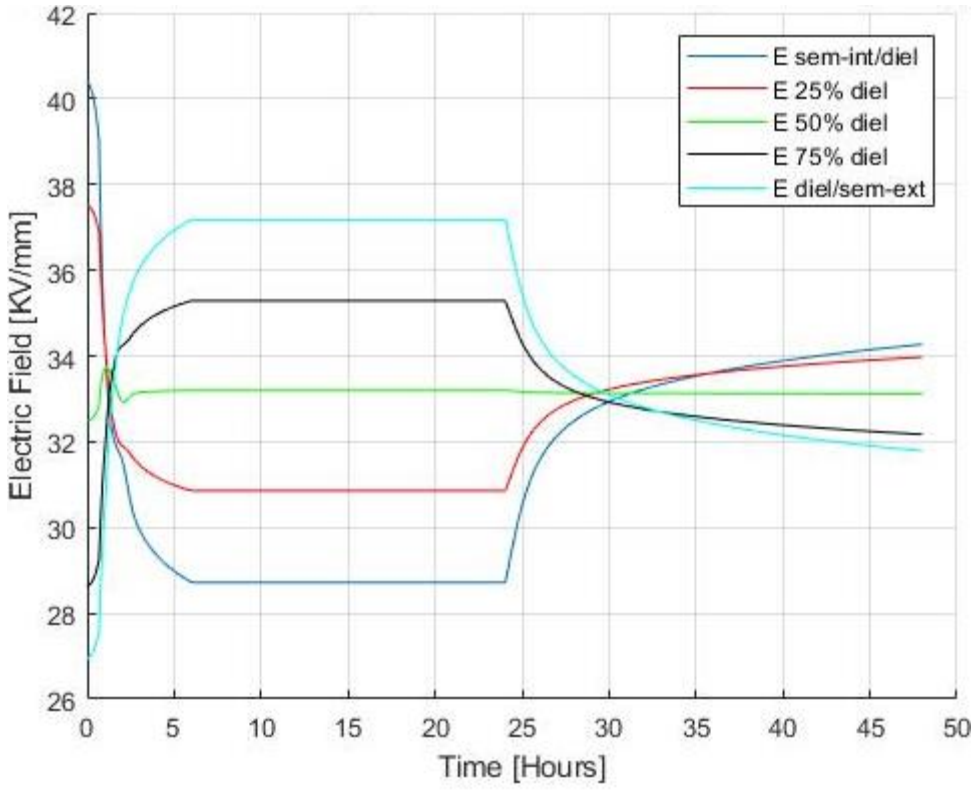

Figure 4.97 – Transient exact electric field during the 1'st cycle of the 48-hour Load Cycles period (LC) under the Type Test conditions at 5 points of the insulation of the sample cable for a_{VH}, b_{VH}.

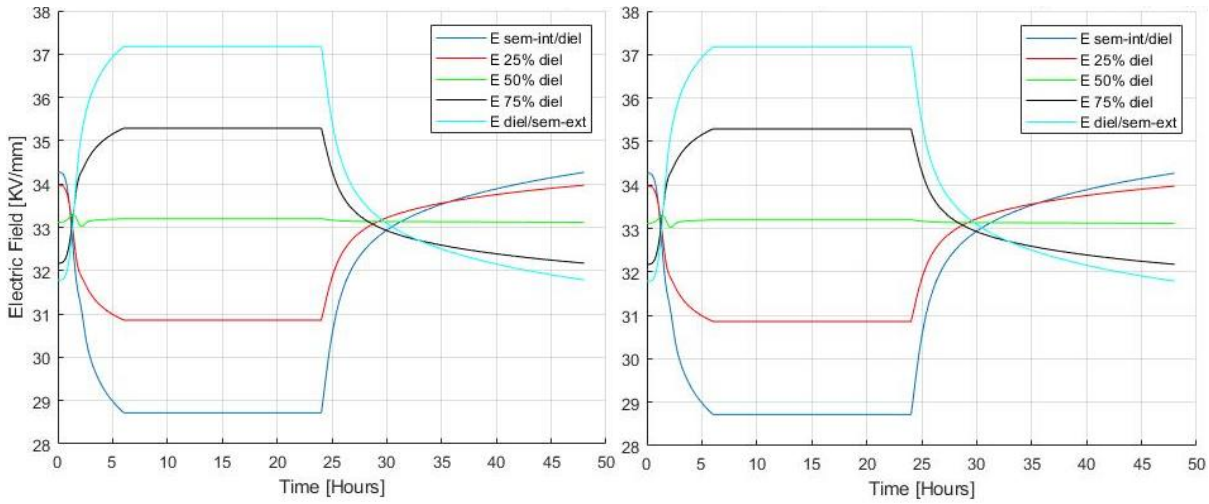

Figure 4.98 – Transient exact electric field during the 2'nd (a) and the 3'rd (b) cycles of the 48-hour Load Cycles period (LC) under the Type Test conditions at 5 points of the insulation of the sample cable for a_{VH}, b_{VH}.

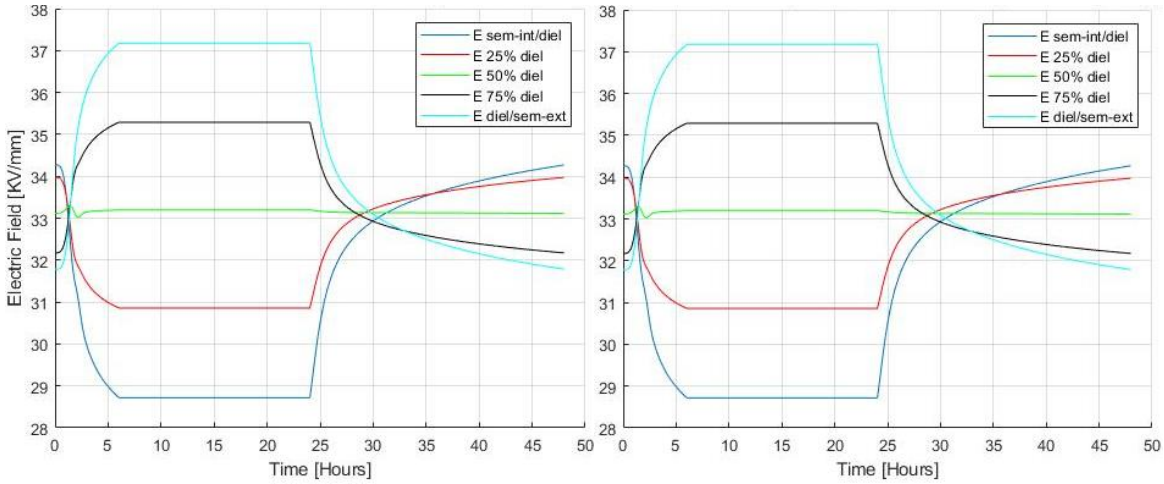

Figure 4.99– Transient exact electric field during the 4'th (a) and the 5'th (b) cycles of the 48-hour Load Cycles period (LC) under the Type Test conditions at 5 points of the insulation of the sample cable for a_{VH}, b_{VH}.

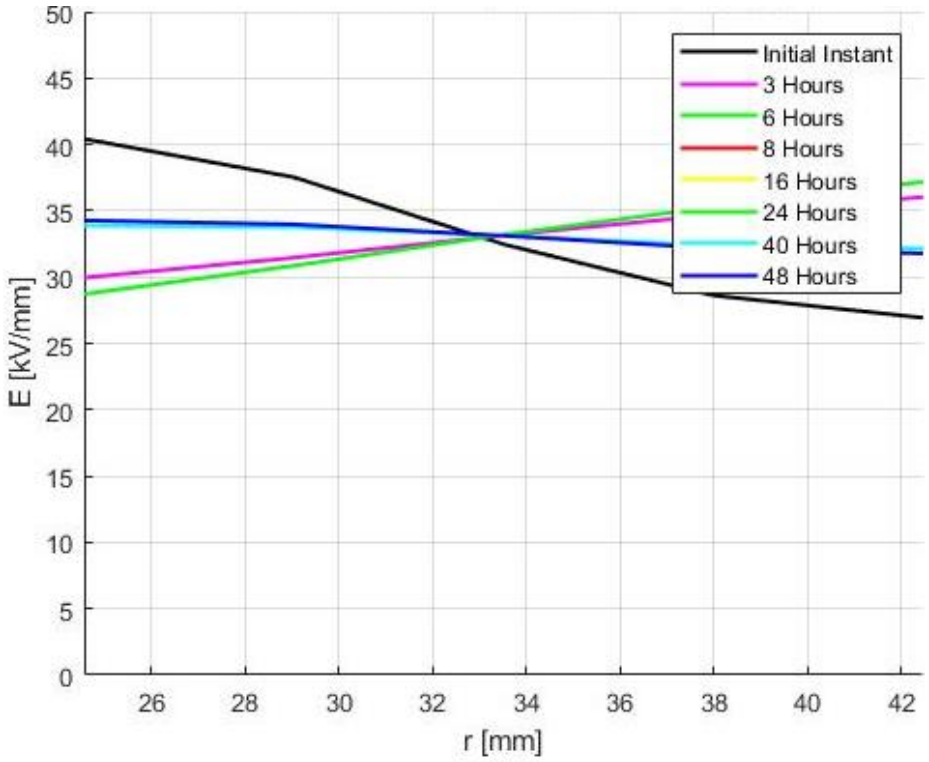

Figure 4.100 – Transient exact electric field profile during the 1'st cycle of the 48-hour Load Cycles period (LC) under the Type Test conditions at 5 points of the insulation of the sample cable for a_{VH}, b_{VH}.

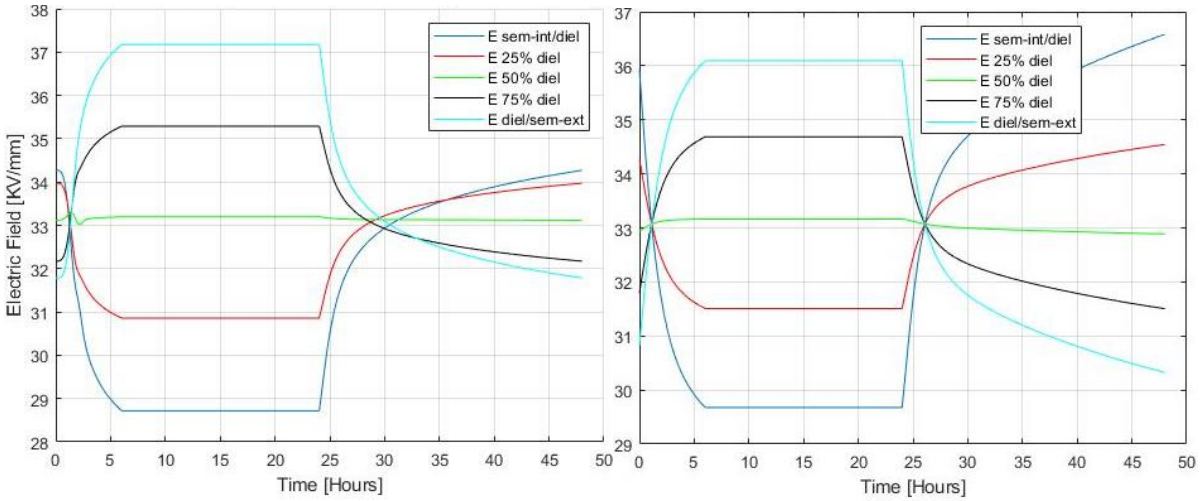

Figure 4.101 – comparison between exact (a) and approximated (b) transient electric field during the 48-hour Load Cycles period (LC) under the Type Test conditions at 5 points of the insulation of the sample cable for a_{VH}, b_{VH}.

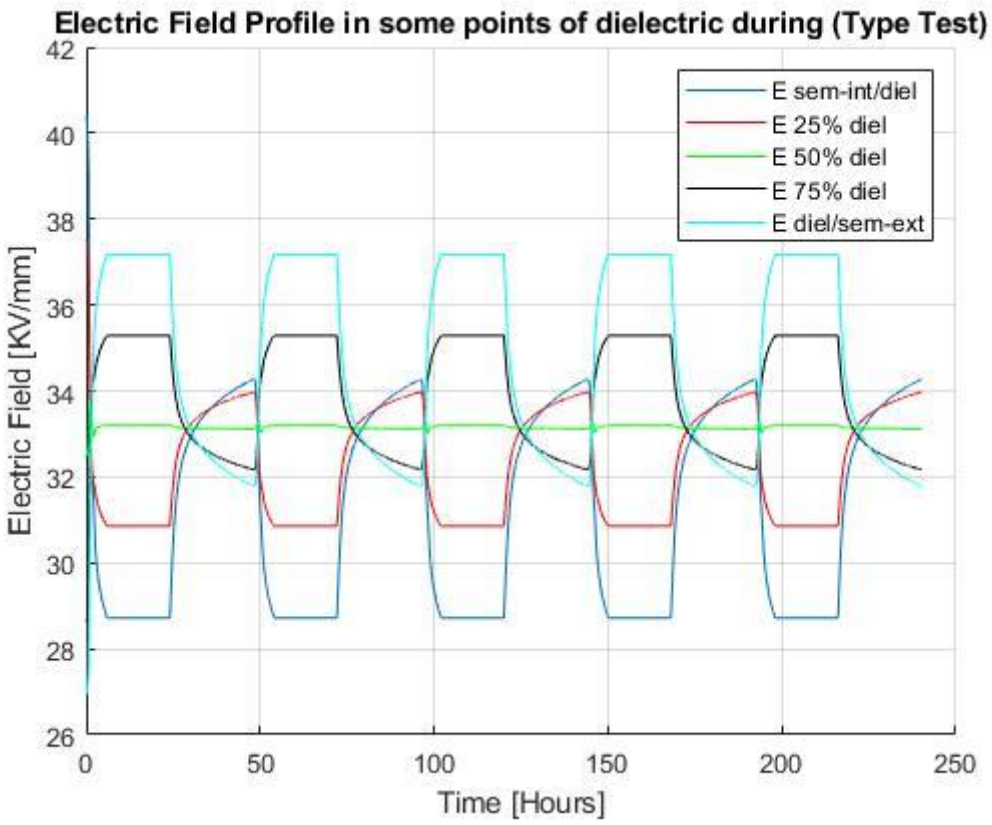

Figure 4.102 – Transient exact electric field profile during the first 5 cycles of the 48-hour Load Cycles period (LC) under the Type Test conditions at 5 points of the insulation of the sample cable for a_{VH}, b_{VH}.

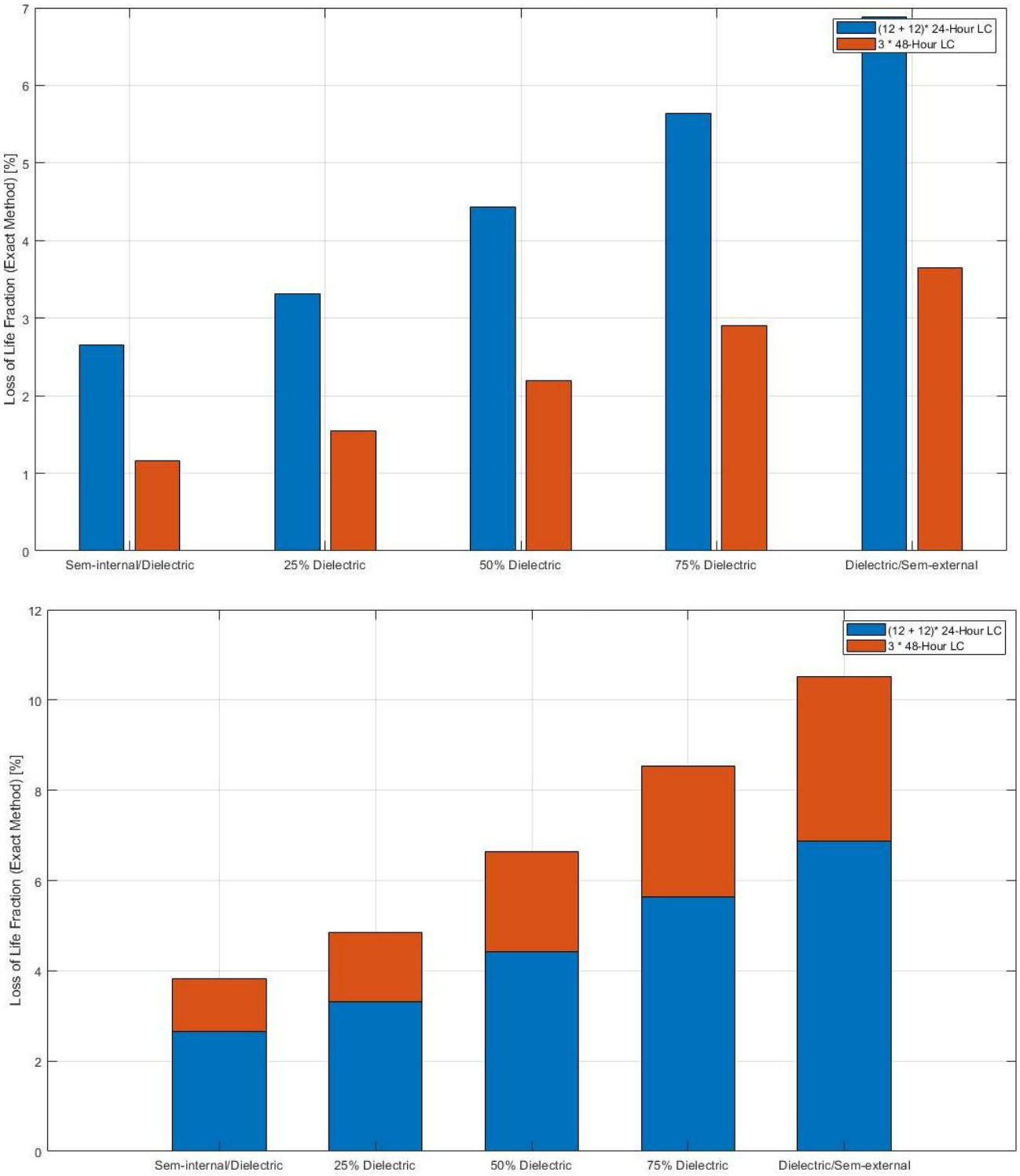

Figure 4.103 – Exact loss-of-life fractions during 12 + 12 cycles of 24-hour Load Cycle (LC) and 3 cycles of 48 hours Load Cycle (LC) under the Type Test conditions at 5 points of the insulation of the sample cable for a_{VH}, b_{VH}.

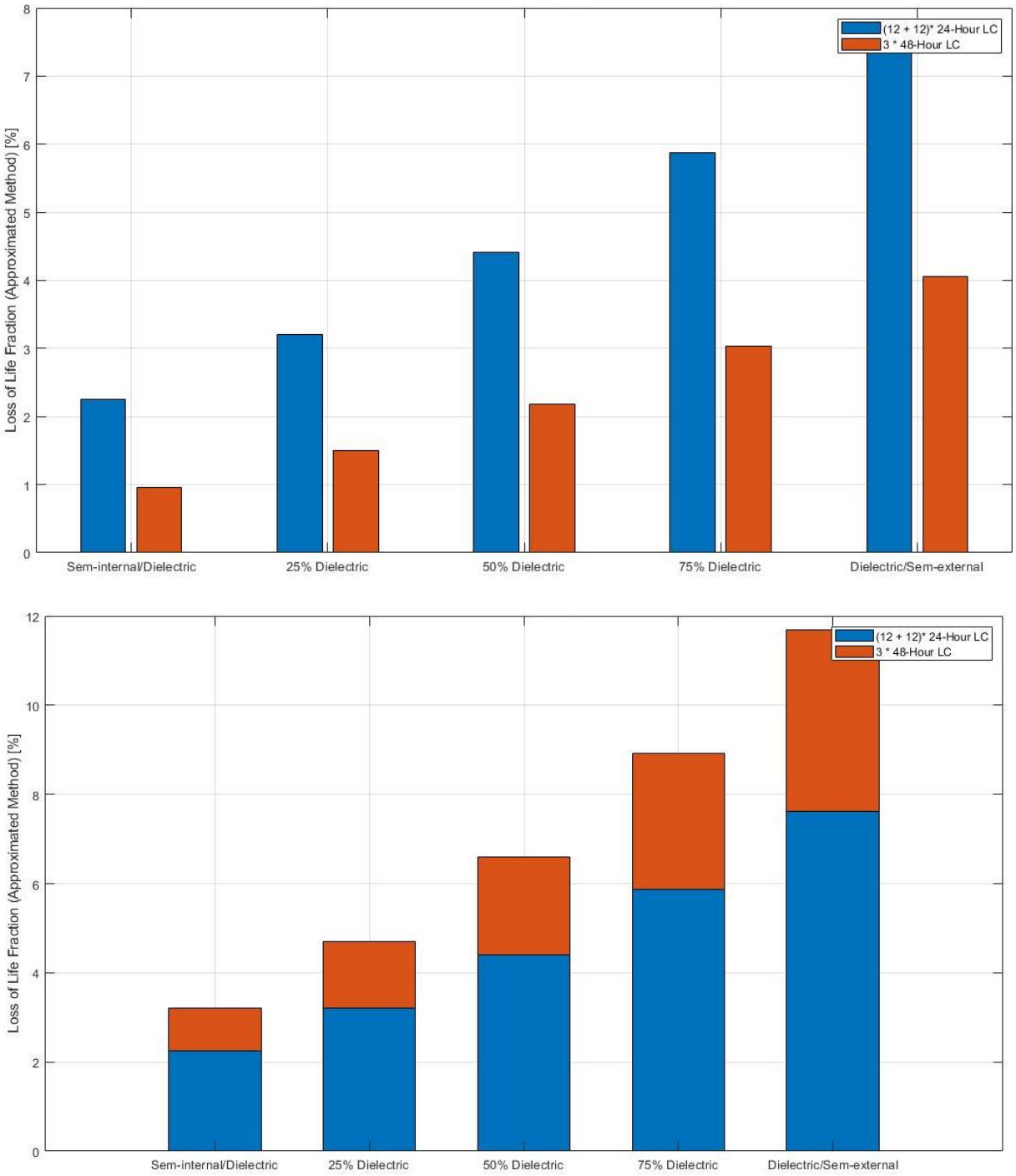

Figure 4.104 – Approximated loss-of-life fractions during 12+12 cycles of 24-hour Load Cycles (LC) and 3 cycles of 48-hour Load Cycles (LC) under the Type Test conditions at 5 points of the insulation of the sample cable for a_{VH}, b_{VH}

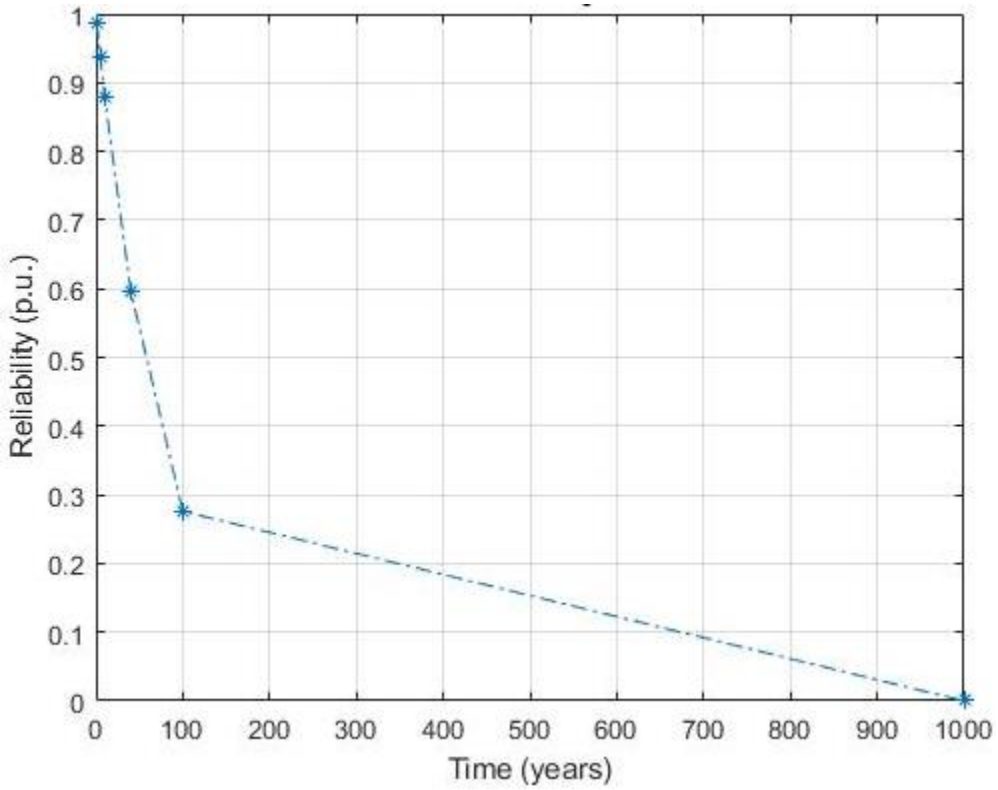

Figure 4.105 – Exact reliability during 12 + 12 cycles of 24-hour Load Cycles (LC) and 3 cycles of 48-hour Load Cycles (LC) under the Type Test conditions of the insulation of the sample cable for a_{VH}, b_{VH}.

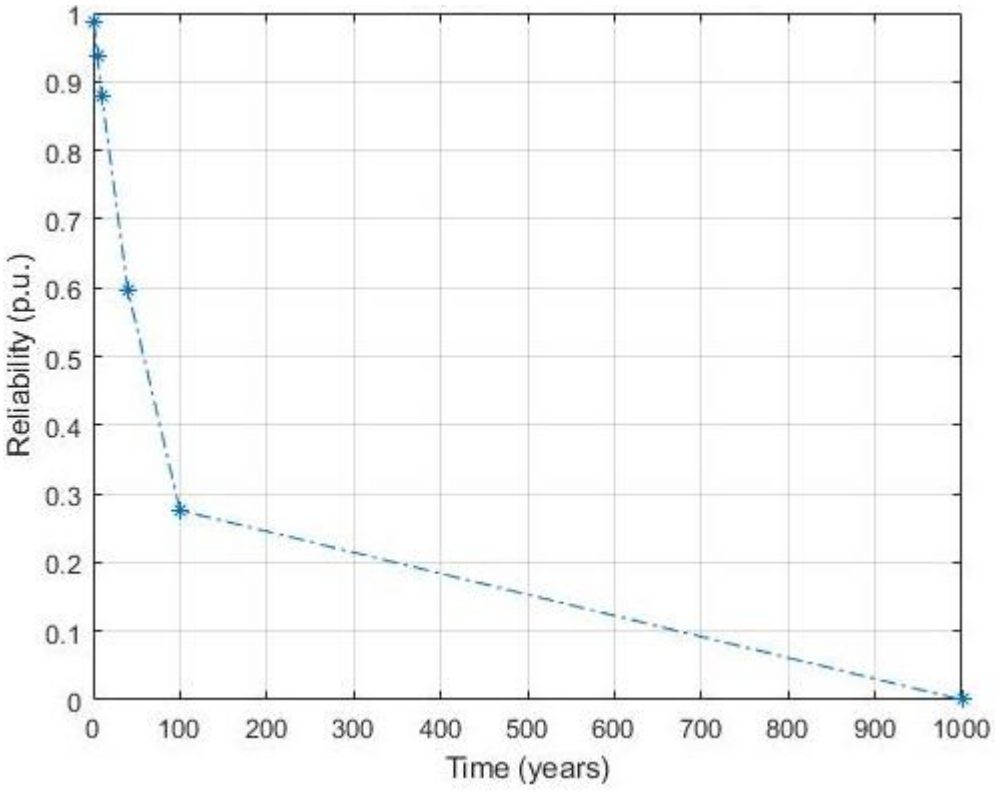

Figure 4.106 – Approximated reliability during 12 + 12 cycles of 24-hour Load Cycles (LC) and 3 cycles of 48-hour Load Cycles (LC) under the Type Test conditions of the insulation of the sample cable for a_{VH}, b_{VH}.

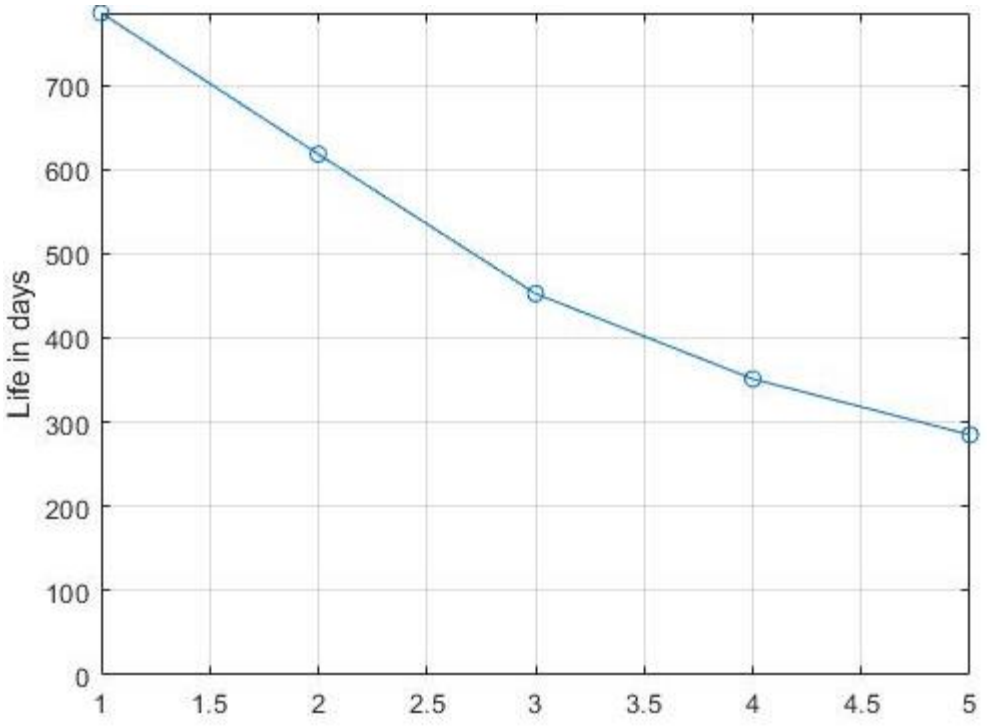

Figure 4.107– Exact life during 12 + 12 cycles of 24-hour Load Cycles (LC) and 3 cycles of 48-hour Load Cycles (LC) under the Type Test conditions at 5 points of the insulation of the sample cable for a_{VH}, b_{VH}.

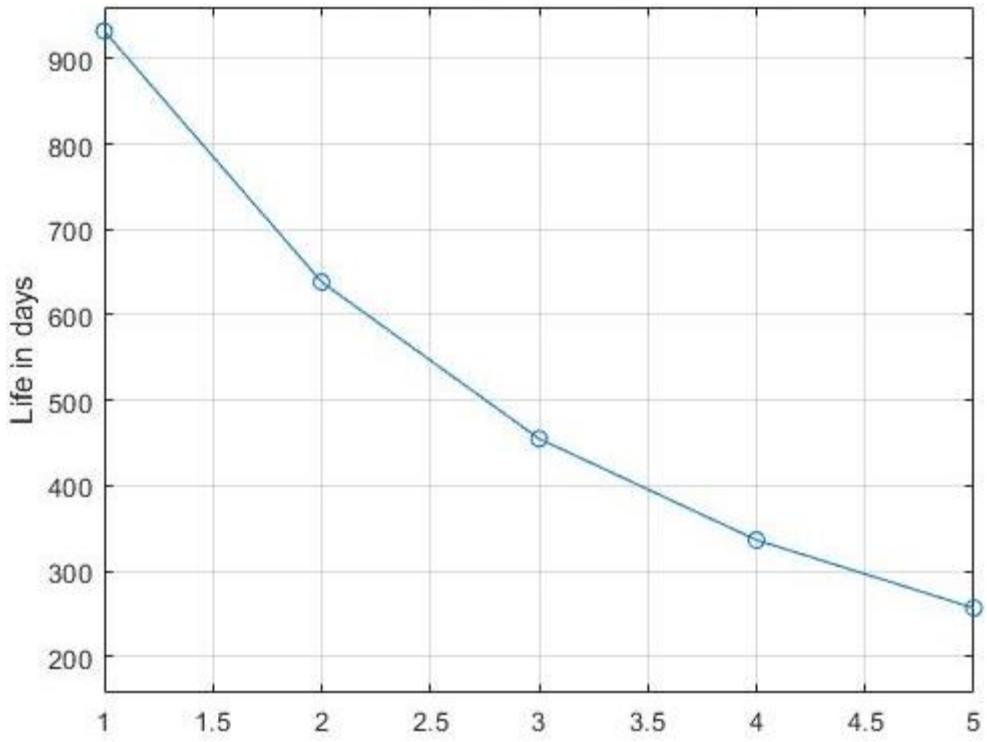

Figure 4.108– Approximated life during 12 + 12 cycles of 24-hour Load Cycles (LC) and 3 cycles of 48-hour Load Cycles (LC) under the Type Test conditions at 5 points of the insulation of the sample cable for a_{VH}, b_{VH}.

Comparison between Type Test and Pre-Qualification test in the case of medium values of *a* and *b*: (PQ test was carried out in previous master theses)[24], [25]

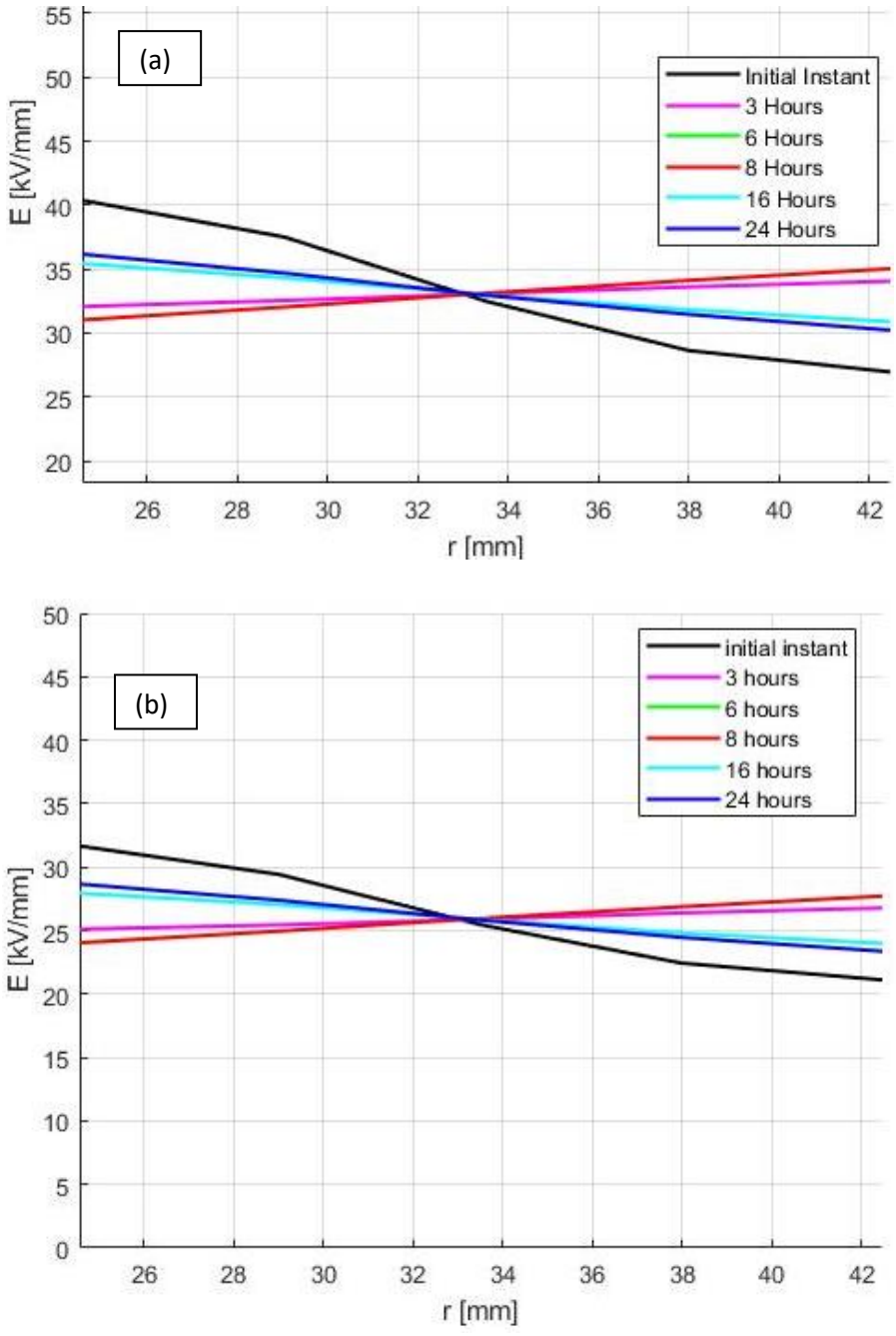

Figure 4.109 – Transient exact electric field profile during the 1'st cycle of the 24-hour Load Cycles period (LC) under the TT (a) & PQ (b) conditions at 5 points of the insulation of the sample cable for a_M, b_M.

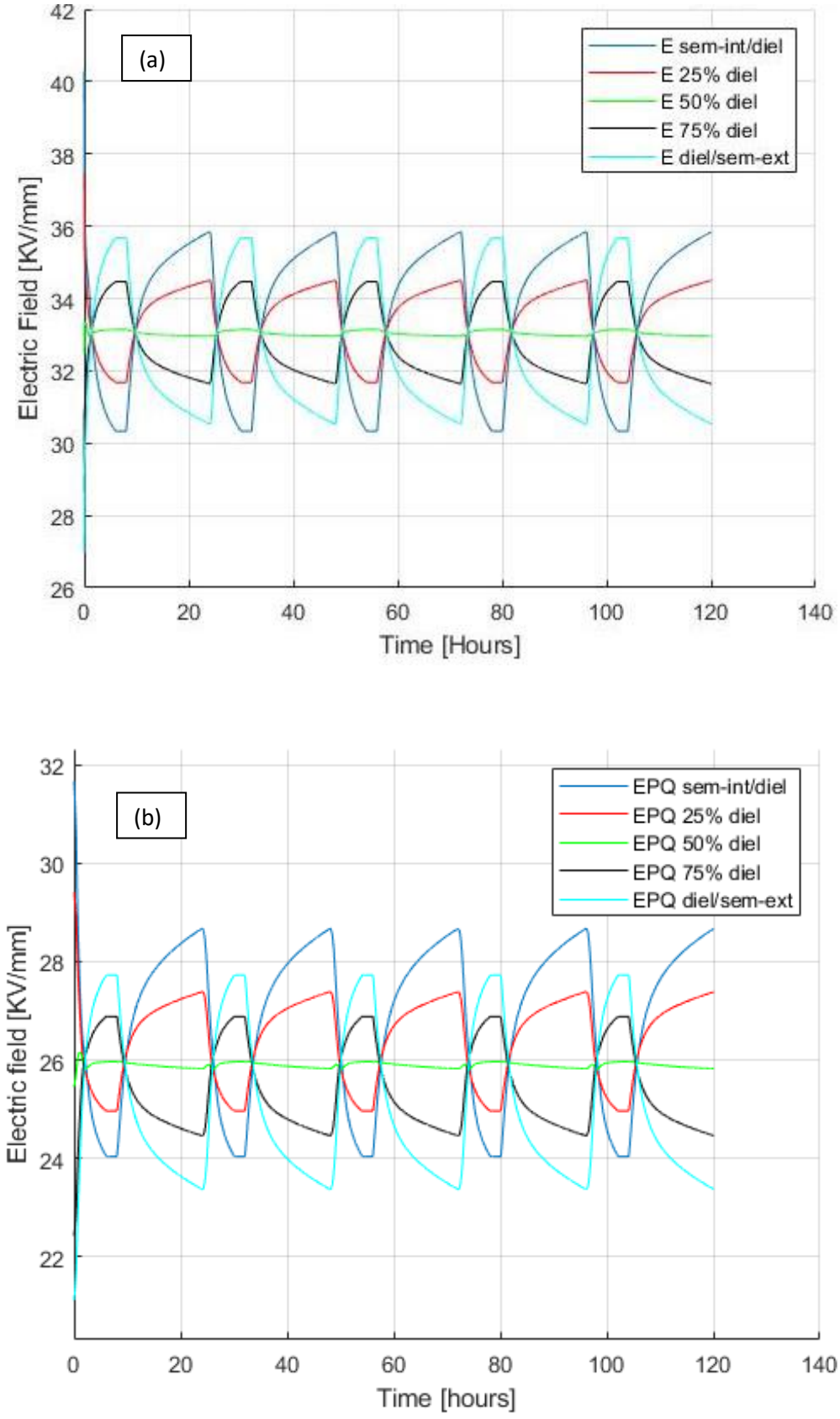

Figure 4.110 – Transient exact electric field profile under the TT (a) & PQ (b) conditions at 5 points of the insulation of the sample cable for a_M, b_M.

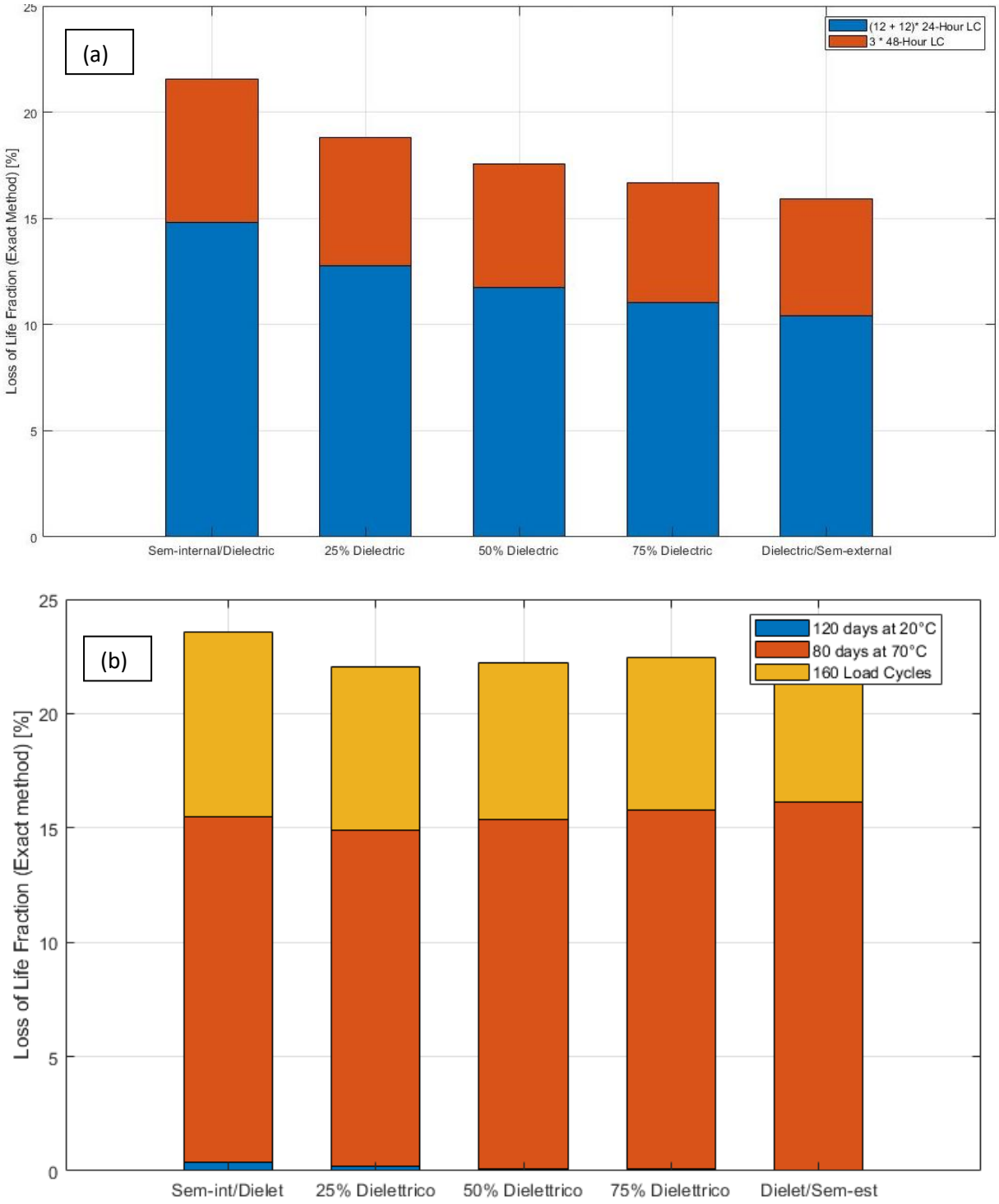

Figure 4.111 – Exact loss-of-life fractions (stacked) under the TT (a) & PQ (b) conditions at 5 points of the insulation of the sample cable for a_M, b_M.

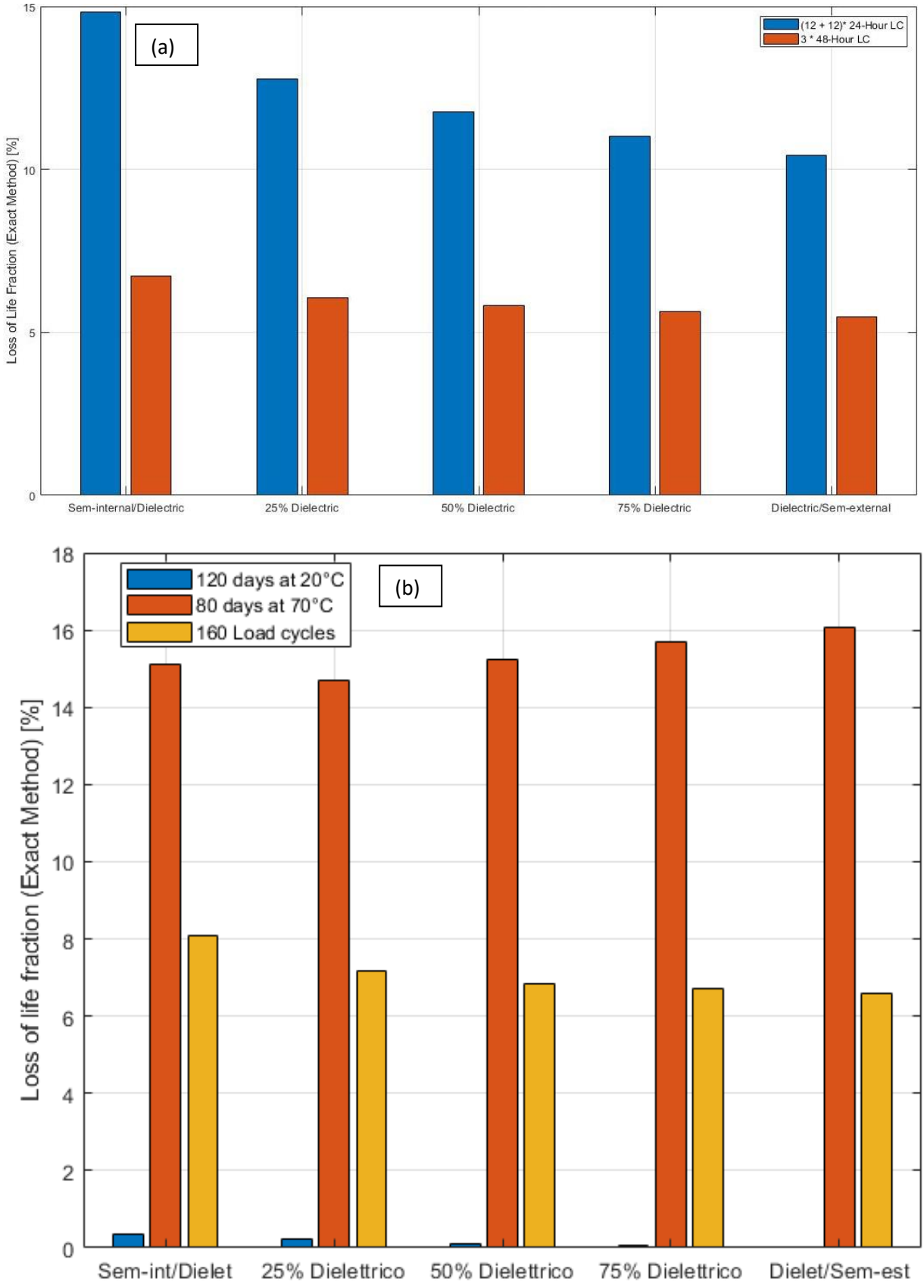

Figure 4.112 – Exact loss-of-life fractions (grouped) under the TT (a) & PQ (b) conditions at 5 points of the insulation of the sample cable for a_M, b_M.

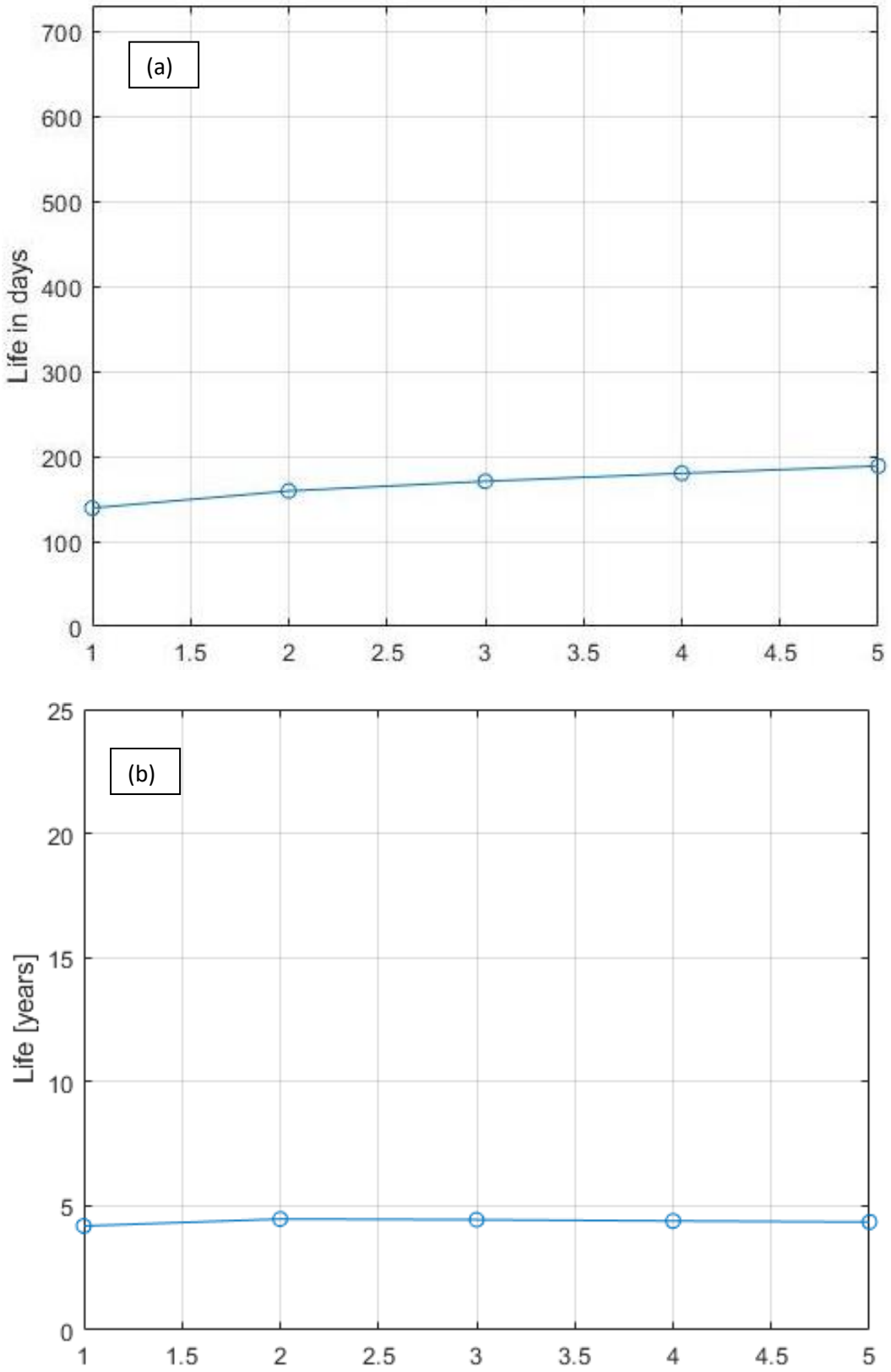

Figure 4.113 – Exact life under the TT (a) & PQ (b) conditions at 5 points of the insulation of the sample cable for a_M, b_M.

Discussion:

It can be noticed from the life figures the following:

- **In case of low values of *a* and *b*:** the life distribution in the insulation thickness reflects a capacitive (Laplacian) distribution of the electric field where the inner insulation surface is subjected to more stress, and in turn, it has a shorter life.
- **In case of medium values of *a* and *b*:** field inversion phenomenon starts to take place showing a stabilization of the electric field distribution in the insulation thickness. Therefore, the life of all points in the insulation are almost the same.
- **In case of high values of *a* and *b*:** field inversion phenomenon takes place showing a resistive distribution of the electric field in the insulation thickness. For this reason, the inner part of the insulation is lesser stressed by the electric field due to the increase of the temperature which leads to an increase in the conductivity.

It is noteworthy to mention that the life of the cable under the Type Test condition (around 100 days) is three times longer than the Type Test duration (30 days) considering the worst case which corresponds to low values of "*a*" and "*b*" (in the inner part of the insulation). Consequently, it is unlikely that the cable fails during the Type Test. This result indicates that the Type Test is not severe from the perspective of the long-term reliability evaluation.

For the sake of comparison, the total life of cable (which corresponds to the life of the point in the cable that has the shortest life) has the following values 100, 170, 190 days for low, medium high and very high values of *a* and *b*, respectively. The following table shows the differences of the results in both the exact and the approximated methods:

Ex = Exact.

App = Approximated.

Rel. err = Relative Error.

Location	L [days]											
	a_L , b_L			a_M, b_M			a_H, b_H			a_{VH}, b_{VH}		
	Ex	**App**	**Rel. err**	**Ex**	**App**	**Rel. err**	**Ex**	**App**	**Rel. err**	**Ex**	**App**	**Rel. err**
Inner	**88**	**110**	0.2564	**139**	170	0.21895	229	278	0.216	785	932	0.1867
25%	161	180	0.1157	159	169	0.064617	235	248	0.0556	618	638	0.0332
50%	282	275	0.0255	170	168	0.010545	225	223	0.0075	452	455	0.0055
75%	443	399	0.101	180	168	0.067740	216	203	0.06	351	336	0.0435
outer	681	556	0.1829	189	**167**	0.114467	**210**	**187**	0.1078	**285**	**256**	0.0989

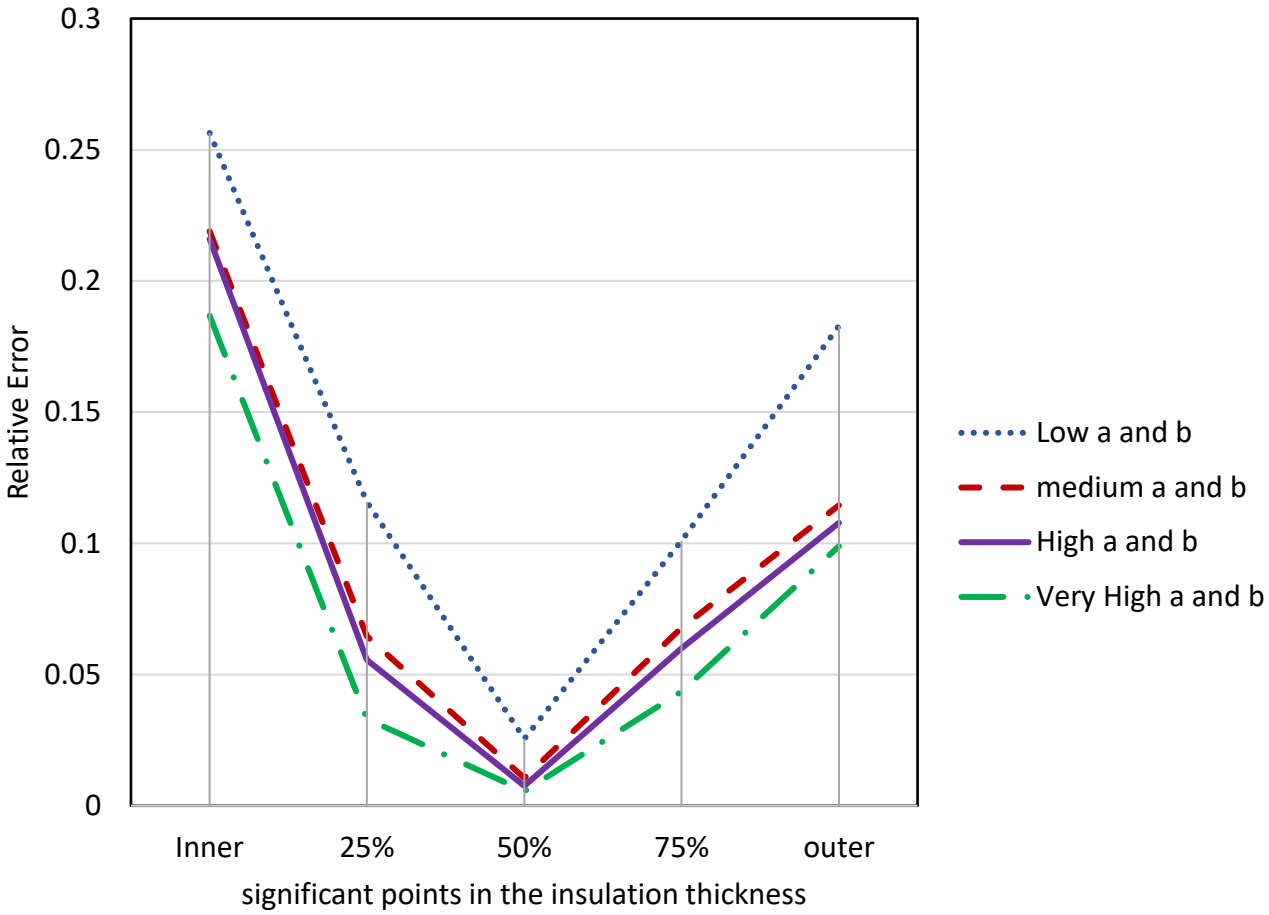

Figure 4.114 - The relative error between the exact and the approximated life models in the insulation thickness for low, medium and high values of *a*, *b* coefficients

The figure (4.114) shows that the maximum error occurs in the inner insulation surface with a considerable error in the outer surface. Whereas, the minimum error takes place in the middle of the insulation thickness.

It is worth noting that the lower the values of *a* and *b*, the higher the error of the approximated model with respect to the exact model. As a result, this may affect the validity of the approximated model where the error is doubled in some points of the insulation thickness comparing to medium and high values of *a* and *b*.

The underlined values in the above-mentioned table are the points with the shortest life, therefore, they represent the life of the cable. It is clear that the cable whose values of *a* and *b* are high, has the longest life amongst the other cables. However, this does not necessarily

mean that the high values of "*a*" and "*b*" are overall better, since there are a lot of considerations to be considered in the selection of "*a*" and "*b*" in the manufacturing process.

It can be seen in the figure (4.112) that the loss of life fraction during 3*48 LC = 6 days is half that of (12 + 12)*24 LC = 24 days, although the period 6/24 is the quarter ¼. This indicates that the loss of life in one 48-hour LC is twice that in two 24-hour LC (equivalent to the same duration of 48 hours). LF (48 LC) ≈ 2 * LF (2*24h LC).

It can be noticed from the figure (4.113) that, for the same values of *a* and *b*, the inversion of the life curve over the insulation thickness in PQ is greater than that in the TT because of the High Load period in PQ test:

- In Type Test: the inner insulation is the most stressed part in both 24-hour and 48-hour LC.
- In Pre-Qualification (PQ) test: the inner insulation is the most stressed in Load Cycles period, whereas the outer insulation is the most stressed in High Load period.

Future improvements:

For the sake of simplicity but without the loss of generality, the implemented life model does not take into consideration many phenomena:

1) Space charge accumulation and dynamics due to:
    a) Polarity reversal in the case of LCC HVDC systems.
    b) Charge injection from the electrode.
    c) Microdefects and inhomogeneity which may be formed during the manufacturing process.
2) Dielectric losses.

References:

[1] IEC 60287-1-1. 2006.

[2] C.K. Eoll.“Theory of Stress Distribution in Insulation of High Voltage d.c. Cables. PartI,” IEEE Trans. Electr. Insul., Vol. EI-10, No. 1, pp. 27–35, March 1975.

[3] M.J.P. Jeroense and P.H.F. Morshuis. “Electric Fields in HVDC Paper-Insulated Cables.” IEEE Trans. Dielectr. Electr. Insul., Vol. 5, No. 2, pp. 225–236, April 1998.

[4] G. Mazzanti and M. Marzinotto, Extruded Cables for High Voltage Direct Current Transmission: Advances in Research and Development, ser. Power Eng. Ser.. Hoboken, NJ, USA: Wiley/IEEE, Jul.2013.

[5] Brochure CIGRE 496. “Recommendations for Testing DC Extruded Cable Systems for Power Transmission at a Rated Voltage up to 500 kV.” CIGRE Working Group B1.32, April 2012, also published on Electra, No. 261, pp. 88–95, April 2012.

[6] G.Mazzanti, “Including the calculation of transient electric field in the life estimation of HVDC cables subjected to load cycles”, IEEE Electr. Insul. Mag., vol. 34, no. 3, pp. 27-37, 2018.

[7] G. Mazzanti, GC Montanari, "Insulation aging models" in Wiley Encyclopedia of Electrical and Electronics Engineering, pp. 308-319, J. Wiley & Sons, 1999.

[8] S. MARINI, “Valutazione Della Vita E Dell’affidabilita’ Di Cavi Ad Alta Tensione Continua In Presenza Di Cicli Di Carico”, Master thesis, University of Bologna, 2015.

[9] G. Chen, M. Hao, Z. Xu, A. Vaughan, J. Cao, H. Wang, "Review of high voltage direct current cables", J. Power Energy Syst., vol. 1, no. 2, pp. 9-21, 2015.

[10] G. Mazzanti, G. Chen, J.C. Fothergill, N. Hozumi, J. Li, M. Marzinotto, F. Mauseth, P. Morshuis, C.W. Reed, A. Tzimas, K. Wu, "A protocol for space charge measurements in full-size HVDC extruded cables", IEEE Trans. Dielctr. Electr. Insul., vol. 22, no. 1, pp. 21-34, 2015

[11] G. Mazzanti, G.C. Montanari, and L. Dissado. “Electrical Aging and Life Models: The Role of Space Charge.” IEEE Trans. Dielectr. Electr. Insul., Vol. 12, pp. 876–890, October 2005.

[12] Y. Zhang, J. Lewiner, C. Alquie and N. Hampton," Evidence ofStrong Correlation Between Space-charge Buildup and Breakdown in Cable Insulation", IEEE Trans. on Dielectr. and Elect. Insul., Vol 3, No.6, pp. 778-783, December 1996.

[13] D Fabiani, GC Montanari, C Laurent, G Teyssedre, PHF Morshuis, R. Bodega , L. A. Dissado , A. Campus and U. H. Nilsson, “Polymeric HVDC Cable Design and Space Charge Accumulation. Part 1: Insulation/Semicon Interface,” IEEE Electr. Insul. Mag., Vol. 23 (6), pp. 11–19, 2007

[14] D. Fabiani, G. C. Montanari, C. Laurent, G. Teyssedre, P. H. F. Morshuis, R. Bodega, L. A. Dissado, "HVDC cable design and space charge accumulation: Part 3 effect of temperature gradient", IEEE Elect. Insu. Mag., 2008.

[15] A. Cavallini, D. Fabiani, G. Mazzanti, and G. C. Montanari, “Life Model Based on Space-Charge Quantities for HVDC Polymeric Cables Subjected to Voltage-Polarity Inversions,” IEEE Trans. Dielectr. Electr. Insul., Vol. 9, 14–523, 2002. 84. 85.

[16] A. Cavallini, D. Fabiani, G. Mazzanti, and G. C. Montanari, “Life Model Based on Space-Charge Quantities for HVDC Polymeric Cables Subjected to Voltage-Polarity Inversions,” IEEE Trans. Dielectr. Electr. Insul., Vol. 9, 14–523, 2002. 84. 85.

[17] W. Choo, G. Chen, and S. G. Swingler, "Space charge accumulation under effects of temperature gradient and applied voltage reversal on solid dielectric DC cable," Proc. of the 9th ICPADM, 1-19, pp.946-949, July 2009.

[18] T.W. Dakin. “Electrical Insulation Deterioration Treated as a Chemical Rate Phenomenon.” AIEE Trans., Vol. 67, pp. 113–122, 1948.

[19] GC Montanari, G. Mazzanti, L. Simoni, "Progress in life electrothermal modeling of electrical insulation over the last decades", IEEE Transactions on Dielectrics and Electrical Insulation, Vol. 9, n. 5, pp.730-745, October 2002.

[20] A L. Dissado, G. Mazzanti, GC Montanari, "Elemental strain and trapped space charge in thermoelectrical aging of insulating materials Life modeling", IEEE Transactions on Dielectrics and Electrical Insulation, Vol.8. 6, pp .966-971, December 2001.

[21] A. Cavallini, G. Mazzanti, GC Montanari, D. Fabiani, A. Contin, "Voltage endurance of electrical components supplied by distorted voltage waveforms", IEEE ISEI, pp.73-76, Anaheim, California USA, in April 2000.

[22] MA Miner, "Cumulative damage in fatigue", J. Appl. Mechanics, pp. A159-A163, September 1945.

[23] CIGRE paper "Current ratings of cables for cyclic and emergency loads. Part.1 Cyclic ratings (load factor less than 100%) and response to a step function", ELECTRA, No. 24, 1972.

[24] G. BLANDINO, “Calcolo del Campo Elettrico Transitorio e Relativi Effetti sulle Stime di Vita dei Cavi ad Alta Tensione Continua”, Master thesis, University of Bologna, 2013.

[25] V. MAZZEO, “Effetto del Campo Elettrico Transitorio sulla Vita dei Cavi Estrusi ad Alta Tensione Continua Soggetti a Cicli di Carico”, Master thesis, University of Bologna, 2014.